2009

Design And Analysis Of Effective Routing And Channel Scheduling For Wavelength Division Multiplexing Optical Networks

Xingbo Gao
University of Central Florida

DESIGN AND ANALYSIS OF EFFECTIVE ROUTING AND CHANNEL SCHEDULING FOR WAVELENGTH DIVISION MULTIPLEXING OPTICAL NETWORKS

by

XINGBO GAO
M.S. University of Central Florida, 2006
B.E. Ocean University of China, 1997

A dissertation submitted in partial fulfillment of the requirements
for the degree of Doctor of Philosophy
in the School of Electrical Engineering and Computer Science
in the College of Engineering and Computer Science
at the University of Central Florida
Orlando, Florida

Fall Term
2009

Major Professor: Mostafa A. Bassiouni

ABSTRACT

Optical networking, employing wavelength division multiplexing (WDM), is seen as the technology of the future for the Internet. This dissertation investigates several important problems affecting optical circuit switching (OCS) and optical burst switching (OBS) networks. Novel algorithms and new approaches to improve the performance of these networks through effective routing and channel scheduling are presented. Extensive simulations and analytical modeling have both been used to evaluate the effectiveness of the proposed algorithms in achieving lower blocking probability, better fairness as well as faster switching. The simulation tests were performed over a variety of optical network topologies including the ring and mesh topologies, the U.S. Long-Haul topology, the Abilene high-speed optical network used in Internet 2, the Toronto Metropolitan topology and the European Optical topology.

Optical routing protocols previously published in the literature have largely ignored the noise and timing jitter accumulation caused by cascading several wavelength conversions along the lightpath of the data burst. This dissertation has identified and evaluated a new constraint, called the wavelength conversion cascading constraint. According to this constraint, the deployment of wavelength converters in future optical networks will be constrained by a bound on the number of wavelength conversions that a signal can go through when it is switched all-optically from the source

to the destination. Extensive simulation results have conclusively demonstrated that the presence of this constraint causes significant performance deterioration in existing routing and wavelength assignment (RWA) algorithms. Higher blocking probability and/or worse fairness have been observed for existing RWA algorithms when the cascading constraint is not ignored.

To counteract the negative side effect of the cascading constraint, two constraint-aware routing algorithms are proposed for OCS networks: the desirable greedy algorithm and the weighted adaptive algorithm. The two algorithms perform source routing using link connectivity and the global state information of each wavelength. Extensive comparative simulation results have illustrated that by limiting the negative cascading impact to the minimum extent practicable, the proposed approaches can dramatically decrease the blocking probability for a variety of optical network topologies.

The dissertation has developed a suite of three fairness-improving adaptive routing algorithms in OBS networks. The adaptive routing schemes consider the transient link congestion at the moment when bursts arrive and use this information to reduce the overall burst loss probability. The proposed schemes also resolve the intrinsic unfairness defect of existing popular signaling protocols. The extensive simulation results have shown that the proposed schemes generally outperform the popular shortest path routing algorithm and the improvement could be substantial. A two-dimensional Markov chain analytical model has also been developed and used to analyze the burst loss probabilities for symmetrical ring networks. The accuracy of the model has been validated by simulation.

Effective proactive routing and preemptive channel scheduling have also been proposed to address the conversion cascading constraint in OBS environments. The proactive routing adapts the fairness-improving adaptive routing mentioned earlier to the environment of cascaded wavelength conversions. On the other hand, the preemptive channel scheduling approach uses a dynamic priority for each burst based on the constraint threshold and the current number of performed wavelength conversions. Empirical results have proved that when the cascading constraint is present, both approaches would not only decrease the burst loss rates greatly, but also improve the transmission fairness among bursts with different hop counts to a large extent.

To my family who offered me unconditional love and support.

ACKNOWLEDGMENTS

From the initial developing stages of this dissertation, to the final draft, I owe an immense debt of gratitude to my advisor, Dr. Mostafa A. Bassiouni. His sound advice, careful guidance and constant support were invaluable throughout my research. I also extend special thanks to my committee member Dr. Guifang Li who has motivated the work on cascaded wavelength conversions and provided valuable help in understanding the operation of wavelength converters. My grateful thanks also go to my committee members Dr. Ratan K. Guha and Dr. Cliff C. Zou for their valued comments, efforts and support.

I am very grateful to my wife Xuhong Zhu. She has been very loving and encouraging throughout the entire course of my Ph.D. studies. It would not be possible without her continuing support. I would thank my mother, sisters and parents-in-law who offered me unconditional love and support. My son Christopher deserves a special mention as he helps keep my spirits high.

I would express special thanks to all my friends for their encouragement and help.

To each of the above, I extend my deepest appreciation.

TABLE OF CONTENTS

LIST OF FIGURES

LIST OF TABLES

CHAPTER 1

INTRODUCTION

In this chapter, we first review briefly WDM optical networks and the background of optical switching mechanisms. We then provide an overview of our motivations and achievements towards this dissertation.

1.1 Optical Switching Network Background

Optical transmission has been playing a critical role in the backbone of current commercial telecommunication networks. Optical transmission is also rapidly expanding toward the customer or business premises, which are the sources or sinks of information. Nowadays, a single wavelength channel can transmit data at a rate of 10 Gb/s and beyond under WDM. Dense WDM (DWDM) technology allows tens or even hundreds of wavelength channels to be transmitted over a single optical fiber. This means that the data rate can reach 10 Tb/s in each individual fiber. Thus, it makes optical networks a logical choice to meet the growing stupendous communication demands, such as faster Internet browsing, video-on-demand, and interactive television. Properly designed

and operated, optical switching technologies can potentially utilize the immense fiber bandwidth and would eventually replace the current traditional networks.

In WDM networks, channels are created by dividing the bandwidth into a number of wavelengths or frequency bands, each of which can be accessed by the end-user at peak electronic rates [CP99]. In order to efficiently utilize this bandwidth, we need to design efficient transport architectures and protocols based on the state-of-the-art optical device technology. Optical transport methodologies have been evolving from generation to generation. In this report, we focus on transport methodologies that are based on optical cross connects (OXC). There are primarily three all-optical transport methodologies, namely, optical circuit switching, optical burst switching, and optical packet switching (OPS).

In wavelength routed WDM networks, end users communicate with each other via all optical WDM channels, which are referred to as lightpaths. A lightpath is necessary to create and keep a connection up in a wavelength routed WDM network and may span multiple fiber links. When wavelength converters are absent, a lightpath must occupy the same wavelength on all the fiber links through which it traverses [ZJM00]. This property is known as the *wavelength continuity constraint*. Given a set of connections, the problem of setting up lightpaths by routing and assigning a wavelength to each connection is called the routing and wavelength assignment (RWA) problem. The wavelength continuity constraint implies that when the RWA protocol is unable to find a path and allocate the same wavelength to all links along the path, the call will be blocked.

Circuit and packet switching have been used in traditional (electronic) communication networks for many years for voice and data communications, respectively. Burst switching, on the other hand, is less common. Switching techniques primarily differ based on whether data will use switch *cut-through* or *store and forward*. In circuit switching, a dedicated path between two end stations is required. A call is established, the data is transferred, and the call is disconnected. Relevant resources are exclusively reserved for the call until it is terminated. In packet switching, the data is assembled into small packets and transmitted. The resources can be shared by different sources. End stations can send and receive data at their own speed. The individual packets can be individually switched or a virtual circuit can be set up. In the first case, the routing decision is done at a packet level while in the later, it is on a virtual channel level. Individual routing may lead to out-of-order message delivery.

Optical circuit switching has been available in the optical domain for the past several years. Its widespread deployment is not yet available since it offers the coarse granularity of switching. On the other side, optical packet switching will not be favorable in the foreseeable future until optical buffers outgrow their immaturity, even though it can switch at the packet level with fine granularity. Circuit switching uses two-way reservation schemes that have a large round trip. Packet switching has a large buffer requirement, complicated control, and strict synchronization issues. Only recently optical burst switching emerges to achieve a good balance between the coarse-grained circuit switching and the fine-grained packet switching by consolidating the currently available

techniques. It uses one-way reservation schemes with immediate transmission, in which the data burst follows a corresponding packet without waiting for an acknowledgment.

1.2 Motivations and Our Proposals

In this dissertation, we investigate several important problems affecting optical circuit switching and/or optical burst switching, and present our approaches to improve system performance, such as lower blocking probability, more effective routing and better fairness.

We evaluate the negative impact of wavelength conversion cascading on the performance of all-optical routing in OCS networks [GBL06]. When data in a circuit-switched connection is routed all optically from source to destination, each wavelength conversion performed along the lightpath of the connection causes some signal-to-noise deterioration. If the distortion of the signal quality becomes significant enough, the receiver would not be able to recover the original data. There is therefore an upper bound (threshold) on the number of wavelength conversions that a signal can go through when it is switched all optically. This new constraint, we refer to as the *conversion cascading constraint*, has largely been ignored by previous performance evaluation studies on all-optical routing. Our simulation studies have shown that the blocking performance of optical routing deteriorates substantially in the presence of the conversion cascading constraint, especially when the connectivity of the network topology is relatively low. Consequently an effective RWA

algorithm needs to take account of the impact of this constraint to avoid the serious negative side effects.

We proceed to propose two constraint-aware dynamic algorithms under the circumstance of bounded cascaded wavelength conversions in optical circuit switching [GBL07]. The first greedy constraint-aware routing algorithm minimizes the number of wavelength conversions for each connection establishing, and the second weighted adaptive constraint-aware routing algorithm considers the distribution of free wavelengths, the lengths of each route and the conversion cascading constraint jointly. Simulation results conclusively demonstrate that the proposed algorithms, especially the latter one, can achieve much better blocking performance in the environments of both full and sparse wavelength conversion.

One of the key components in the design of optical burst-switched networks is the development of efficient adaptive routing. In most existing studies of optical burst-switched networks, adaptive routing is based on deflection routing and/or feedback from the past intervals which often introduces excessive transmission delay and architectural complexity. We propose three novel adaptive routing schemes which consider the transient link congestion at the moment when the bursts arrive; moreover they can utilize the same offset times for the same node pairs implying zero additional transmission delay and simplicity [GB08a, GB09]. The proposed schemes also aim to address the intrinsic unfairness defect of existing popular signaling protocols by increasing the effective link utilization. In performance results, we show that with our routing techniques, the fairness among the bursts with different hop counts can be greatly improved; and our methods can

decrease the burst loss probability substantially as well in large-scale optical burst-switched WDM mesh networks.

The three novel adaptive routing schemes described above aim to improve both loss fairness among bursts with various hop counts and overall burst loss performance in optical burst-switched networks. We continue to present a reduced load fixed point approximation analysis to evaluate burst loss probabilities for symmetrical ring networks operated under the proposed routing [GB08b, GB09]. The analysis is based on a two-dimensional Markov chain model and its accuracy is validated by simulation.

As it happens on OCS networks, we presuppose that the conversion cascading constraint would cause similarly substantial negative impact on OBS routing algorithms. Due to the inherent differences of signaling protocols between the two switching mechanisms, we need to further investigate this negative impact in OBS to design effective methods to resolve or alleviate this problem. Effective proactive routing [GBL08b, GBL08a, GBL09a] and preemptive channel scheduling [GBL09b] have been proposed as the solutions. The proactive routing approach is based on the previously presented hop-based adaptive routing, while the preemptive scheduling approach uses a dynamic priority for each burst based on the constraint threshold and the current number of performed wavelength conversions. Extensive comparative simulation results have illustrated that by limiting the negative cascading impact to the minimum extent practicable, the proposed approaches can dramatically decrease the blocking probability and improve the transmission fairness among bursts with different hop counts.

1.3 Outline of the Dissertation

The remainder of this dissertation is organized as follows. Chapter 2 identifies the conversion cascading constraint and evaluates the negative impact it brings to optical circuit-switched networks. In Chapter 3, two constraint-aware dynamic algorithms are presented in the environment of cascaded wavelength conversions. Chapter 4 introduces a set of fairness-improving adaptive routing mechanisms in optical burst-switched networks. We also develop analytical loss models for symmetrical ring networks and verify the analytical results by simulation. Chapters 5 and 6 present the proactive routing scheme and the preemptive channel scheduling to address the cascaded wavelength conversions in OBS environments. Chapter 7 concludes the dissertation and discusses our future ideas to extend the work we have accomplished.

CHAPTER 2

IMPACT OF CASCADED WAVELENGTH CONVERSIONS

In wavelength-routed (circuit-switched) WDM networks, due to the wavelength continuity constraint, if wavelength converters are absent a lightpath accommodating a new connection request must occupy the same wavelength on all the fiber links through which it traverses. It implies that when not being able to find a path and allocate the same wavelength to all links along the path, the RWA protocol will block the call. To remedy the high connection blocking rates caused by this problem, wavelength converters are introduced. As its name suggests, wavelength converters can convert one wavelength to another, which would help establish more connections successfully. However, we can not perform wavelength conversions for an individual connection unlimitedly as each wavelength conversion would deteriorate the quality of the data being transmitted, resulting in the data being rendered useless at the end nodes. In this chapter, we evaluate the impact on blocking performance if an upper bound on the number of wavelength conversions per connection is applied (hence the conversion cascading constraint). To the best of our knowledge, we are the first to conduct this evaluation empirically.

2.1 Introduction

Many efforts have been done in obtaining the call blocking performance of wavelength-routed networks [RS97, JX01]. Since the technology of optical wavelength conversion can significantly improve the network blocking performance and network throughput, it has received considerable attention in the optical community [Bir96, SAS96, LL93b, LL93a, EB03]. The performance improvement obtained by wavelength converters depends on the topology of the network, the traffic demand, and the number of available wavelengths, among other factors [SAS96].

The full-range wavelength converter (FWC) is one of the most important wavelength converters and it can convert an incoming wavelength to any of the outgoing wavelengths of the WDM network [XL99, QY02]. Since converters are very costly, there are trade-offs between the number of converters deployed in a WDM network and how much performance improvement is achieved. Subramaniam et al. [SAS96] studied the effects of topological connectivity and wavelength conversion in circuit-switched all-optical wavelength networks. They combined their analytical model and numerical simulation together to show the strong correlation between the benefits of conversion and network topology as well as the number of available wavelengths. Lee and Li [LL93b] examined networks with partial wavelength conversion, where a small number of full-range wavelength converters are shared by different wavelengths within one node architecture. They showed that the problem of finding the optimal RWA solution with incomplete wavelength conversion is non-deterministic polynomial NP-complete. Houmaidi et al. [HBL03, EB03] presented the *k*-

minimum dominating set (k-MDS) algorithm to place the FWC's optimally in optical networks and proved to gain better blocking performance than the approach that placed the converters in nodes that have the highest blocking probabilities [IM99, SS02]. They have also presented a new link-dependency analytical model that is useful for enhancing the k-MDS algorithm [EB06].

However, all of the above efforts on all-optical networks disregarded the practical impediments and constraints that face the deployment of the wavelength conversion technology, such as the conversion cascading constraint. Our study in this chapter is mainly motivated by the observation that the conversion cascading constraint may have noticeable or even significant negative impact on blocking performance of existing routing algorithms in optical environments with sparse and/or full wavelength conversion. We evaluate this negative impact in all-optical networks and show that it indeed can be substantial and that RWA needs to take it into account.

The rest of the chapter is organized as follows. In Section 2.2, we discuss briefly wavelength conversion mechanisms and the conversion limitation from the perspective of physical layer. In Section 2.3, we discuss the potential impact of the conversion cascading constraint on optical routing algorithms. In Section 2.4, we review briefly the routing and wavelength assignment algorithms studied in this chapter. In Section 2.5, we evaluate the blocking performance of the existing static routing algorithms at the presence of the conversion cascading constraint in different topologies, and we also discuss the performance measures in terms of sparse converters placement. Finally, Section 2.6 summarizes the chapter.

2.2 Wavelength Conversion Mechanisms and Physical Limitations

In general, the core of the wavelength converter is a three terminal device consisting of input, output, and control terminals [Yoo96]. Depending on the mapping functions and the form of control signals, wavelength converters can be classified into three categories: optoelectronic, optical gating, and wave-mixing [Yoo96, RM98]. In this chapter, we focus on all-optical routing, i.e., the optical signal travels from the source node to the destination node without being converted to electronic signal. Specifically, the performance results discussed in this chapter do not apply to the case when the signal is subjected to O/E & E/O conversions in the intermediate OXC's along the lightpath of the connection.

There are countless issues to be considered when comparing wavelength conversion techniques. These issues can be grouped in three large categories: signal quality, configuration, and performance [Yoo96]. Signal quality includes signal-to-noise ratio, chirp, amplitude distortion, and extinction ratio, and it largely determines the bit-error-rate and the cascadability of wavelength converters. Configuration is related to the actual implementation of the wavelength conversion in the OXC, and is closely linked to the mapping function of the wavelength converter and the resulting OXC architecture. The configuration issue includes control requirements, dynamic ranges of input signals, polarization dependence, filtering requirements, and power requirements. Lastly, performance includes conversion efficiencies, conversion bandwidths, and bit-rate limits.

Future optical networks are expected to rely on optical technologies not only for transmission but also for signal processing. Wavelength conversion and optical buffering are two envisioned all-optical signal processing technologies to facilitate and enable the switching and routing of optical signals. It is well understood that wavelength conversion degrades the quality of the signal and reduces the signal to noise ratio; cascading wavelength conversion further aggravates this problem and must be carefully dealt with [LGV97]. The extinction ratio of the converted signal is typically low, and the reduced extinction ratio leads to power penalties measured right after wavelength conversion. In addition, some types of wavelength conversion produce chirp in the converted signal, which leads to excessive pulse broadening after fiber transmission. Because of all of these factors, wavelength conversion cannot be repeatedly cascaded without a bound. Although the signal deterioration problems associated with wavelength conversion and with conversion cascadability have been investigated at the physical layer level, the rich literature on the performance evaluation of optical routing has largely ignored this problem. Ideally, a connection should be discarded (blocked) if the number of wavelength conversions employed to switch the connection causes the signal quality to degrade to a point of no return. In this chapter, we present the results of a study to evaluate the level of deterioration of the blocking performance of all-optical routing due to a constraint on the maximum number of allowed wavelength conversion within the lightpath of circuit-switched optical connections.

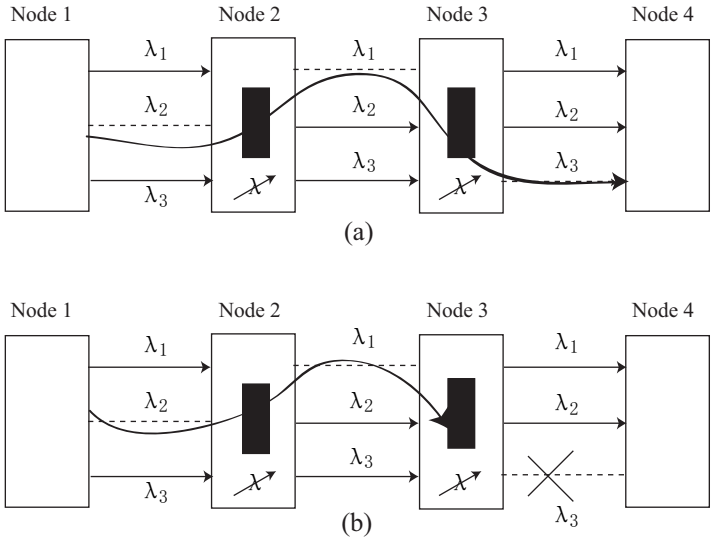

Figure 2.1: Example blocking due to the conversion cascading constraint.

2.3 Negative Impact of Conversion Cascading Constraint

As aforementioned in previous sections, it is inferred that the enforcement of the conversion cascading constraint would inevitably degrade the blocking performance. In this section, let us briefly look at how the entire system can be affected by this constraint through an example.

In Figure 2.1, there are four optical nodes and three available wavelengths on each directional link between any two nodes. The arrowed solid lines represent that the corresponding wavelengths are currently in use, while the wavelengths represented by the dotted lines are still available. As shown in Figure 2.1a, a control packet tries to schedule a wavelength channel and related resources for a data burst traversing from node 1 to node 4. At node 2, it finds only λ_1 is available and thus one wavelength conversion from λ_2 to λ_1 has to be set up and conducted when the burst arrives. A

similar situation happens at node 3 which will convert further from λ_1 to λ_3 in order to reach node 4. If we do not consider the conversion cascading constraint or if the constraint has a threshold larger than one (i.e., two or more cascaded conversions are permitted in total for each data transmission), the control packet is able to finish reservation as usual. However, if the system can only accept a maximum of one wavelength conversion per data transmission, the burst would be dropped at node 3 as showed in Figure 2.1b (if the burst is not discarded, it will arrive at the receiver as a useless signal that cannot be recovered). When bursts get excessively discarded due to the conversion cascading constraint, the burst loss performance will be degraded, and the wavelengths already utilized by the dropped bursts and other related resources are wasted as well.

2.4 Routing Algorithms in Study

In the dynamic traffic situation, it is desirable to choose a route and a wavelength that maximize the probability of setting up a given connection, while at the same time attempting to minimize blocking for future connections. Consequently, RWA algorithms play a key role in improving the blocking performance of wavelength-routed all-optical networks.

Shortest path routing has been widely used in telecommunication networks because it consumes less resource and has very simple complexity. Shortest path routing can be classified into two categories: static routing and dynamic (or adaptive) routing. In static routing, the routes are

usually pre-computed without considering the current network state; while in dynamic routing, the route selection is based on the current network state. Typical examples of algorithms that utilize static routes are fixed shortest-path routing (FSR) and fixed-alternative shortest-path routing (FAR). For dynamic routing, the two well-known algorithms - least-loaded routing (LLR) [KA98] and least-congested-path (LCP) [CY94] routing were proposed.

Static routing provides simplicity of control for setting up and tearing down lightpaths without requiring extensive support from the control and management protocols to continuously update the routing tables as in adaptive routing [RS97]. Fixed-alternative routing can provide some degree of fault tolerance upon link failures. In this chapter, we focus on evaluating the impact of the conversion cascading constraint on the FSR and FAR algorithms through simulation.

While deploying full conversion capability in all nodes of a large optical network would be very expensive, the sparse placement of full wavelength converters in selected nodes is a good compromise between cost and blocking performance. Therefore, we also carry out simulation with sparse wavelength conversion based on the k-MDS ($k = 1$) sparse converter placement algorithm [HBL03].

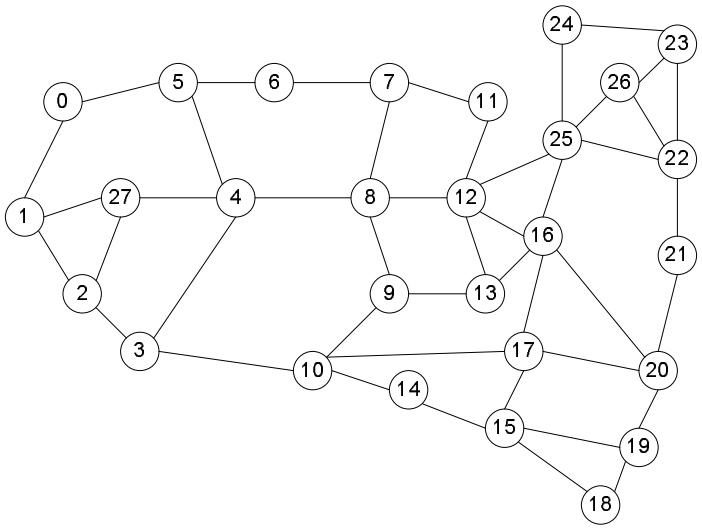

Figure 2.2: U.S. Long-Haul Network.

2.5 Impact Evaluation

We have conducted extensive simulations to evaluate the impact of the conversion cascading constraint on the blocking performance of the FSR and FAR static routing algorithms. The performance tests use a variety of network topologies including the U.S. Long-Haul network (shown in Figure 2.2), 5 x 5 mesh-torus, 10 x 10 mesh-torus, 20-node ring and 40-node ring networks. The lightpath connection requests arrive to the network according to a Poisson process with rate λ, and the connection holding time is exponentially distributed with mean $1/\mu$. For each connection request, the source and destination nodes are uniformly selected. So all the source-destination node pairs have the same traffic load in Erlangs, $\rho = \lambda/\mu$. The number of wavelengths, W, is the same on all fiber links. In the tests, we use $W = \{32, 48, 64\}$. For the FSR routing, the connection is blocked if the chosen shortest path cannot accommodate it. For the FAR routing, one more edge-

disjoint candidate route is added so that the blocking events on the two routes can be considered to be independent. If the connection fails on the primary path, it re-attempts on the alternative path. Wavelengths are assigned to a session randomly from the set of free wavelengths on the associated path.

For each topology, we compare the performance of the FSR algorithm under the full wavelength conversion environment with and without the presence of the conversion cascading constraint. We also present simulation results for the FAR algorithm on the 20-node ring network and the U.S. Long-Haul network. Finally, the case of sparse deployment of wavelength conversion is tested on the U.S. Long-Haul topology using FAR.

We use the notation c_j to represent a constraint when the maximum allowed number of wavelength conversions in the lightpath of a connection is j. If constraint c_j is in effect, then any path that requires $j+1$ or more wavelength conversions is not acceptable. Another notation *nc*, no constraint, indicates that the cascading constraint is ignored.

2.5.1 U.S. Long-Haul Network

Figures 2.3a and 2.3b depict the blocking performance of the fixed shortest-path routing algorithm for the U.S. Long-Haul network with full wavelength conversion at $W = 32$ and $W = 48$, respectively. U.S. Long-Haul has 28 nodes, 45 links and its longest shortest-path between source and

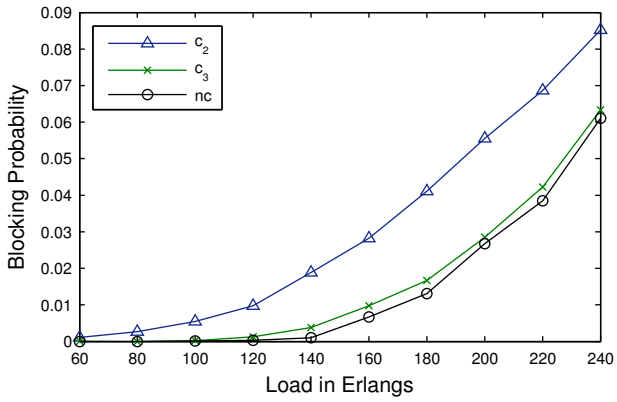

(a) $W = 32$

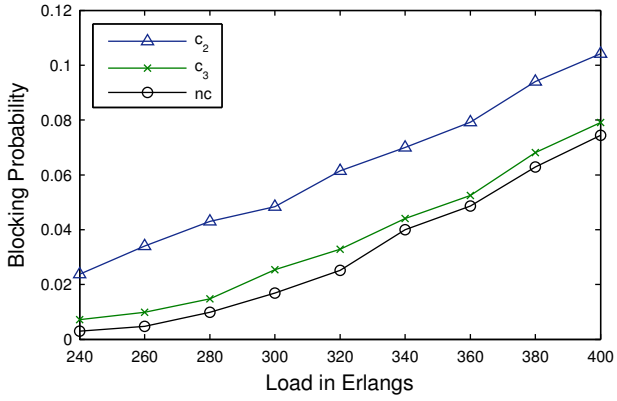

(b) $W = 48$

Figure 2.3: U.S. Long-Haul Network, FSR, Full Wavelength Conversion.

destination has six intermediate OXC's. Therefore no connection needs more than six wavelength conversions to reach its destination. However, most source-destination pairs in the U.S. Long-Haul network have lightpaths with much less number of intermediates OXC's. We have found that the constraint c_j when $j > 3$ does not affect most connections in the Long-Haul network and thus imposes very little impact on the network blocking performance. The constraint c_3 has slightly little negative impact but both the constraint c_2 and c_1 cause noticeable performance degradation.

The two figures highlight the negative performance impact when the constraint c_2 is in effect, i.e., when the maximum allowed number of conversions in the lightpath is two. In Figure 2.3a under a load of 180 ($W = 32$) without the enforcement of the constraint, the blocking percentage is around 1.3%. When we apply the c_2 constraint, the blocking percentage is increased to 4%, which is three times worse than when the constraint is ignored. Similarly in Figure 2.3b when $W = 48$, load is equal to 300, the blocking percentage is increased from 1.7% without conversion constraints to 4.8% with the c_2 constraint. Figures 2.3a and 2.3b show that there is a persistent significant deterioration of the blocking performance of the U.S. Long-Haul network when the c_2 constraint is present.

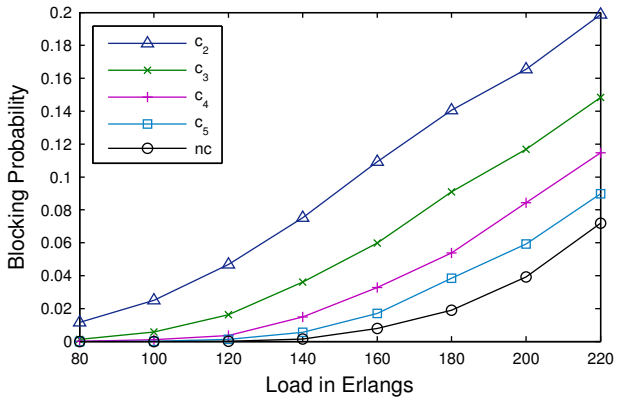

(a) Ring with 20 nodes, $W = 48$

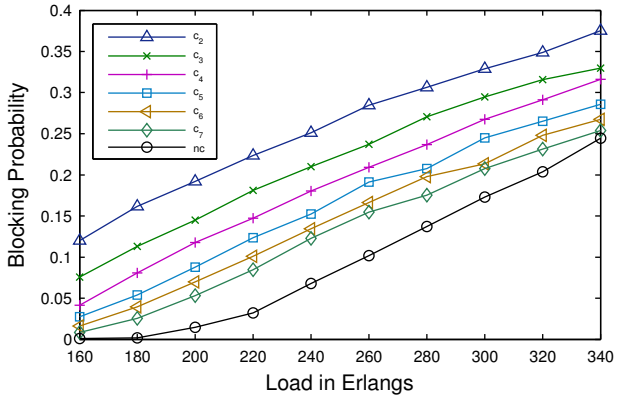

(b) Ring with 40 nodes, $W = 64$

Figure 2.4: Ring Networks, FSR, Full Wavelength Conversion.

2.5.2 20-node and 40-node Ring Topologies

The impact of the conversion cascading constraint on the sparsely connected ring topology is quite noticeable and is more apparent than on the Long-Haul and mesh topologies. Figure 2.4a compares the blocking probabilities for the 20-node ring at different loads for the constraints c_2, c_3, c_4 and c_5, while Figure 2.4b compares the blocking probabilities for the 40-node ring at different loads for the constraints $c_2 - c_7$. In all cases, the negative impact of the constraint c_j increases as the value of j decreases. The constraint c_j with a relatively high value of j has been found to cause clear deterioration on the blocking performance of the ring networks. This is attributed to the unique nature of the ring topology: every node has only two neighbors and thus a lot of wavelength conversions are needed to help establish the connection requests.

2.5.3 5 x 5 and 10 x 10 Mesh Topologies

Similar to the U.S. Long-Haul network, the 5 x 5 mesh network has a limited number of intermediate hops in any lightpath and only the constraint c_2 (and of course c_1) has a noticeable impact on the blocking performance. For the constraint c_2 in the 5 x 5 mesh, the biggest deterioration in terms of blocking probability is observed at load 800 in Figure 2.5a when it is increased from 1.6% to 2.96%. The graphs for $W = 32$ and $W = 64$ have similar trends and are thus omitted. An interesting observation in Figure 2.5a is that the two curves labelled c_2 and *nc* are interleaved when

the loads are high. This is because at high loads the connections dropped due to the constraint would leave some wavelengths free and help with the setup of the next incoming requests. This fluctuation is often observed at very high loads. The 10 x 10 mesh network has a larger diameter and consequently has a larger average number of intermediate OXC's between pairs of nodes. As demonstrated in Figure 2.5b, the constraints c_4, c_3 and c_2 all cause noticeable impact. As expected, the impact of the cascading constraint c_j becomes worse as the value of j decreases.

The simulation results so far have shown that the level of impact of the conversion cascading constraint on routing performance depends greatly on the network topology and traffic load. In conclusion, a network with a small diameter and low/moderate traffic load would typically need very few wavelength conversions and its blocking rate would not be affected much by the presence of an upper bound on the number of cascaded wavelength conversions. A network with a large diameter and heavy dynamic traffic will frequently use wavelength conversion and its blocking rate will rise when there exists a maximum threshold on the number of cascaded wavelength conversions.

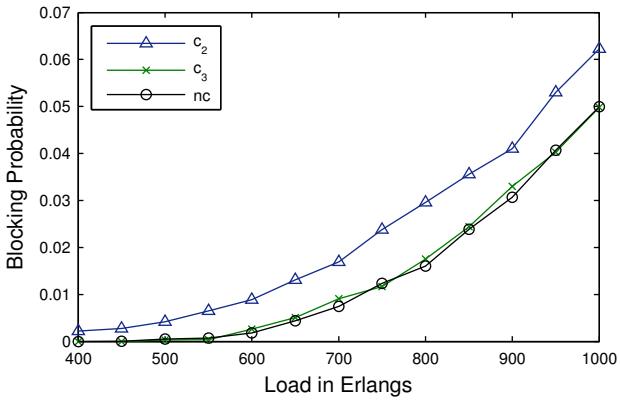

(a) Mesh-torus (5 x 5), $W = 48$

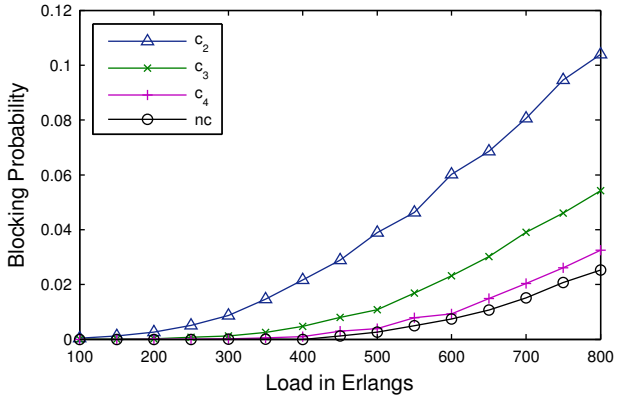

(b) Mesh-torus (10 x 10), $W = 32$

Figure 2.5: Mesh-torus Networks, FSR, Full Wavelength Conversion.

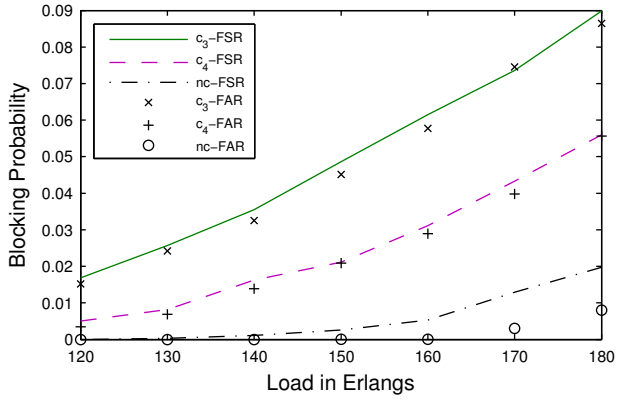

Figure 2.6: Ring with 20 nodes, $W = 48$, FSR and FAR, Full Wavelength Conversion.

2.5.4 FAR algorithm and Sparse Wavelength Conversion

To better investigate the impact of wavelength conversion cascading on blocking performance of optical routing algorithms, we conduct simulation tests using the fixed-alternative shortest-path routing (FAR) algorithm that provides a primary path and an alternative path.

The performances of the FSR and FAR algorithms on the 20-node Ring network in the environment of full deployment of wavelength conversion are compared in Figure 2.6. When there is no conversion cascading constraint, FAR performs better than FSR with respect to the blocking probability which is expected. However when the conversion cascading constraint is in effect, there is almost no difference between FSR and FAR even for c_3 and c_4. The reason is that the usually much longer alternative path in the ring network cannot generally provide less number of conversions than the shorter primary path and thus blocking would still often occur on the alternative path.

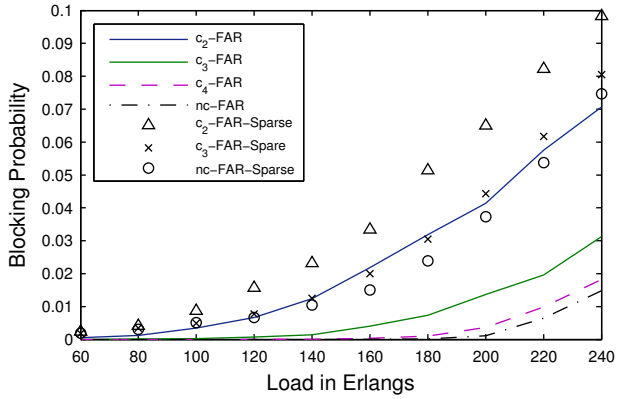

Figure 2.7: U.S. Long-Haul, $W = 32$, FAR, Full and Sparse Wavelength Conversion.

Figure 2.7 plots the performance comparison for the U.S. Long-Haul network under the two different environments: sparse deployment of wavelength conversion and full deployment of wavelength conversion. The FAR algorithm is used in both cases. Sparse wavelength converters are allocated according to the k-MDS ($k = 1$) converter placement algorithm [HBL03]; more specifically, the optical nodes in the set $\{1,3,4,5,8,10,12,15,17,20,22,25,27\}$ in Figure 2.2 are equipped with full-range wavelength converters (FWC). In the environment of full deployment of wavelength conversion (i.e., there are converters in every node), the blocking performance deteriorates significantly for c_2 (curves labeled *c_2-FAR* versus *nc-FAR*) for the similar reason happening on the 20-node Ring, which was explained in the previous paragraph. When every node is equipped with converters, the blocking performance for c_4 is very close to *nc* (curves labeled *c_4-FAR* versus *nc-FAR*). As expected, FAR performs worse for the same constraint with sparse deployment of wavelength conversion than with full deployment. For sparse deployment, FAR almost has the same performance for c_3 and *nc* (markers labeled *c_3-FAR-Sparse* versus *nc-FAR-Sparse*). But the

difference between c_2 and *nc* in sparse deployment is noticeable (markers labeled c_2-*FAR-Sparse* versus *nc-FAR-Sparse*). This indicates clearly that the impact of the cascading constraint cannot be ignored even if only sparse deployment of wavelength conversion is used.

2.6 Summary

In this chapter, we have evaluated the impact of the conversion cascading constraint on the performance of static optical routing algorithms in OCS networks. The simulation tests used popular optical network topologies, including U.S. Long-Haul, mesh-torus, and ring. The results show that the negative impact of cascaded conversions can be substantial and should not be ignored. In next chapter, we extend the tests to other network topologies and dynamic routing. To solve the problem, adaptive constraint-aware routing algorithms are proposed, and extensive associated empirical results are also presented.

CHAPTER 3

CONSTRAINT-AWARE ADAPTIVE ROUTING

Our study in this chapter is mainly motivated by the observation that the conversion cascading constraint may have noticeable or even significant negative impact on the conventional dynamic routing algorithms in optical environments with full and sparse wavelength conversion, similar as what we have discovered on the static all-optical routing algorithms in last chapter [GBL06]. While the dynamic routing algorithms in [YAK03, ZBL05, LS99] have shown that they could obtain good network-wide blocking performance by selecting a path with the maximum available wavelengths in a wavelength-routed all-optical network without wavelength converters, we find that they do not perform well when being simply extended for the environment of wavelength conversion. Moreover they can be significantly impacted by the conversion cascading constraint especially under the environment of full wavelength conversion. We propose two dynamic RWA algorithms to take the wavelength conversion and/or the conversion cascading constraint into account. The two algorithms named Greedy Constraint-aware Routing (GCAR) and Weighted Adaptive Constraint-aware Routing (W-ACAR) perform source routing using both link connectivity and the global state information of each wavelength. They also consider the wavelength conversion capability of OXC's and additionally recognize the limitation of the conversions cascading constraint. We carry

out extensive performance studies of the proposed dynamic algorithms over a variety of topologies including the U.S. Long-Haul topology, ring topology and mesh-torus topology. The results conclusively demonstrate that the two constraint-aware GCAR and W-ACAR algorithms especially the latter one can achieve much better performance than fixed shortest-path routing, fixed-alternative routing and conventional dynamic routing algorithms, in the environment of full or/and sparse wavelength conversion.

3.1 Overview of Optical Adaptive Routing

In static routing, the routes are usually pre-computed without considering the current network state; while in dynamic (adaptive) routing, the route selection is based on the current network state. The two well-known algorithms - least-loaded routing (LLR) [KA98] and least-congested-path (LCP) [CY94] routing were proposed. The major advantage of adaptive routing is that it often results in higher resource utilization and lower connection blocking than static routing. Adaptive routing combined with full-wavelength converters in each optical node usually offers very low blocking probability. In this sense, the conversion cascading constraint might not have noticeable impact on adaptive routing. However, it has been shown that the average hop counts of connections set up with dynamic routing are much higher than FSR and FAR [YAK03]. To further improve the blocking performance and reduce the path lengths as well, Chu et al. [CLZ03] proposed a dynamic RWA algorithm called weighted least-congestion routing and first-fit wavelength

assignment (WLCR-FF) in a wavelength-routed all-optical network with wavelength converters. Given appropriate weights to wavelength conversion, shorter path length and better blocking probability can be achieved. But, as the other proposed algorithms, WLCR-FF ignored the negative impact of the conversion cascading constraint. While converters get more involved, the negative impact caused by the conversion cascading constraint may be noticeable. Furthermore, in certain cases, e.g., in ring networks with full wavelength conversion, the LLR algorithm actually resulted in worse performance compared to that of the static fixed-alternative routing algorithm [CLZ03], where the wavelength conversion cascading constraint may also impose their probably most significant impact.

Based on the principle of least-congested-path routing [CY94], a variety of dynamic routing algorithms have been proposed to select the lightpaths with the maximum idle wavelengths which proved to achieve good blocking performance, as well as good link utilization (load balancing). The authors in [LS99] proposed dynamic routing using congestion and neighborhood information which searches only the neighborhood including the links up to distance k on the pre-computed paths and then determines the maximum idle wavelengths. Zhou et al. [ZBL05] showed the efficiency and effectiveness of logical link representation and bitwise computation in single-fiber and multiple-fiber optical networks by adopting a modified Dijkstra algorithm that chooses the lightpaths with the maximum free wavelengths dynamically. Yoo et al. [YAK03] further presented four adaptive routing algorithms that favor paths with near-maximum number of available wavelengths between two nodes and concluded NAW (near-maximum available wavelength) was the

best routing algorithm. However, when the least-congested-path based routing is simply extended to incorporate the wavelength converter deployment, it may not perform well as desired and more importantly it may be significantly impacted by the conversion cascading constraint since the available wavelengths likely get fragmented (explained in Section 3.2 in more depth). Therefore, we need to take the impact of the conversion cascading constraint into account and thus propose the two constraint-aware dynamic algorithms GCAR and W-ACAR in the following section.

3.2 Adaptive Constraint-Aware Routing and Wavelength Assignment

The proposed set of algorithms requires the support of Open Shortest Path First (OSPF) extensions that provide information on wavelengths being used at each link of the entire network. Using this information, source routing is performed to search for a route with the near-minimum number of wavelength conversions at the arrival time of a connection request, in a similar fashion to the Dijkstra shortest path algorithm. We first demonstrate an extension of NAW [YAK03] called Near-maximum Available Wavelength Routing with Wavelength Conversion (NAW-WC) by incorporating wavelength converter deployment, and then propose two adaptive algorithms based on this extension, which additionally consider the impact of the conversion cascading constraint under the environment of full and sparse wavelength conversion. As aforementioned, they are called Greedy Constraint-aware Routing (GCAR) and Weighted Adaptive Constraint-aware Routing (W-ACAR).

3.2.1 Near-maximum Available Wavelength Routing with Wavelength Conversion

Extending the NAW algorithm proposed in [YAK03] for routing in circuit-switched networks, we consider both full and sparse placement of FWC's in the network. The resulting algorithm searches for a route that has the largest number of free wavelengths with the required wavelength conversions subject to an upper limit of the conversion cascading constraint. If there is a tie, the algorithm selects the route having the smallest hop count. We investigate the negative impact of the conversion cascading constraint on NAW-WC through the following method: when the searched route needs more wavelength conversions than the upper bound of the cascading constraint, the connection request will be discarded.

The pseudo-code given in Figure 3.1 describes the NAW-WC algorithm as it finds a route with the near-maximum number of free wavelengths between two nodes subject to the conversion cascading constraint. We use the notations and data structures similar to the ones used in [ZBL05]. The operator "$\cap$" denotes the logical intersection (bitwise *AND*) operation and the operator "$\bullet$" denotes string concatenation. NAW-WC accepts three inputs: source node S, destination node D, and the array *LinkState* that records the free wavelengths on each link. The algorithm returns the selected path from S to D, the length of this path, the number of wavelength conversions required to fulfill the connection request and the largest free wavelengths that can be used in this path. The data structures used by the algorithm are as follows. For each node v, we use the following notations:

- *Route*$[v]$: a string that stores the route selected so far from source S to node v.
- *HopCount*$[v]$: the length (i.e., number of hops) of *Route*$[v]$.
- *Nconversions*$[v]$: the number of wavelength conversions required by *Route*$[v]$.
- *Avail*$[v]$: the mask bit array representing the free wavelengths that can be used in *Route*$[v]$.

As we mentioned at the beginning of this section, up-to-date information on wavelengths being used at each link of the entire network is required to support the NAW-WC routing algorithm. The array *LinkState* records the free wavelengths available on each link. We assume each link to be a bidirectional fiber and also assume that all links in the network have the same W wavelengths. The variable *LinkState*$[C,v]$ is used to keep track of the free channels on the link connecting the two nodes from C to v. The kth bit in this variable is set to one if the kth wavelength is free and is set to zero if this wavelength is used. The function $NF(X)$ is used to calculate the number of free wavelengths along the path. For instance, $NF($*Avail*$[v])$ returns the number of 1-valued bits stored in *Avail*$[v]$, which is the number of free wavelengths that can be used in *Route*$[v]$.

In Step One, the algorithm does the initialization work by setting the initial values of the data structures for the source node. It also marks all the optical nodes except the source node as unvisited. In Step Two, it tries to find the next better node(s) that has the larger number of free wavelengths from all or some of the neighbor nodes directly connected to the current node, depending on whether they have been selected before or not. Two situations are considered here: 1)

Near-Maximum Available Wavelength Routing with Wavelength Conversion (NAW-WC)

Input parameters: S, D, array LinkState

Step 1: */* Initialization */*
Set current node C = S;
Avail[C] = $2^n - 1$ */* All n bits of Avail[C] have a value 1, i.e. all n wavelengths are free */*
Route[C] = "S"; HopCount[C] = 0; Nconversions[C] = 0;
Insert all nodes of the graph except node S into the set L;
Mark all members of L as unvisited;

Step 2: */* Update the values computed for every neighbor of C */*
for every neighbor of current node C, say v, which is a member of L
do
    if (v is unvisited) { */* First time to reach v */*
        Mark v as visited;
        Route[v] = Route[C] ● "v";
        HopCount[v] = HopCount[C] + 1; Nconversions[v] = Nconversions[C];
        Avail[v] = Avail[C] ∩ LinkState[C, v];
        if (Avail[v] == 0 AND LinkState[C, v] ≠ 0 AND (Node C has FWC)) {
            / Conversion is needed to reach v from C */*
            Nconversions[v] = Nconversions[C] + 1;
            Avail[v] = LinkState[C, v];
        }
    } else { */* v has been visited before */*
        TempAvail = Avail[C] ∩ LinkState[C, v];
        TempHopCount = HopCount[C] + 1; TempNconv = Nconversions[C];
        if (TempAvail == 0 AND LinkState[C, v] ≠ 0 AND (Node C has FWC)) {
            / Conversion is needed to reach v from C */*
            TempNconv = Nconversions[C] + 1;
            TempAvail = LinkState[C, v];
        }
        / Check if this is a better path to reach node v */*
        *// **CHECK_START***
        if ((TempAvail > NF(Avail[v])) OR
            (NF(TempAvail) == NF(Avail[v]) AND TempHopCount < HopCount[v])) {
            / Better path to node v has been found via node C */*
            Route[v] = Route[C] ● "v"; Nconversions[v] = TempNconv;
            HopCount[v] = TempHopCount; Avail[v] = TempAvail;
        }
        *// **CHECK_END***
    }
done

Step 3: */* Find next current node */*
if (L is not empty) {
    Select a node v from L having the largest value of NF(Avail[v]);
    If there is a tie, select the node v having the smallest value of HopCount[v];
    Remove v from L; set C = v; go to step 2;
}

Step 4: */* Return success or failure */*
if ((Avail[D] == 0) OR (Nconversions[D] > ConversionBound) {
    Failure: the NAW-WC algorithm failed to find a valid path from S to D;
} else {
    Success: return (Route[D], HopCount[D], Nconversions[D], Avail[D]);
}

Figure 3.1: Algorithm NAW-WC.

if the neighbor node is unvisited so far, only its associated data structures need to be updated based on the path $Route[C]$ found by the current node; 2) if the neighbor node has been visited, comparison on the number of free wavelengths owned by the original path and the new projected path is needed in order to distribute the load to less congested links. If the new projected path proves to be better because of either larger free wavelengths or fewer hop counts, then it is picked and the associated variables are updated accordingly. In Step Three, the node having the largest number of free wavelengths from all eligible nodes in the set L is chosen and a shorter path breaks a tie. The algorithm repeats Step Two until all the nodes have been selected. In Step Four, the algorithm returns the resulting route to the destination node if the total number of conversions required does not exceed the upper bound, otherwise failure is returned.

The major disadvantage of NAW-WC is that it does not take the conversion cascading constraint into consideration during the searching process for an admittable route. In Step Two, when a conversion is required to reach v from C, $Avail[v]$ or $TempAvail$ is defined to be equal to $LinkState[C,v]$ instead of the intersection set of $LinkState[C,v]$ and $Avail[v]$ like when no wavelength converter is used. In this way, the path with the conversion has a higher probability of being picked in Step Three because of its probably larger set of available wavelengths. The preference of conversion may lead to longer average hop lengths of established connections and significant impact when the cascading constraint is applied, which would eventually result in worse blocking performance.

3.2.2 Greedy Constraint-Aware Routing Algorithm

By recognizing the drawbacks of the NAW-WC routing algorithm, we improve the checking process for a better path to an already visited node in Step Two by looking for less number of conversions before comparing the free wavelengths. Figure 3.2 depicts this important change based on the relevant block of pseudo code of NAW-WC (corresponding to the pseudo code between the two labels *CHECK_START* and *CHECK_END* in Figure 3.1) for the GCAR algorithm. The new algorithm is called Greedy Constraint-Aware Routing algorithm as it continuously searches for the routes with the least wavelength conversions greedily. Step Three is also modified to comply with the new algorithm as follows: the next current node will be chosen based on a series of parameters in order of the smallest $Nconversions[v]$, the largest $NF(Avail[v])$ and lastly the smallest $HopCount[v]$. In fact, all the lightpaths set up by the GCAR algorithm use the minimum number of wavelength conversions as possible based on the current network state information according to the principle of Dijkstra's algorithm.

Since the GCAR algorithm is aware of the conversion cascading constraint and thus fewer connections will be discarded due to the constraint, it should not be surprising to conclude that it would perform better than NAW-WC when the constraint is enforced. GCAR still has certain advantage over NAW-WC even if no cascading constraint exist because GCAR assigns higher priority to the $Nconversions[v]$ in Step Three when selecting the next node to be traversed, which eventually leads to overall shorter average hop lengths of the established connections. This can

```
/* Check if this is a better path to reach node v */
// CHECK_START
if ( (Avail[v] == 0 AND TempAvail > 0) OR
     (TempNconv < Nconversions[v] AND TempAvail > 0) OR
     (TempNconv == Nconversions[v] AND NF(TempAvail) > NF(Avail[v]) ) OR
     (TempNconv == Nconversions[v] AND NF(TempAvail) == NF(Avail[v])
        AND TempHopCount < HopCount[v]) )
           /* Better path to node v has been found via node C */
           Route[v] = Route[C] ● "v"; Nconversions[v] = TempNconv;
           HopCount[v] = TempHopCount; Avail[v] = TempAvail;
}
// CHECK_END
```

Figure 3.2: Pseudo code regarding better path checking (GCAR).

be explained through a simplified example depicted in Figure 3.3 that shows a subset of an entire optical network where a connection request having node 9 as its destination comes to node 5. The symbol *AND* represents the number of available wavelengths as computed by the logical-*AND* of the two wavelength sets on the current link and the uplink; and *NUW* is the number of unreserved wavelengths on each edge. The two dotted edges (7, 8) and (6, 10) indicate a wavelength conversion would be required if a connection flow from the former node to the latter one. If a wavelength conversion occurs, the common free wavelengths between the two involved nodes will be updated to use those available on the relevant downlink according to the algorithm (implying *AND* is equal to *NUW*), which usually embraces a higher probability of having a larger value than what is gotten through several successive logical-*AND*s. Both NAW-WC and GCAR will choose node 7 first and then node 8. However, NAW-WC will then select nodes 6, 10 and finally node 9 because larger free wavelengths are available on this partial path. Nevertheless, GCAR will choose node 9 directly for fewer number of wavelength conversions despite larger

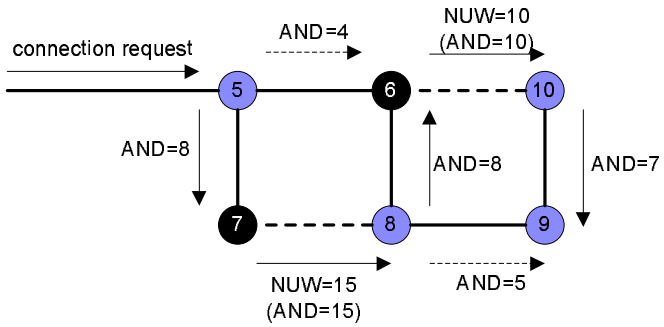

Figure 3.3: GCAR uses fewer hops than NAW-WC under certain scenario without enforcing the conversion cascading constraint.

available wavelengths on the other route which also has more hops. In fact, assuming wavelength conversions are required in the two nodes 6 and 7, GCAR will always result in an equal or shorter path than NAW-WC as long as there is a feasible lightpath available. Although sometimes GCAR may have longer paths than NAW-WC, with overall shorter paths of successful connections and its awareness of the constraints, GCAR usually performs better than NAW-WC regarding the blocking probability.

3.2.3 Weighted Adaptive Constraint-Aware Routing Algorithm

We may draw a conclusion from the previous dynamic routing algorithm GCAR that the dominating factors of impacting the blocking performance in the networks are as follows: the number of wavelength conversions, the availability of common free wavelengths and the lengths of the paths. It may be a good idea to integrate them into a single factor using a weight function (or penalty

function):

$$Weight[v] = \frac{Avail[v]}{HopCount[v]} + \delta \times \theta(v) \tag{3.1}$$

A feasible route from the source S to the destination D with the maximum weight is then picked. In the weight function, the natural logarithm part $\theta(v)$ contributes to the negative impact of the conversion cascading constraint as follows:

$$\theta(v) = \ln\left(1 - \frac{Nconversion[v]}{ConversionBound + 1}\right) \tag{3.2}$$

The parameter δ controls the contribution of $\theta(v)$ in the weight function and with bigger values it would generally make the impact of the cascading constraint more obvious. Except to investigate the trend of the impact when varying δ, we assume $\delta = 1$ in most of our performance tests in Section 3.3 (exceptions will be clearly noted). The natural logarithm function in $\theta(v)$ has the following good properties that interpret the negative impact of the cascading constraint very well:

- $\theta(v)$ is always non-positive. When $Nconversions[v]$ equals zero, $\theta(v)$ (which is also zero) has no impact at all. When $Nconversions[v]$ increases, $\theta(v)$ becomes smaller (negative) which has a larger negative influence on the decision question whether the current route indicated by $Route[v]$ should be chosen for the node v.

- When *ConversionBound* is fixed, the non-linear logarithm degradation of $\theta(v)$ caused by the increasing of $Nconversions[v]$ matches the expected real-world situation: if $Nconversions[v]$

is small we may not care about it much because appropriate conversions can improve the blocking performance; but if $Nconversions[v]$ is becoming larger its negative impact also is becoming accumulatively noticeable and thus it should be suppressed.

- The same value of $Nconversions[v]$ has different degrees of negative impacts when *ConversionBound* varies which is also desired. For instance, it is obviously more urgent to restrain further cascading conversions when *ConversionBound* is set to two than it is set to four if the wavelength conversion already occurred once (i.e., $Nconversions[v] = 1$).

We select the weight function $Weight[v]$ mainly because of the following consideration: first, it is important to decrease resource consumption by reducing lightpath lengths, which can be achieved through FSR routing; second, routing through least congested paths (LCP) allows load sharing and thus preserves resources on critical links for future connections. Intuitively, these two techniques reduce the blocking probability. However, they run in opposite directions. In fact, since FSR routing is not aware of the network status, it cannot perform load sharing. On the other hand, LCP routing may choose longer paths in order to avoid congested links, which is resource wasteful. Finally, to prevent the number of cascading conversions required by the selected lightpaths from exceeding the upper bound, it should be controlled gradually. Thus in summary, in order to achieve a good blocking performance, the weight function should be proportional to the number of free wavelengths, and be inversely proportional to the length of the route, and decrease gradually

when the number of conversion cascading conversions approaches to the limit, which is the main reason why we select the proposed weighted function.

3.3 Numerical Results and Analysis

We have conducted extensive simulations to evaluate call blocking performance of the three algorithms: NAW-WC, GCWR and W-ACAR, and the other two static methods: the FSR and FAR algorithms, under the environment of full/sparse wavelength conversion and the impact of the conversion cascading constraint. The performance tests use a variety of network topologies including the U.S. Long-Haul network (shown in Figure 2.2), 5 x 5 mesh-torus, 10 x 10 mesh-torus, 20-node ring and 40-node ring networks. The lightpath connection requests arrive to the network according to a Poisson process with rate λ, and the connection holding time is negatively exponentially distributed with mean $1/\mu$. For each connection request, the source and destination nodes are uniformly selected. So all the source-destination node pairs have the same traffic load in Erlangs. This assumption adheres to the model of uniform traffic used in [EB06]. The number of wavelengths, W, is the same on all fiber links. For the FSR routing, the connection is blocked if the chosen shortest path cannot accommodate it. For the FAR routing, one more edge-disjoint candidate route is added so that the blocking events on the two routes can be considered to be independent. If the connection fails on the primary path, it re-attempts on the alternative path. We use hop-based routing with forward reservation in both FSR and FAR, which is different from what we adopt in

the three dynamic algorithms. Wavelengths are assigned to a session randomly from the set of free wavelengths on the associated path. All simulation results are given with 95% confidence intervals by use of the batch means method with 50 batches or more.

For each topology, we compare the performance of FSR, FAR and the three dynamic algorithms under the full/sparse wavelength conversion environment with and without the presence of the cascading constraint. We include the graphs of FSR and FAR presented in Chapter 2 here to make the comparisons complete. Since how to allocate converters in the network is not the focus of this chapter and the k-MDS converter placement algorithm [HBL03,EB03,EB06] has proved to achieve good blocking performance both empirically and theoretically, we adopt the k-MDS algorithm for our sparse deployment of wavelength converters. The simulation results for the FAR algorithm as well as the dynamic algorithms on the 40-node ring network and the 10 x 10 mesh-torus network are ignored due to the similarity.

Same as in Chapter 2, we use the notation c_j to represent a constraint when the maximum allowed number of wavelength conversions in the lightpath of a connection is j. If constraint c_j is in effect, then any path that requires $j+1$ or more wavelength conversions is not acceptable. Another notation *nc*, no constraint, indicates that the cascading constraint is ignored. These notations will not be explained again when they are used in the following chapters.

3.3.1 Blocking Performance Analysis of U.S. Long-Haul Network

Figures 3.4a-3.4f depict the blocking performance of different RWA algorithms in the U.S. Long-Haul network with full or/and sparse wavelength conversion. U.S. Long-Haul has 28 nodes, 45 links and its longest shortest-path between source and destination has six intermediate OXC's. Therefore no connection needs more than six wavelength conversions to reach its destination. However, most source-destination pairs in the U.S. Long-Haul network have lightpaths with much less number of intermediates OXC's. In Figures 3.4a and 3.4b we have found that for the primitive FSR algorithm, the conversion constraints c_j when $j > 3$ do not affect most connections in the Long-Haul network and thus have very little impact on the network blocking performance. The constraint c_3 has slightly little negative impact but both the constraint c_2 and the constraint c_1 cause noticeable performance degradation. We can also observe in Figure 3.4a that the FAR algorithm works much better than the FSR algorithm, which is expected. For FAR, the performance degradation is still significant when the constraint c_3 or c_2 is in effect. Moreover, the gap between the two curves labeled C_2-*FAR* and C_3-*FAR* is even larger than the gap between the other two curves labeled C_2-*FSR* and C_3-*FSR* at high loads. It can be explained as follows: when we provide two candidate routes for a node pair, the blocking events of these two routes can be considered to be independent; hence the blocking probability can be decreased a lot at high loads even if the c_3 or c_4 constraint exists. Nevertheless, because the alternative paths are typically longer than the primary paths, blocking would still often occur on the alternative paths when only two cascaded

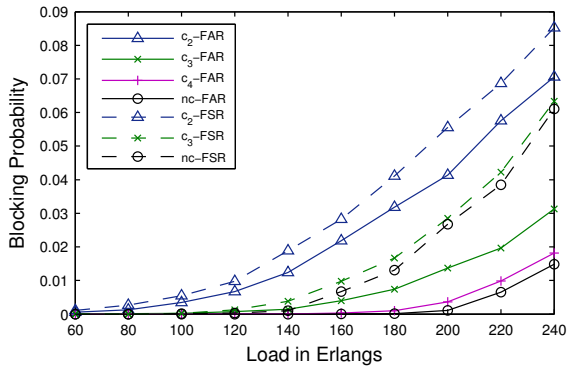

(a) FSR vs. FAR

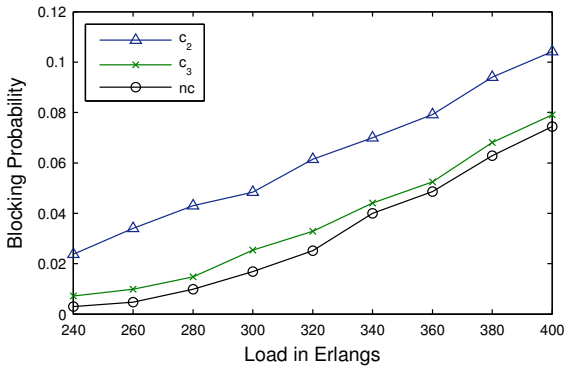

(b) FSR, $W = 48$

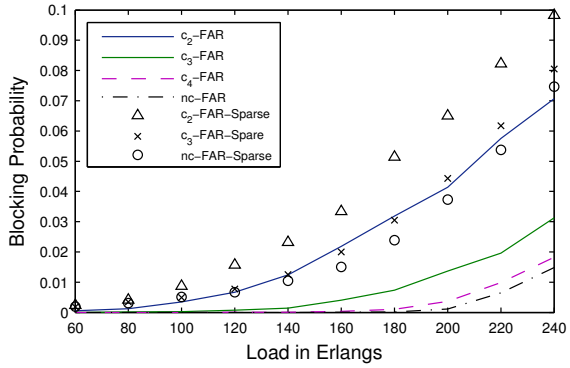

(c) FAR, Full Conversion vs. 1-MDS

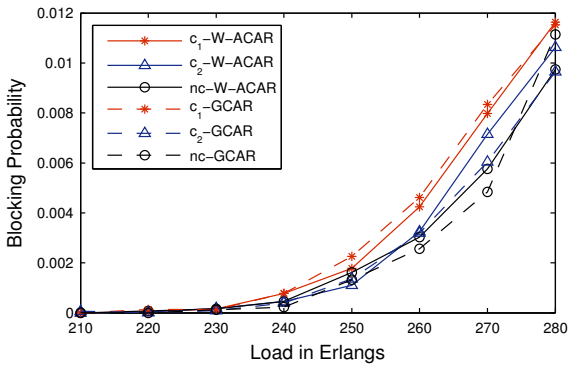

(d) W-ACAR vs. GCAR

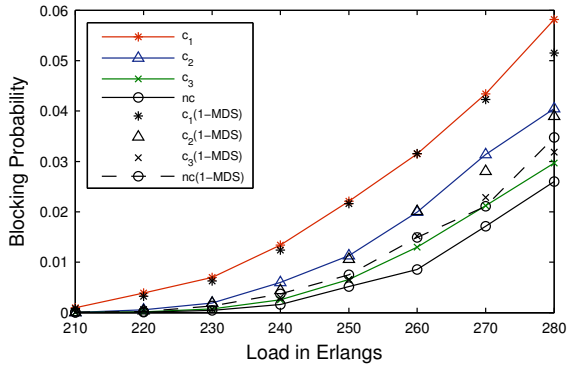

(e) NAW-WC, Full Conversion vs. 1-MDS

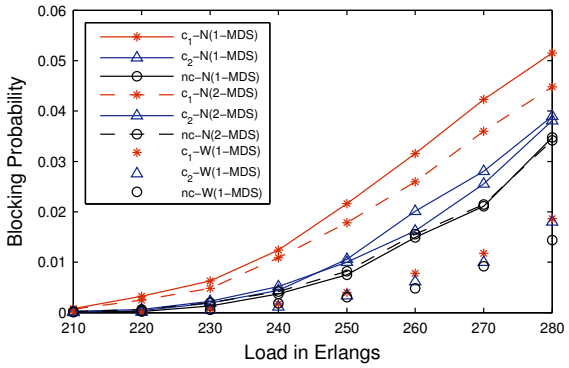

(f) W-ACAR vs. NAW-WC

Figure 3.4: Blocking probability versus traffic load in U.S. Long-Haul network. Unless specified otherwise, all graphs imply full wavelength conversion with $W = 32$. In (f), C_1-*N* stands for C_1-*NAW-WC* while C_1-*W* stands for C_1-*W-ACAR* and so on.

wavelength conversions are allowed at maximum. Thus C_2-*FAR* has a smaller improvement over C_2-*FSR* than C_3-*FAR* over C_3-*FSR* with respect to blocking performance.

Figure 3.4c plots the performance comparison for the U.S. Long-Haul network under the two different environments: full wavelength conversion and sparse wavelength conversion using 1-MDS. The FAR algorithm is used in both cases. Sparse wavelength converters are allocated according to the k-MDS ($k = 1$) converter placement algorithm; more specifically, the optical nodes in the set $\{1,3,4,5,8,10,12,15,17,20,22,25,27\}$ in Figure 2.2 are equipped with full-range wavelength converters (FWC). In the environment of full wavelength conversion, the blocking performance deteriorates significantly for c_2 for the same reason explained in the previous paragraph. When every node is equipped with converters, the blocking performance for c_4 is very close to *nc*. As expected, FAR performs worse for the same constraint with sparse conversion than with full conversion. For sparse conversion, FAR almost has the same performance for c_3 and *nc*. But the difference between c_2 and *nc* with sparse conversion is still noticeable. This indicates clearly that the impact of the cascading constraint cannot be ignored even if only sparse wavelength conversion is used.

Figures 3.4d-3.4f show that the blocking performance of the NAW-WC, GCAR and W-ACAR algorithms is a significant improvement over FSR and FAR. It is primarily because the network state is known when the requests come and more wavelengths are left free for future connections in dynamic algorithms. We can also observe that overall the GCAR and W-ACAR algorithms have similar blocking performance, while they are better than the NAW-WC algorithm that is a con-

ventional dynamic algorithm without considering the negative impact of the conversion cascading constraint in the environment of either full or sparse wavelength conversion. The performance results with sparse conversion for GCAR are omitted because they are very close to the results for W-ACAR. This indicates that this negative impact cannot be ignored even in dynamic algorithms. Furthermore, without the presence of the cascading constraint (curves labeled *nc*) GCAR and W-ACAR still perform better than NAW-WC, which we have discussed the reason when introducing these two algorithms in Section 3.2. In Figure 3.4d we can observe all the four curves representing the different conditions of the two algorithms GCAR and W-ACAR are interleaved. It is basically because they get similar average hop lengths of the established connections and similar link utilization under these conditions. We will look into this scenario in a quantitative way when discussing the ring and mesh-torus topologies in the following subsections.

Figure 3.4e compares the performance for NAW-WC with full conversion and with 1-MDS sparse conversion, while Figure 3.4f compares the performance between W-ACAR and NAW-WC both with 1-MDS or 2-MDS sparse conversion. The 2-MDS sparse conversion indicates the optical nodes in the set $\{4, 8, 12, 17, 25\}$ in Figure 2.2 are equipped with FWC's. If no constraints exist the blocking performance decreases when the U.S. Long-Haul network is switched from full conversion to 1-MDS sparse conversion, but the difference is kept small; and there is almost no degradation from 1-MDS to 2-MDS. This observation is mainly attributed to the effectiveness of the *k*-MDS algorithm and is consistent with the common conclusion obtained in many past researches [SAS96, LL93b, IM99, KA98] that sparse conversion can achieve similar blocking per-

formance as full conversion when an appropriate number of converters are allocated in the right place. However, if any cascading constraint exists, the imposed negative impact on NAW-WC is still obvious. Figure 3.4f shows W-ACAR also performs much better than NAW-WC in the environment of 1-MDS sparse conversion.

3.3.2 Performance Analysis of 20-node and 40-node Ring Topologies

The impact of the conversion cascading constraint on the sparsely connected ring topology is quite noticeable and is more apparent than on the Long-Haul and mesh topologies. Figures 3.5a-3.5c compare the blocking probabilities for the static FSR and FAR algorithms with full wavelength conversion in the 20-node ring and the 40-node ring, respectively. In all cases, the negative impact of the constraints c_j increases as the value of j decreases. The constraints c_j with relatively high value of j have been found to cause clear deterioration on the blocking performance of the ring networks. This is attributed to the unique nature of the ring topology: every node has only two neighbors and thus a lot of wavelength conversions are needed to help establish the connection requests. The more wavelength conversions are involved, the more apparent will be the impact of the conversion cascading constraint. When there is no cascading constraint, FAR performs better than FSR with respect to the blocking probability which is expected. However, when the cascading constraint is in effect, there is almost no difference between FSR and FAR even for the c_3 and c_4 constraints (Figure 3.5c). The reason is that for most node pairs in a ring topology, one route is

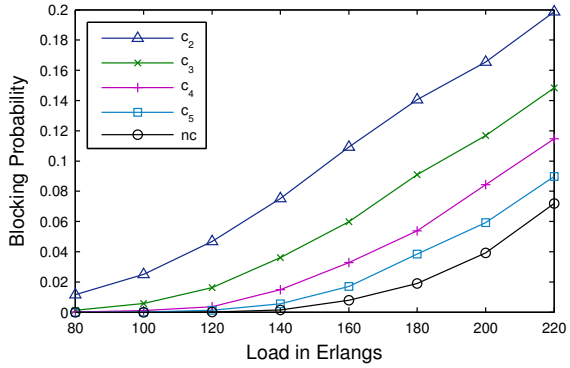

(a) FSR

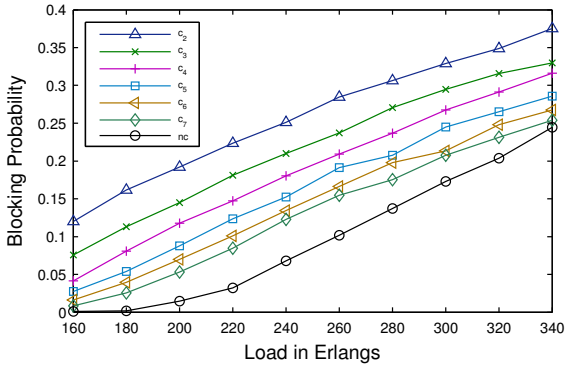

(b) 40-node Ring, FSR, $W = 64$

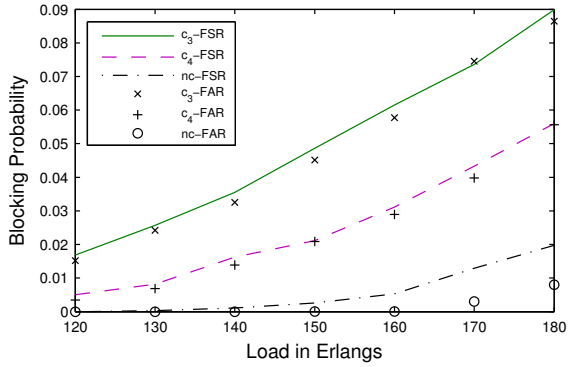

(c) FSR vs. FAR

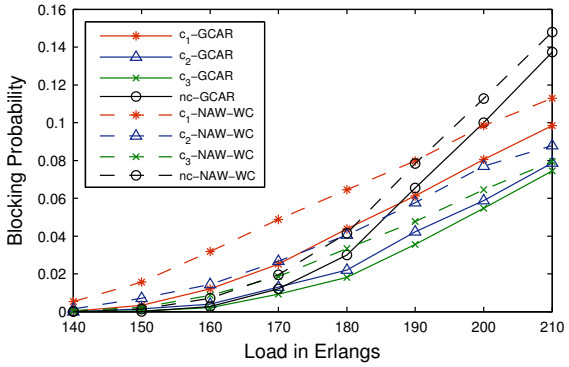

(d) NAW-WC vs. GCAR

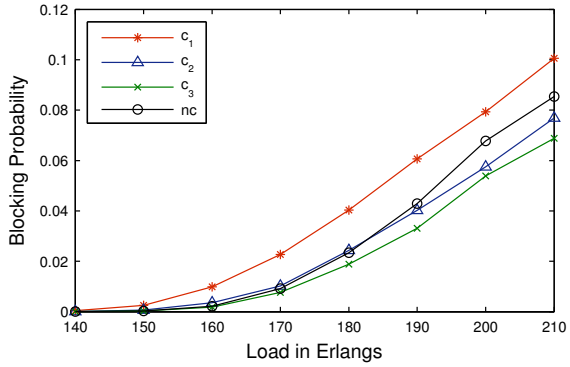

(e) W-ACAR

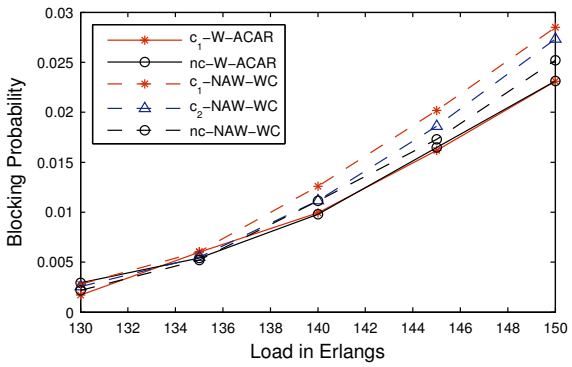

(f) W-ACAR vs. NAW-WC, 1-MDS

Figure 3.5: Blocking probability versus traffic load in ring networks (unless specified otherwise, all graphs imply 20-node ring and full wavelength conversion with $W = 48$).

very short and another route is very long. Due to this nature, a connection request using FAR is very likely to get rejected on the much longer alternative route when it cannot go through the shorter primary route due to the restriction of the conversion cascading constraint.

As expected, the NAW-WC, GCAR and W-ACAR algorithms perform much better than FSR and FAR. Figure 3.5d and Figure 3.5e show the GCAR algorithm is slightly better than the NAW-WC algorithm and W-ACAR is the best. Although GCAR is constraint-aware, it has the same very few choices as NAW-WC when selecting the routes for the connection requests in the ring networks, and thus it has only minor advantages over NAW-WC. On the other side, by considering the path length and the conversion cascading constraint jointly, the W-ACAR algorithm gains better performance. It is also important to observe that at high loads, the blocking probability is higher for all the dynamic algorithms when there is no cascading constraint than when c_j ($j = 2$ or 3) is in effect. We call it high load abnormality because it is typically observed when loads are very high. Many factors contribute to this abnormality, e.g., network topology, network connectivity, traffic load and RWA algorithms. In the ring networks, it is mainly because if no cascading constraint exists many connections with long routes can be easily set up by dynamic algorithms with the sacrifice of many more potential connection requests having shorter routes which results in poorer blocking performance. We observe in Figure 3.5e this high load abnormality is alleviated in the W-ACAR algorithm because it suppresses a lot of long-route connections.

Figure 3.5f demonstrates the performance comparison between W-ACAR and NAW-WC in the environment of 1-MDS sparse conversion where each other node in the 20-node Ring is placed a

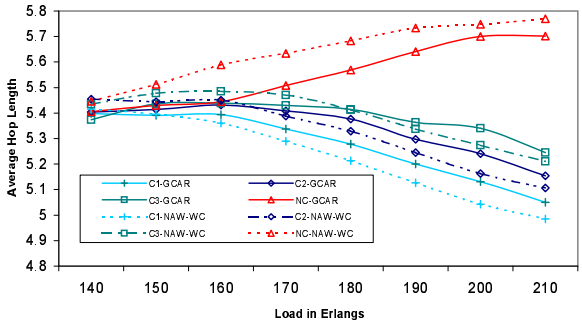

(a) Average hop length, NAW-WC vs. GCAR

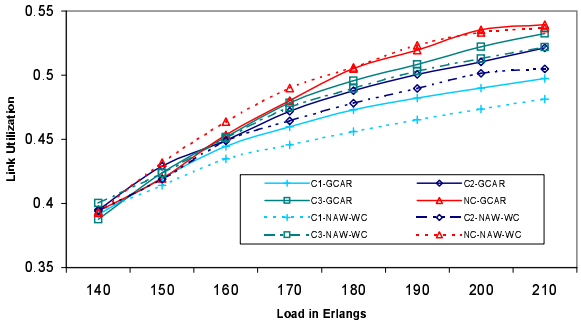

(b) Link utilization, NAW-WC vs. GCAR

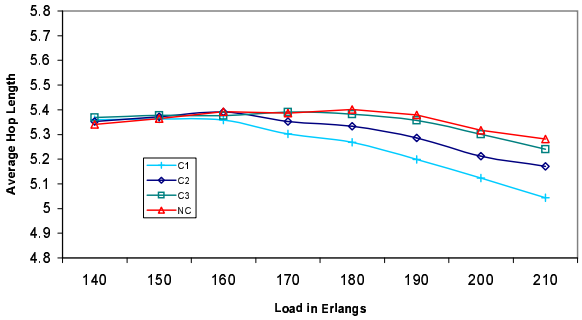

(c) Average hop length, W-ACAR

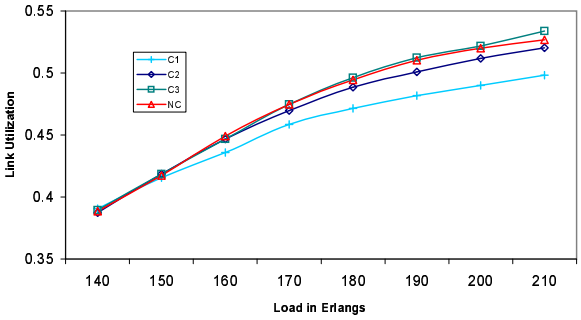

(d) Link utilization, W-ACAR

Figure 3.6: Average hop length (link utilization) versus traffic load in 20-node ring network, full wavelength conversion, $W = 48$.

FWC. The performance result of GCAR is very close to that of NAW-WC in this environment and is thus omitted. We can observe that there is still noticeable performance degradation for NAW-WC when c_2/c_1 is applied, but W-ACAR has almost the same better performance for c_1 and nc. This is also determined by the unique ring topology as we have discussed earlier.

To better understand the performance of the three dynamic algorithms, we plot the link utilization of the entire network and average hop length of all successful connections with full wavelength conversion in Figures 3.6a-3.6d. Figure 3.6a shows for NAW-WC and GCAR when there is no ef-

fective cascading constraint and when the load gets higher, both routing algorithms would have to search more links for admittable routes to accommodate new connection requests, as the nearby links were already congested by the existing connections. This has resulted in the continuously growing average hop lengths until a saturation point at around the load equal to 200 Erlangs. However, the more links a route has to traverse, the more wavelength conversions it requires. Therefore, when the c_2 and c_3 constraints are in effect, the long paths requiring over-the-limit wavelength conversions could not be fulfilled. It turns out the hop numbers of the dropped connection requests due to the cascading constraint are typically more than twice of the average hop length, which causes the average hop length to drop when the load gets higher. Usually, when the entire network is loaded appropriately higher average hop lengths mean higher resource consumption and thus higher blocking probabilities. We conclude that the large gap among the average hop lengths corresponding to the no constraint conditions and the c_2/c_3 constraint conditions showed in Figure 3.6a determines the high load abnormalities occurred in Figure 3.5d as well in Figure 3.5e.

3.3.3 Blocking Performance Analysis of 5 x 5 and 10 x 10 Mesh Topologies

Similar to the U.S. Long-Haul network, the 5 x 5 mesh network has a limited number of intermediate hops in any lightpath and only the constraint c_2 (and of course c_1) has a noticeable impact on the blocking performance for the FSR and FAR algorithms (Figure 3.7a). The FAR algorithm has much higher blocking probabilities with the c_2 constraint enforced than with the c_3 constraint. The

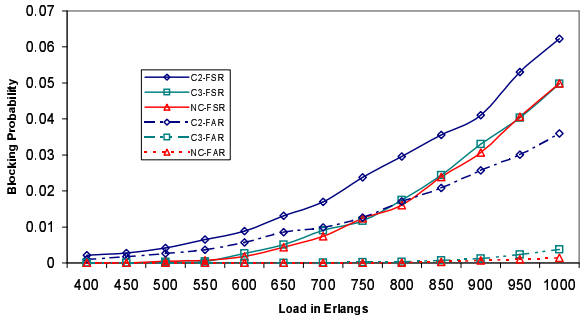

(a) FSR vs. FAR, $W = 48$

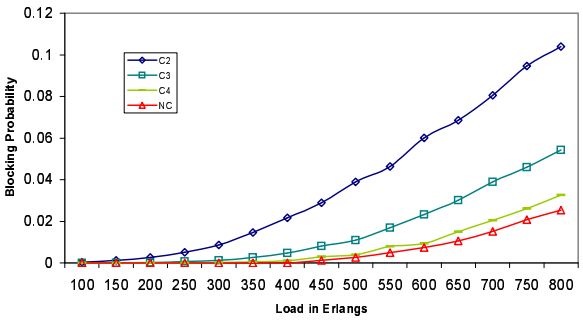

(b) 10 x 10 mesh-torus, FSR, $W = 32$

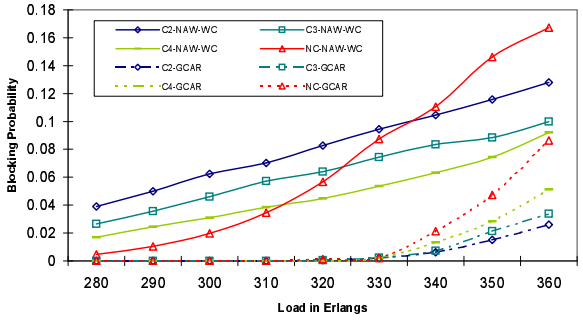

(c) NAW-WC vs. GCAR

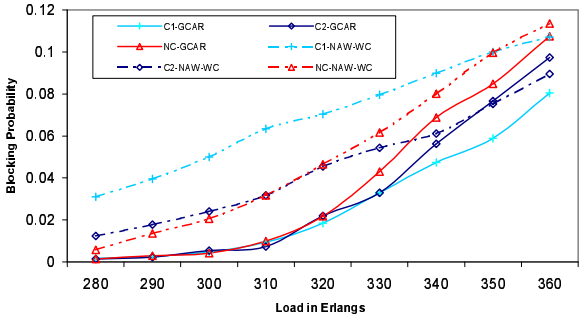

(d) NAW-WC vs. GCAR, 1-MDS

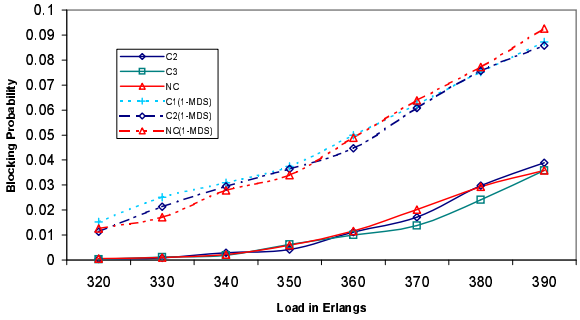

(e) W-ACAR, Full Conversion vs. 1-MDS

Figure 3.7: Blocking probability versus traffic load in mesh-torus networks (unless specified otherwise, all graphs imply 5 x 5 mesh-torus and full wavelength conversion with $W = 16$).

reason is similar to our analysis on FAR that we conducted in the U.S. Long-Haul network except that the 5 x 5 mesh is denser and smaller. Another interesting observation in Figure 3.7a is that the two curves labeled C_3-*FSR* and *nc*-*FSR* are interleaved when the loads are high. This fluctuation is also an alleviated phenomenon of high load abnormality due to the high density of mesh-torus. The 10 x 10 mesh network has a larger diameter and consequently has a larger average number of intermediate OXC's between pairs of nodes. As demonstrated in Figure 3.7b, the constraints c_4, c_3 and c_2 all cause noticeable impact. As expected, the impact of the conversion cascading constraint c_j becomes worse as the value of j decreases.

Figure 3.7c and Figure 3.7e depict the simulation results on the 5 x 5 mesh network of the three dynamic algorithms W-ACAR, GCAR and NAW-WC (in order of blocking performance) in the environment of both full and sparse wavelength conversion. The 1-MDS algorithm chooses to allocate FWC's to the optical nodes in the set {(0,4), (2,4), (1,3), (3,3), (0,2), (2,2), (4,2), (1,1), (3,1), (2,0), (4,0)} in 5 x 5 Mesh-torus. The link utilization of the entire network and average hop lengths of all successful connections with full wavelength conversion are demonstrated in Figures 3.8a - 3.8d. Figure 3.8c shows that the W-ACAR algorithm almost has the same average hop lengths when no constraint exists or c_j (j = 2, 3) is in effect across different loads. Simultaneously, its link utilization increases gradually as the load increases but the differences between different c_j and no constraint keep very small. These can explain well why the blocking performances are so close for c_j and *nc* in Figure 3.7e. On the other hand, we can observe in Figure 3.8a that the NAW-WC algorithm has the largest average hop length with *nc* but smaller values at the same loads under the

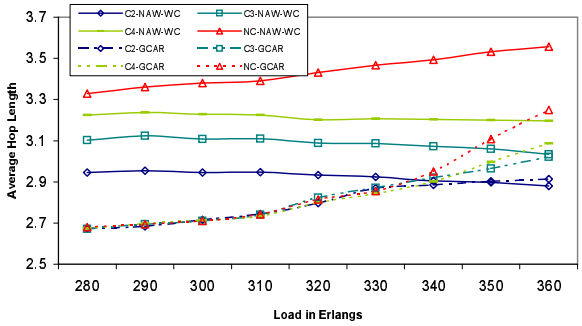

(a) Average hop length, NAW-WC vs. GCAR

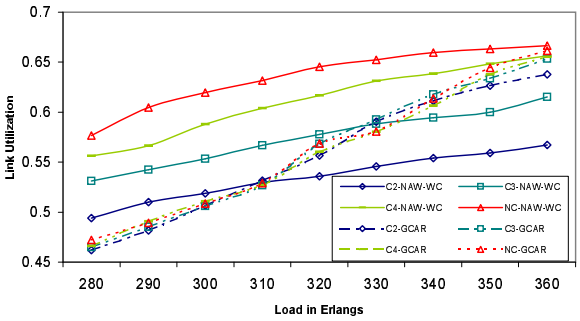

(b) Link utilization, NAW-WC vs. GCAR

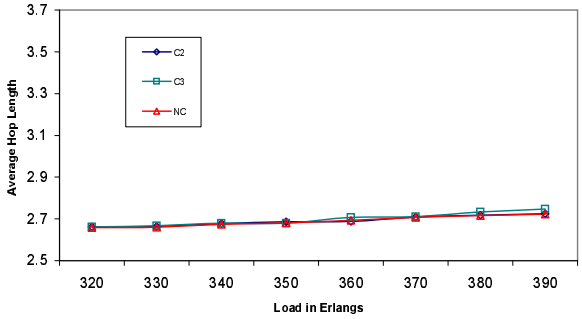

(c) Average hop length, W-ACAR

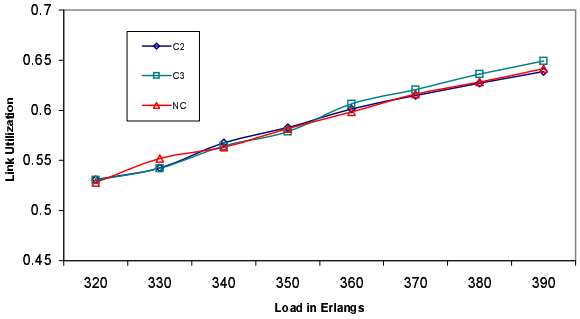

(d) Link utilization, W-ACAR

Figure 3.8: Average hop length (link utilization) versus traffic load in 5 x 5 mesh-torus network, full wavelength conversion, $W = 48$.

impact of the cascading constraint c_j as j decreases. However, it has obviously lower link utilization with c_j as j decreases and the highest link utilization with *nc* (Figure 3.8b). When the loads are less than 310 Erlangs, the connections having longer hops are compensated through higher link utilization and the system keeps balanced which contributes to the steady performance degradation with c_j as j decreases. When the traffic loads exceed 310 Erlangs, the *nc* case in the NAW-WC algorithm begins to have steadily growing average hop lengths but it does not have the same fast increase on the link utilization. This breaks the system balance and thus its blocking performance degrades faster than with c_j ($j = 2,3,4$). Actually this can be used to explain quantitatively the blocking performance of the GCAR algorithm as well.

As showed in Figure 3.7d with 1-MDS sparse conversion (less than 50% nodes have converters), the NAW-WC also has similar trend as the full conversion condition regarding the negative impact imposed by the cascading constraint and c_1 still causes a large performance degradation. In Figure 3.7e, W-ACAR has significant performance deterioration with 1-MDS sparse conversion compared to full conversion but the negative impact of cascading constraint is very small.

The simulation results so far have shown that the level of impact of the conversion cascading constraint on routing performance depends greatly on the network topology and traffic load. In conclusion, a network with a small diameter and low/moderate traffic load would typically need very little wavelength conversion and its blocking rate would not be affected much by the presence of an upper bound on the number of cascaded wavelength conversions. A network with a large diameter and high dynamic traffic patterns will frequently use wavelength conversion and its

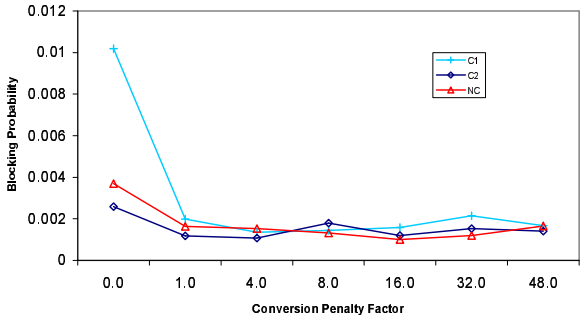

(a) U.S. Long-Haul, *Load = 250*, *W = 32*

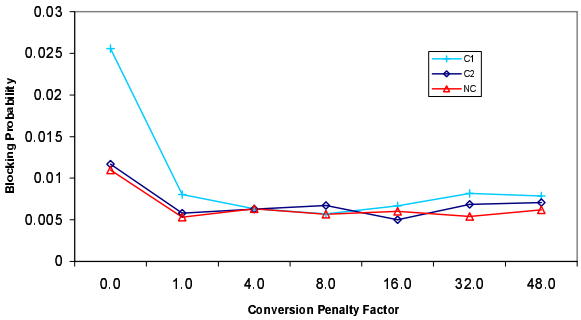

(b) U.S. Long-Haul, *Load = 270*, *W = 32*

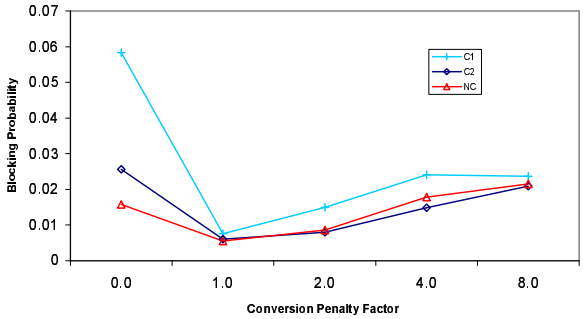

(c) 5 x 5 Mesh-torus, *Load = 350*, *W = 16*

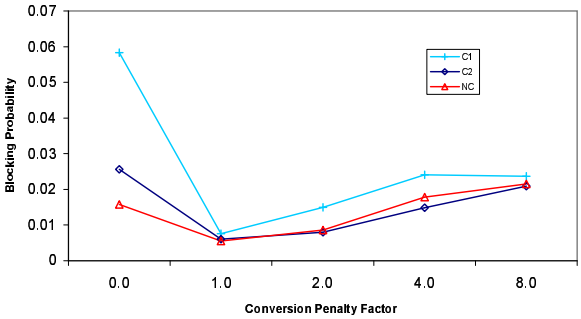

(d) 5 x 5 Mesh-torus, *Load = 370*, *W = 16*

Figure 3.9: Blocking probability versus conversion penalty factor, full wavelength conversion.

blocking rate will rise when there exists a maximum threshold on the number of cascaded wavelength conversion.

3.3.4 Performance Trend Analysis of W-ACAR by Varying Conversion Penalty Factors

To investigate how the performance of W-ACAR fluctuates when varying the conversion penalty factor δ, we re-run the simulation for U.S. Long-Haul and 5 x 5 Mesh-torus networks with full wavelength conversion by using different δ values. Figures 3.9a-3.9b depict the blocking perfor-

mance for U.S. Long-Haul at load = 250 and load = 270, respectively; while Figures 3.9c-3.9d show for 5 x 5 mesh-torus at load = 350 and load = 370, respectively. All the graphs demonstrate when δ changes from 0.0 to 1.0 the blocking performance has an obvious improvement even for *nc* conditions and thus it is critical to take the wavelength conversion as well as the cascading constraint into account. When δ grows gradually from 1.0 to larger values, the performance fluctuation in the U.S Long-Haul network is not big; but in 5 x 5 mesh-torus network there is a near-linear performance degradation until δ reaches a relatively large value. Therefore, through careful tuning, it is possible to find an optimal or near-optimal δ for each network i.e., $\delta = 1.0$ for 5 x 5 mesh-torus and $\delta = 32.0 - 48.0$ for U.S. Long-Haul so that the overall blocking probability is the lowest and the high load abnormality problem that occurred previously gets minimized.

3.4 Summary

In this chapter, we have examined the impact of the conversion cascading constraint on the performance of optical routing algorithms. We proposed two new dynamic algorithms GCAR and W-ACAR algorithms based on NAW-WC, in wavelength-routed all-optical networks. The GCAR and W-ACAR algorithms take into account the negative impact of the conversion cascading constraint when they make a route decision. Furthermore, the W-ACAR algorithm considers the distribution of free wavelengths, the lengths of each route and the conversion cascading constraint jointly and hence has the best blocking performance in most cases. The results demonstrated that the

two constraint-aware algorithms could improve the blocking performance significantly compared to conventional dynamic RWA algorithms in the environment of full or/and sparse wavelength conversion.

CHAPTER 4

FAIRNESS-IMPROVING DYNAMIC ROUTING

In most existing studies of optical burst-switched networks, adaptive routing is based on deflection routing and/or feedback from the past intervals which often introduces excessive transmission delay and architectural complexity. Our proposed novel adaptive routing schemes, however, consider the transient link congestion at the moment when the bursts arrive and have potential to reduce the overall burst loss probability. Moreover, they can utilize the same offset times for the same node pairs implying zero additional transmission delay and simplicity. The proposed hop-by-hop routing schemes also aim to address the intrinsic unfairness defect of existing popular signaling protocols by increasing the effective link utilization. The results show that the proposed schemes generally outperform shortest path routing and depending on the routing strategy involved, the network topology and the traffic load, this improvement can be substantial. We develop analytical loss models to demonstrate the need for such an adaptive routing scheme at each hop and show its effectiveness. We also verify the analytical results by simulation.

4.1 Introduction

Optical burst switching has been considered as one of the most promising technologies for the next-generation optical Internet based on wavelength division multiplexing. In OBS networks, data packets are aggregated into much larger sized bursts before transmission. A data burst is preceded in time by a control packet which is sent on a separate control wavelength and requests resource allocation at switches. Data bursts can be transmitted in an all-optical fashion. Unlike bursts, control packets would have to experience O/E/O conversion for resource reservation at each intermediate optical node. The signaling protocol plays a crucial role in the burst transmission. The well-known Just-Enough-Time (JET) is the one most widely adopted among several signaling protocols proposed for OBS networks in the literature [QY99, YQD00, WM00]. In this chapter and after, we will consider OBS networks using JET.

In the JET protocol, an output wavelength is reserved with a control packet just before the arrival of the burst (Delayed Reservation). The wavelength is released just after the burst transmission with a timer. When there are no available wavelengths at the arrival time of the corresponding burst, the control packet is rejected and the burst is lost. The time duration between a control packet and its associated burst is called the *offset time*. For a successful burst transmission in JET, its control packet must always be ahead of time at each hop, otherwise the burst will arrive before completion of bandwidth reservation and will be dropped.

One of the primary objectives in the design of an OBS network is to minimize burst loss. Burst loss occurs primarily due to the contention of bursts in the bufferless core nodes. Approaches for resolving contention include wavelength conversion, optical buffering, and deflection routing [WL04, YQD00, WMA00, HLH02, CWX03, ZVR04, ZVR07]. Apart from the three contention resolution approaches, burst segmentation and preemption techniques were also proposed [VJS02, CCE03]. In general, the above contention resolution techniques are reactive such that they attempt to resolve contentions rather than avoid them. A more proactive alternative is to prevent contention before it happens by policing the traffic at the source, or by routing traffic in a way that the congestion in the network is minimized. The authors in [TVJ03] proposed two dynamic congestion-based load balanced routing techniques to avoid congestion. In the schemes, a list of link-disjoint alternate paths are pre-calculated for each pair of source and destination nodes. The routes are re-computed periodically based on certain dynamic traffic information such as link congestion or number of contentions, and one specific route is selected/used for a chosen time interval. In order to achieve good performance, each source node must frequently gather information concerning the link utilization and switch the selected path. The authors in [YR06] focused on presenting a suite of path selection strategies, each utilizing a different type of information regarding the link congestion status. In the two adaptive path selection mechanisms proposed in [TVJ03] and [YR06], the average transfer delay always exceeds that of the shortest-path routing because alternative paths with a larger transfer delay are also utilized in the multi-path routing. The paper [OA05] proposed a decentralized routing scheme based on multiple paths in which each

source node splits the traffic load according to the measured loss rate instead of link utilization. Moreover, load splitting ratios for the multiple paths are autonomously adjusted to minimize the average transfer delay based on the condition that the required loss rate of optical bursts is satisfied. However, this proposed load splitting method is more complex and thus requires more processing overheads at the source nodes.

On the other hand, it is highly desirable to support Quality of Service (QoS, e.g., to achieve fairness) when designing a channel scheduling algorithm or routing scheme in OBS [VJ03, ZVJ04, CTZ07]. In this chapter, we newly propose three adaptive routing schemes to resolve the unfairness among bursts with different numbers of hop count. Each scheme performs hop-by-hop routing using local and/or immediate neighborhood link congestion information based on link connectivity. They are named *hop-by-hop routing using forward channel reservation* (Hop-FCR), *hop-by-hop routing using link connectivity* (Hop-LC) and *hop-by-hop routing using neighborhood forward channel reservation* (Hop-N-FCR). In contrast to most existing feedback-based dynamic routing algorithms, the Hop-FCR scheme considers the transient output wavelength reservation status at the epoch when the control packets arrive to select the next hop. The total channel reservation on the output link ahead of this epoch is called *forward channel reservation* (FCR). Additionally, the Hop-LC algorithm takes the connectivity of the immediate candidate nodes into account. The third routing technique, Hop-N-FCR, also considers the state information of the next candidate links ahead of time.

Our proposed routing schemes not only improve fairness remarkably but also improve burst loss performance to a large extent. They are relatively easy to implement which is very important especially in high-speed optical networks. In conventional deflection routing [WMA00, HLH02], the burst is deflected to an alternate port in case of a contention on the primary port. Nevertheless, the deflection in the network results in several side effects including burst transmission delay, and out-of-order packet arrival at the destination. Furthermore, in general buffer is not necessary for the deflection routing mechanism. However, optical buffer is required to enable deflection routing to function correctly in JET-based OBS networks as showed in [HLH02, YR06]. Our schemes do not suffer from these disadvantages, neither would they enforce the optical buffer requirement because they can utilize the same offset times for the same node pairs during the dynamic routing process. We shall further elaborate on this in later sections.

This chapter is organized as follows. Section 4.2 discusses related work about designing channel reservation algorithms and routing techniques to achieve fairness in OBS networks. Section 4.3 describes the proposed fairness-improving dynamic routing schemes in-depth. The analytical performance model is provided in Section 4.4. Section 4.5 demonstrates analysis validation and simulation results. Finally Section 4.6 summarizes the chapter.

4.2 Related Work

Many aspects of burst switching have been extensively studied in the OBS literature, which include but are not limited to signaling and reservation protocols, routing and scheduling, burst assembly at the ingress nodes and contention resolution at the core nodes. However, there have been very few attempts to design and evaluate schemes to reduce the effect of the fairness problem in the OBS networks.

In the OBS networks, the fairness problem indicates the loss probabilities of optical bursts traveling through lightpaths with larger hop counts tend to be higher than those whose paths have a smaller number of hops. This fairness problem, which is common to most networks, has been investigated in several papers as a secondary consideration in the evaluation of routing and wavelength-assignment algorithms [WMA00, OAM01]. For instance, the authors in [WMA00] proposed a deflection routing algorithm and showed that it can evenly decrease the blocking probabilities of the bursts with various hop counts under a variety of traffic loads; i.e., their proposed deflection routing could neither improve nor aggravate fairness between bursts with large hop counts. In [OAM01], an OBS reservation scheme using parallel backward reservation paradigm was proposed for OBS networks operated under the wavelength-continuity constraint (i.e., no converters). The authors achieved fairness by classifying bursts into several groups according to their total hop counts and then limiting the number of wavelengths dedicated to the group composed of shorter-hop bursts. The simulation results reported in [OAM01] showed that the overall mean

blocking probability was slightly increased while better fairness was achieved. Requiring that the traffic load of bursts be known a priori in order to derive an effective wavelength-partitioning method is another drawback of this scheme.

The work in [ZBL04] was dedicated to improve fairness in OBS networks. The authors proposed two approaches - balanced just-in-time scheme (BJIT) and prioritized random early dropping scheme (PRED). BJIT dealt with the fairness problem by adjusting the size of the search space for a free wavelength based on the number of hops traveled by the burst. PRED adapted the concept of random early discard (RED) to the OBS environment and prioritized the levels of discarding at the network access stations on the basis of the length of the lightpath. The detailed performance results presented in the chapter showed that both schemes can alleviate the fairness problem without negatively affecting the overall throughput of the system. Since BJIT is more practical than PRED in regards to implementation and has slightly better performance too, we shall focus on BJIT thereafter. More specifically, the scheduler in the BJIT scheme is only allowed to search for a free wavelength out of total n_i number of wavelengths for an incoming burst arriving at its ith hop, where $n_i < n_j$ if $i < j$, which is different from the approach in [OAM01]. The value of n_i is determined according to (4.1)

$$n_i = (1-g) \times W + g \times i \times W/D, \qquad 0 \leq g \leq 1. \tag{4.1}$$

where W is the number of wavelengths on a fiber link and D is the maximum hop count of any shortest lightpath in the network topology. The parameter g controls the degree of effectiveness of resolving fairness. Generally speaking, the larger we assign a value to g, the better fairness we can obtain. As the authors mentioned, BJIT becomes BJET if this technique applies to a JET-based network, and when $g = 0$ BJET is exactly equivalent to the standard JET scheme. However, the authors did not describe which subset of n_i wavelengths should be searched from the entire W wavelength set $[1, W]$ at the burst's ith hop. Two simple policies can be employed — choose the first n_i applicable wavelengths sequentially, i.e., search the subset $[1, n_i]$; or select a total of n_i wavelengths randomly. We name them BJET-F and BJET-R, respectively, in our performance comparison section (Section 4.5).

4.3 Proposed Adaptive Routing

There are several important criteria to consider when designing and implementing an adaptive OBS routing scheme: burst loss probability, resource utilization, system complexity and fairness. Most of all, a dynamic OBS routing scheme should be very careful when selecting a route and a wavelength for a burst so that it does not severely harm burst loss performance and utilization on the whole. Simultaneously, in order to address the inherent unfairness issue in JET, we have to favor bursts with longer paths in a certain method, which often results in slight or noticeable overall burst loss performance degradation in the conventional fairness solutions. In this section,

we propose three simple adaptive routing schemes, considering the routing and wavelength reservation problems jointly. Furthermore, by exposing a larger proportion of underutilized network resources to the longer-path bursts, we are able to improve fairness as well as overall burst loss performance. Since our schemes are distributed, the network architecture still remains simple and scalable. They are called *Hop-FCR*, *Hop-LC* and *Hop-N-FCR*, as aforementioned. In this work, we use JET as our signaling protocol and assume that each OBS switch in the network has full wavelength conversion capabilities, which are used in the case of wavelength contention.

In order to examine and measure the burst loss fairness quantitatively, we adopt a variation of the standard *coefficient of variance* (CoV) for expression purpose. Compared with the standard deviation, the metric *CoV* still offers a good view of fairness even when the overall burst loss ratios are quite different for various experiments. We slightly revise the standard *CoV* for our usage as follows. Given a network topology, we compute the number of hops that the longest path has by using any shortest-path algorithm. We use p_i to indicate the burst loss probability for i-hop bursts, where $1 \leq i \leq n$ and n is the largest number of hops. The term p_0 indicates the overall burst loss probability for all bursts. Hence, the standard *CoV* expressed as a percentage (also known as *relative standard deviation*) is modified as follows:

$$CoV' = \frac{\sigma'}{p_0} \times 100\%, \tag{4.2}$$

where

$$\sigma' = \sqrt{(n-1)^{-1} \sum_{i=1}^{n} (p_i - p_0)^2}. \tag{4.3}$$

In the above expression, p_0 replaces the loss mean of all bursts with individual hops, as explained previously. Thus CoV' represents the degree to which the burst loss probabilities for bursts with different hops deviate from p_0. When assessing the fairness, the lower the variation percentage, the better the loss fairness is for bursts with various path lengths.

4.3.1 Foward Channel Reservation

We first give a general definition of forward channel reservation. Its computation shown later mainly depends on the wavelength state information managed by the wavelength scheduler deployed at each optical fabric.

Consider a unidirectional link ℓ_{ij} of the OBS network which transmits incoming bursts from node i to node j. Let W_k denote the kth index of the wavelength set $[1,W]$ on link ℓ_{ij} and let $FCR_{\ell_{ij}}(k,t)$ denote the current state of forward channel reservations of wavelength W_k at time t. Generally, $FCR_{\ell_{ij}}(k,t)$ is defined as the sum of the residual channel reservation time of any burst(s) in transmission and the channel reservation time of the burst(s) to be transmitted, if any. How we actually compute $FCR_{\ell_{ij}}(k,t)$ would depend on the system implementation, i.e., what information each optical switch is supposed to track and process. In particular, we intend to utilize

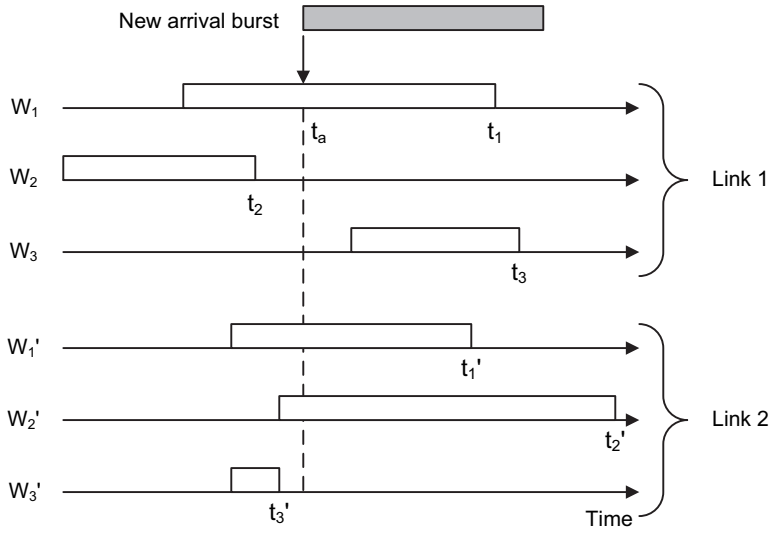

Figure 4.1: Computing *FCR* on candidate links.

the available wavelength state information provided by the wavelength scheduling algorithm in order to avoid adding extra system overhead. Two widely-used scheduling algorithms called LAUC (latest available unscheduled channel) and LAUC-VF (LAUC with void filling) were proposed in [XVC00]. LAUC, which is very similar to the Horizon algorithm [Tur99], maintains a single variable recording the latest reservation time of each channel and assigns the channel with the latest starting time that is still earlier than the arrival time of the incoming burst. On the other hand, LAUC-VF additionally keeps track of all void intervals within the channel space and assigns the intervals that would give the minimum of gaps or voids. We shall show how to compute $FCR_{\ell_{ij}}(k,t)$ for LAUC and LAUC-VF, respectively.

Let $\{b_k(z,t), z = 1,...,m_k\}$ be the set of m_k scheduled bursts (in transmission and to be transmitted) on wavelength W_k of link ℓ_{ij} at time t (for simplicity, we omit the subscript ℓ_{ij} in $b_k(z,t)$).

Consider any burst $b_k(z,t)$, let $s_k(z,t)$ and $e_k(z,t)$ denote its starting time and ending time, respectively. According to LAUC, only $e_k(m_k,t)$ is tracked on wavelength W_k. Let t_a denote the arrival time of a new burst (Figure 4.1 draws an example of link state at t_a for two adjoining candidate links). At time t_a, $FCR_{\ell_{ij}}(k,t)$ is obtained as

$$FCR_{\ell_{ij}}(k,t_a) = \begin{cases} e_k(m_k,t_a) - t_a, & \text{if } e_k(m_k,t_a) > t_a; \\ 0, & \text{otherwise.} \end{cases} \tag{4.4}$$

When LAUC-VF is selected for scheduling, $s_k(z,t)$ and $e_k(z,t)$ are assumed to be known for any burst $b_k(z,t)$. Let $b_k(z^*,t)$ denote the only burst (if there is such one) that satisfies $s_k(z^*,t_a) \leq t_a < e_k(z^*,t_a)$ and let $\Lambda = \{z : s_k(z,t_a) > t_a\}$ be the set of index z that their corresponding bursts are scheduled to be transmitted after t_a. In consequence, $FCR_{\ell_{ij}}(k,t)$ at time t_a is calculated as

$$FCR_{\ell_{ij}}(k,t_a) = \left[e_k(z^*,t_a) - t_a\right] + \sum_{\forall z \in \Lambda} \left[e_k(z,t_a) - s_k(z,t_a)\right] \tag{4.5}$$

Specially, if $e_k(m_k,t_a) \leq t_a$ then $FCR_{\ell_{ij}}(k,t_a) = 0$, same as it was defined in LAUC.

After $FCR_{\ell_{ij}}(k,t_a)$ is known, we can add up them for all $k \in [1,W]$ to get the total forward channel reservations for link ℓ_{ij}. In this chapter, we choose LAUC scheduling (hence Equation (4.4)) for the purpose of demonstration.

4.3.2 Hop-based Routing Using Forward Channel Reservation

The Hop-FCR routing scheme selects paths using information on immediate candidate link state. The motivation behind Hop-FCR is to dynamically route bursts hop-by-hop to one of the designated paths based on the metric of forward channel reservation.

In Hop-FCR, as a burst control packet (BCP) proceeds toward its destination, it instantaneously chooses the next node with the lowest preference value among the candidate nodes that are ahead of the current node. The preference is the barometer indicating the state of the forward channel reservations of the immediate candidate link. Obviously, the smaller preference value is, the less congested the candidate link would be at the epoch. Consider a source-destination pair (s,d) and a BCP destined for node d from node s has arrived at an intermediate node i. The data counterpart of this BCP will arrive at time t_a. Let $\Psi = \{j : L_{jd} < L_{id}\}$ be the set of candidate neighbor nodes of node i that are closer to node d. L_{id} (respectively, L_{jd}) denotes the shortest-path length (in number of hops) from node i (respectively, node j) to node d. Here we choose hop count instead of physical distance as the path-length metric because it has been shown in [TVJ03] that lower blocking performance could be scored with the former metric. As a consequence, $L_{jd} = L_{id} - 1$. The preference value for node j as the next routing hop at t_a, denoted as $Pref_i(j,t_a)$, is defined as follows:

$$Pref_i(j,t_a) = \sum_{k=1}^{W} FCR_{\ell_{ij}}(k,t_a). \tag{4.6}$$

The burst will be routed to the next node whose index id j^* is determined by

$$j^* = \arg \min_{\forall j \in \Psi'} Pref_i(j, t_a). \tag{4.7}$$

To ensure that the burst can be scheduled on link ℓ_{ij^*}, we define the set $\Psi' = \{j : j \in \Psi$ *and the scheduler returns success on link* $\ell_{ij}\}$ by excluding those nodes that fail the scheduler on their link counterparts.

Equation (4.7) shows that the proposed routing selects the next neighboring node from the set Ψ' with the least preference value. Since we limit the candidate nodes to those that are closer to the destination, Hop-FCR always finds shortest paths with the same number of hops as that found by any conventional fixed shortest-path routing. Using multiple shortest paths with the same number of hops ensures that the same offset times for the same node pairs can be used. The multiple paths may share one or more common links, though. This property in conjunction with dynamic routing makes Hop-FCR superior to conventional deflection routings in many regards, as explained in Section 4.1. We confine our search for immediate candidate nodes for two main reasons: 1) If a request moves to the nodes farther away from the destination, the path length may increase too much, resulting in wasted network resources; 2) It can keep a simple network architecture and fast processing speed, as we do not require optical buffers at the intermediate nodes to accommodate bursts because of insufficient offset time if they are deflected to a longer lightpath.

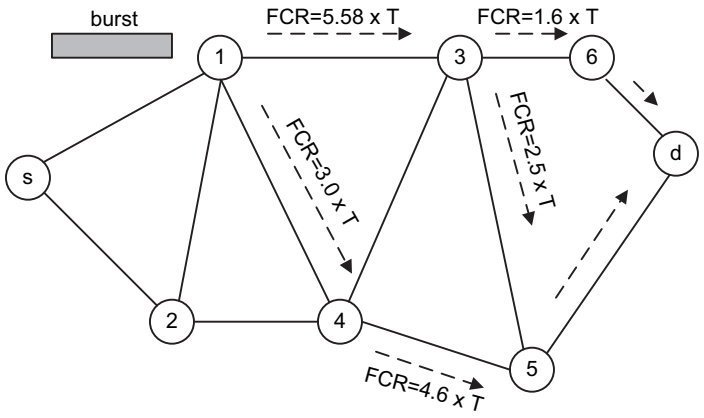

Figure 4.2: Demonstration of hop-by-hop routing using *FCR*.

Figure 4.2 shows a sample forwarding process for a BCP through the schemes that utilize forward channel reservation. *FCR* in the figure is the sum of forward channel reservations for all wavelengths on the related links (T is a given time unit). Assuming that a control packet originated from node s to node d arrives at node 1, the request can move to node 3 or node 4, since only these two nodes are closer to the destination d. According to (4.6)

$$Pref_1(3,t_a) = 5.58 \times T,$$

$$Pref_1(4,t_a) = 3.0 \times T.$$

Same as before, time t_a refers to when the data counterpart of the control packet will arrive at node 1. Therefore, the control packet is forwarded to node 4 (assuming it satisfies (4.7)) — a less congested node at the current point indicated by the preference values, and the same forwarding process occurs until it arrives at the destination. If the control packet arrives at the destination node, a routing lightpath has been chosen and the required channel on each link along the path

has been successfully reserved. After the offset time elapses, the data burst can be transmitted all optically.

4.3.3 Hop-based Routing Using Link Connectivity

This algorithm (Hop-LC) is the same as Hop-FCR except for the equation used to compute the preference value. In the preference calculation, Hop-FCR uses the sum of *FCRs* of all wavelengths on each candidate outgoing links along which a control packet can be delivered. Hop-LC additionally takes the connectivity of the immediate candidate nodes into account. In other words, consider a data burst that reaches an intermediate node i between a source-destination pair (s,d) at time t_a, let node j be one of the possible next hops and $\Omega = \{y : L_{yd} = L_{jd} - 1\}$ be the set of neighbor nodes of node j that are closer to node d. We define *forward* connectivity index of node j (to node d) as $C_f(j,d) = |\Omega|$, which is the number of next candidate nodes ahead of node j assuming the burst will be forwarded to node j from the current node i. The preference of node j as the next hop is defined and calculated as follows:

$$Pref_i(j,t_a) = \frac{Pref_i(j,t_a)'}{C_f(j,d)}. \tag{4.8}$$

where $Pref_i(j,t_a)'$ is the same preference computed using (4.6). After $Pref_i(j,t_a)$ is obtained for all candidate nodes, the node with the least preference value will be selected for the next hop,

same as (4.7). By taking the forward connectivity index into account as in (4.8), we incline to direct bursts along the node with more future routing options which may further decrease burst loss probabilities. The selection of the denominator is heuristic. We also undertake experiments on other weighted $C_f(j,d)$ choices like $\sqrt{C_f(j,d)}$ and $C_f^2(j,d)$, nevertheless we have found that (4.8) performs best for all example network topologies examined in this work.

It is worth mentioning that $C_f(j,d)$ is not the same as the node degree $D(j)$. Instead, its value depends on how many shortest paths exist between node j and node d, so $C_f(j,d) \leq D(j)$. In Figure 4.2, as we have discussed in Subsection 4.3.2, when a control packet arrives at node 1 it can move to either node 3 or node 4. Assuming the request arriving at node 3, it has two next candidate nodes 5 or 6 that are closer to the destination d to choose (hence, $C_f(3,d) = 2$). However, if the request selects node 4 instead of node 3, node 5 would be the only next candidate node (hence, $C_f(4,d) = 1$). From this perspective, choosing node 3 instead of node 4 that was chosen by Hop-FCR may be a better choice depending on the value of *FCRs*. Therefore, we have:

$$C_f(3,d) = 2, Pref_1(3,t_a) = 5.58/2 = 2.79 \times T,$$

$$C_f(4,d) = 1, Pref_1(4,t_a) = 3.0/1 = 3.0 \times T.$$

Since $Pref_1(3,t_a) < Pref_1(4,t_a)$, node 3 is selected as the next hop by the algorithm Hop-LC.

4.3.4 Hop-based Routing Using Neighborhood Forward Channel Reservation

In the last two algorithms Hop-FCR and Hop-LC, we only considered the *FCRs* on the immediate candidate links. It has been well-known that in optical circuit-switched networks dynamic routing algorithms utilizing global link-state information often achieve better blocking performance than those utilizing only local link state information. Nevertheless, due to the bursty characteristic and the nature of optical burst switching, it would cause a lot excessive overhead and outdated link-state information if we want to exchange channel reservation messages in an intensive way (beyond next candidate links) as in optical circuit switching. In this regard, our third routing scheme, called Hop-N-FCR, not only takes the *FCRs* on the immediate candidate links into account, but also checks the *FCRs* on the next candidate links. We assume that the control plane of the OBS network provides support for the collection and dissemination of information on the next candidate links. Consider a source-destination pair (s,d) and assume that a burst arrives at an intermediate node i at time t_a. Let node j be one of the candidate next hops, and let $\Omega = \{y : L_{yd} = L_{jd} - 1\}$ be the set of neighbor nodes of node j that are closer to node d, then the preference of node j is defined as follows:

$$Pref_i(j,t_a) = Pref_i(j,t_a)' + \xi \times \frac{\sum_{k\in\Omega} Pref_j(k,t_a)'}{C_f^2(j,d)}. \tag{4.9}$$

$Pref_i(j,t_a)'$ and $Pref_j(k,t_a)'$ have the same definitions as in (4.6), while $C_f(j,d)$ has the same meaning as in (4.8). Responding to possibly large summation of preference values on those next

candidate links compared with (4.8) where a single immediate candidate link is considered, we select $C_f^2(j,d)$ heuristically as the denominator in the second part of the above expression (4.9). Because when calculating the final preference value $Pref_i(j,t_a)$ at time t_a, $Pref_j(k,t_a)'$ is computed earlier than when the burst arrives at node j (as there is a link propagation delay), it may not be accurate if many bursts come to node j during the link propagation delay. Therefore, the parameter ξ $(0 < \xi < 1)$ is introduced to diminish this negative impact by giving the contribution of the neighborhood $Pref_j(k,t_a)'$ aggregation a relatively smaller weight. Same as (4.7), in the end the node with index id j^* having the least $Pref_i(j,t_a)$ will be selected for the next hop.

In the example Figure 4.2, when a control packet arrives at node 1 by following (4.9) we have (ξ is set to 0.8 here):

$$Pref_1(3,t_a) = 5.58 + 0.8 \times (2.5+1.6)/4 = 6.4 \times T,$$

$$Pref_1(4,t_a) = 3.0 + 0.8 \times (4.6)/1 = 6.68 \times T.$$

Since $Pref_1(3,t_a) < Pref_1(4,t_a)$, node 3 is selected as the next hop by the scheme Hop-N-FCR as Hop-LC selected previously.

4.3.5 Fairness Capability, Complexity and Extensibility

As mentioned earlier, the proposed routing methods also bear fairness-solving in mind, which distinguishes them from the other path-based adaptive routing mechanisms [OA05, TVJ03, YR06].

To achieve better fairness, our proposed routing methods allow longer-hop bursts to have more routing choices. For example, in Figure 4.2 there are three hops from node 1 to node d. According to the routing principle, data bursts can take three different paths:

node 1 $\rightarrow$ node 3 $\rightarrow$ node 6 $\rightarrow$ node d

node 1 $\rightarrow$ node 3 $\rightarrow$ node 5 $\rightarrow$ node d

node 1 $\rightarrow$ node 4 $\rightarrow$ node 5 $\rightarrow$ node d

However, two-hop data bursts traversing from node 3 to node d can only take the following two paths:

node 3 $\rightarrow$ node 6 $\rightarrow$ node d

node 3 $\rightarrow$ node 5 $\rightarrow$ node d

And all one-hop bursts always have only one routing choice. By being offered more routing opportunities, those longer-hop bursts will obtain relatively greater possibilities of passing through intermediate optical nodes. Consequently, better fairness can be achieved as desired.

The running time for the three routing schemes is described as follows. It includes static path computation and dynamic routing/scheduling times. Let N denote the number of nodes in the network topology. The path computation for all the three schemes is the same, which typically takes $O(N^2)$ for one source node using Dijkstra's algorithm. Compared with the simple shortest path routing, we would additionally use a path finding algorithm such as depth-first search to find all shortest paths between two given nodes, but it takes only linear time. All candidate next hops

from the current node to the destination are stored in the routing table of this node and let $\bar{M}$ denote the average of this value in the network. $\bar{M}$ is generally very small, such as $2-5$. For Hop-FCR, it takes $O(\bar{M}W)$ to calculate *FCRs* on the candidate links for routing comparison, and takes $O(logW)$ for burst scheduling via LAUC (with its best implementation). Hop-LC adds a little division overhead for the routing comparison process. Since Hop-N-FCR considers neighborhood link state information, the time complexity for its routing comparison is $O(\bar{M}W+\bar{M}^2W)$, while the running time for its burst scheduling is the same as the other two. Besides the increased time complexity, Hop-N-FCR requires support of neighborhood link state dispatching and gathering.

Although Hop-FCR and the other two strategies, in general, are expected to outperform shortest path routing, they have limitations. More specifically, since they compute only (multiple) shortest paths between source-destination pairs, the network topology plays an important role in achieving their advantages. Denser networks are usually expected to perform better than sparser ones operated under the same routing strategy. To make the hop-by-hop routing work well in the diverse network environments, we can relax path computing by allowing extended routes with a longer hop count, i.e., shortest hops plus η more hops. The threshold η is tunable for different networks. It is also well-known that the average path length of admissible bursts has significant impact on burst loss performance, so we suggest that the extended routing be applied to sparse networks like Ring topologies and/or if optical buffering is available to compensate the increased offset time.

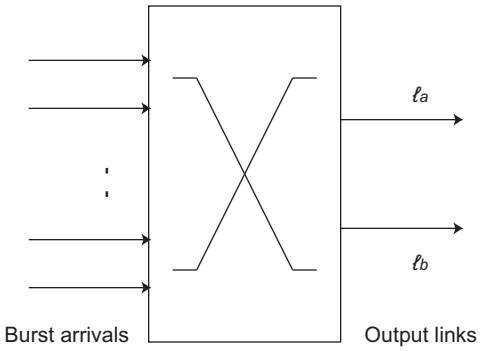

Figure 4.3: An Nx2 OBS Fabric with *FCR*-based adaptive routing.

4.4 Analysis

In this section, we develop burst loss models to demonstrate the need for a *FCR*-based adaptive routing at each hop and show its effectiveness. We first derive the burst loss probability in an Nx2 OBS switch operated under the specified adaptive routing. Figure 4.3 shows a sketch of this fabric with its two output links (or ports), denoted as ℓ_a and ℓ_b. Afterwards, for the sake of simplicity, we apply the adaptive routing to symmetrical Ring networks and further compute the end-to-end burst loss rate approximately through analysis. The possibility of extending the model to general mesh networks is also discussed.

4.4.1 Notation and Assumptions

Let us consider the following notation.

λ Rate of total Poisson burst arrivals to the node including arrivals of bursts locally generated in this node and arrivals of external bursts received from neighboring nodes.

λ_a Arrival rate of bursts destined for ℓ_a only.

λ_b Arrival rate of bursts destined for ℓ_b only.

λ_{ab} Arrival rate of bursts that can be switched to either ℓ_a or ℓ_b, i.e., $\lambda = \lambda_a + \lambda_b + \lambda_{ab}$.

p_a Probability that arriving bursts with λ_{ab} are switched to ℓ_a.

p_b Probability that arriving bursts with λ_{ab} are switched to ℓ_b, i.e., $p_b = 1 - p_a$.

μ Service rate of arriving bursts.

W Total number of wavelengths per output link.

ρ Normalized traffic load of all burst arrivals, i.e., $\rho = \lambda/(W\mu)$.

We assume bursts (i.e., with λ_a, λ_b and λ_{ab} respectively) come to the node fabric according to independent Poisson processes and burst transmission time on each link are independently and exponentially distributed with a common mean of $1/\mu$. To make it clear, let us look at a six-node Ring network operated under the designated adaptive routing through Figure 4.4a. According to the routing principle, the arrowed dotted lines demonstrate all the possible routes of the bursts that are originated from node r_0 to the rest of five nodes (r_1 - r_5). Without loss of generality,

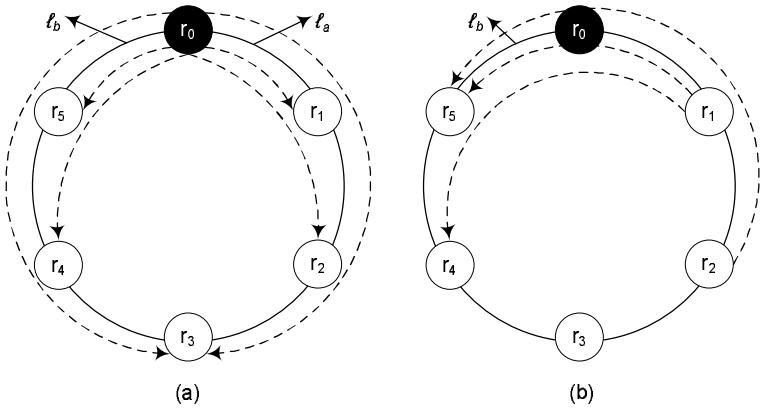

Figure 4.4: A six-node Ring with first-hop adaptive routing.

we designate output link ℓ_a of node r_0 as the port used to reach the immediate neighbor in the clockwise direction (node r_1) and output link ℓ_b as the port to reach the immediate neighbor in the anticlockwise direction (node r_5). The two nodes r_1 and r_2 are within two-hop distance from the sender and thus their shortest paths can be reached only via ℓ_a in the clockwise direction. Similarly, the two nodes r_4 and r_5 can be reached only via ℓ_b in the anticlockwise direction. On the other hand, to reach node r_3, the sender r_0 would choose either ℓ_a or ℓ_b depending on their *FCRs*.

4.4.2 Loss Model for Single Node Switch

We model the OBS node in Figure 4.3 using a two-dimensional Markov chain with the state defined as $Q = \{i, j\}$, where i is the number of wavelengths that are reserved on ℓ_a and j is the number of wavelengths that are reserved on ℓ_b. The state transition diagram for the Markov chain is shown in

Figure 4.5 and the state transition rates are as follows:

$$q_{(i,j)(i,j+1)} = \begin{cases} \lambda_1 = \lambda_b + p_b \cdot \lambda_{ab}, & i < W \\ \lambda_3 = \lambda_b + \lambda_{ab}, & i = W, \end{cases}$$

$$q_{(i,j)(i+1,j)} = \begin{cases} \lambda_2 = \lambda_a + p_a \cdot \lambda_{ab}, & j < W \\ \lambda_4 = \lambda_a + \lambda_{ab}, & j = W, \end{cases}$$

$$q_{(i,j)(i,j-1)} = \begin{cases} j \cdot \mu, & j > 0 \\ 0, & \text{otherwise}, \end{cases}$$

$$q_{(i,j)(i-1,j)} = \begin{cases} i \cdot \mu, & i > 0 \\ 0, & \text{otherwise}. \end{cases} \tag{4.10}$$

Denote the steady state probability that the system in state $\{i, j\}$ as $p(i, j)$, and it is subject to

$$\sum_{i=0}^{W} \sum_{j=0}^{W} p(i, j) = 1. \tag{4.11}$$

By solving the $(W+1) \times (W+1)$ linear equations representing the state transitions and (4.11), we can get the steady state probabilities of the system. A burst gets dropped as all of the wavelengths on both output links are busy, or when all the wavelengths are occupied on either link and,

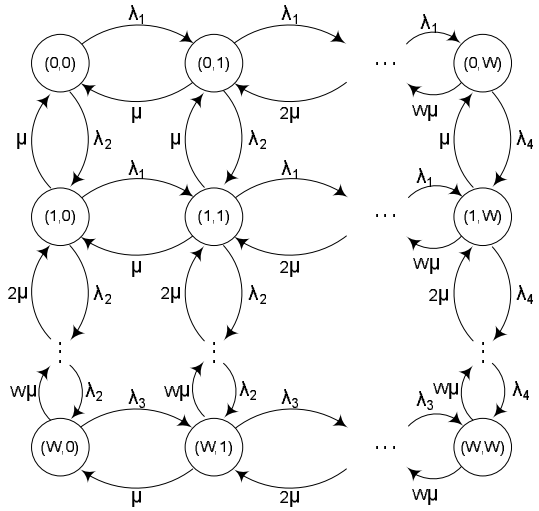

Figure 4.5: Markov chain for a single optical switch with two output links.

if and only if the burst is not designated to use the other link, regardless when there is some free wavelength(s) on that link. Therefore, the loss probabilities at output link ℓ_a and ℓ_b are derived by

$$P_{\ell_a} = \frac{\lambda_a + p_a \cdot \lambda_{ab}}{\lambda} \cdot p(W,W) + \frac{\lambda_a}{\lambda} \cdot \sum_{j=0}^{W-1} p(W,j), \tag{4.12}$$

$$P_{\ell_b} = \frac{\lambda_b + p_b \cdot \lambda_{ab}}{\lambda} \cdot p(W,W) + \frac{\lambda_b}{\lambda} \cdot \sum_{i=0}^{W-1} p(i,W). \tag{4.13}$$

Accordingly, the total burst loss probability at the optical switch is given as (4.14).

$$P_{loss} = P_{\ell_a} + P_{\ell_b}. \tag{4.14}$$

4.4.3 Loss Model for Ring Topology

Due to the unique node connectivity property of Ring networks, the proposed hop-by-hop routing applied to ring networks behaves in the same way as first-hop adaptive routing. Furthermore, Hop-LC is the same as Hop-FCR, and Hop-N-FCR is also projected to perform closely as them. As suggested in Subsection 4.3.5, extended routing may be adopted for Rings with a small η. Therefore, we consider extended Hop-FCR only and η is set to one to avoid undesirable vibration effects, as explained in [ZVR04, ZVR07].

Let us first consider the six-node Ring network shown in Figures 4.4a-4.4b, and then we generalize to Ring networks with an arbitrary number of nodes. As we can see, when $\eta = 1$ all node pairs in an even-numbered Ring still utilize only shortest paths, because any extended route requires at least two more hops. By symmetry and the Poisson arrivals assumption, the blocking probability B on each link in Figure 4.4a is the same. Let $\bar{\lambda}$ denote the arrival rate of bursts offered to each source-destination (SD) pair; therefore the total traffic locally generated in any node in Figure 4.4a is $5 \cdot \bar{\lambda}$. As aforementioned, bursts arrive at each optical node independently. Each optical node can be modeled as an Nx2 OBS switch which has been depicted in the former subsection. Without loss of generality, we take node r_0 for example. The directed link from node r_0 to r_5 (or r_1) is denoted as ℓ_b (or ℓ_a). Using the notation defined in 4.4.1, we can easily show the following

$$\lambda_b = \bar{\lambda} + \bar{\lambda} + (1-B) \cdot \bar{\lambda} + (1-B) \cdot \frac{\bar{\lambda}}{2} + (1-B)^2 \cdot \frac{\bar{\lambda}}{2}. \tag{4.15}$$

We shall explain the above equation using the help of Figures 4.4a and 4.4b. In (4.15), the first two components (single $\bar{\lambda}$) represent the burst arrivals directed to ℓ_b from the traffic destined from node r_0 to the two nodes r_5 and r_4 (shown by dotted arrowed lines in Figure 4.4a). The term $(1-B)\cdot\bar{\lambda}$ represents the burst arrivals directed to ℓ_b from the traffic destined from node r_1 to r_5 (shown by dotted arrowed line in Figure 4.4b). These latter bursts have arrived at node r_0 by traversing the link $r_1 \rightarrow r_0$ whose blocking probability is B. Similarly, $(1-B)\cdot\frac{\bar{\lambda}}{2}$ and $(1-B)^2\cdot\frac{\bar{\lambda}}{2}$ stand for the burst arrivals directed to ℓ_b from the traffic destined from node r_1 to r_4 and from node r_2 to r_5 (shown by dotted arrowed lines in Figure 4.4b). Before arriving at node r_0, the traffic from node r_1 to r_4 suffers blocking on link $r_1 \rightarrow r_0$ while the traffic from node r_2 to r_5 suffers blocking on both link $r_2 \rightarrow r_1$ and link $r_1 \rightarrow r_0$. Since the traffic destined from node r_1 to r_4 (or from node r_2 to r_5) has two selectable paths, only half the bursts in this traffic travel in the anticlockwise direction from node r_1 to r_0 (or from node r_2 to r_1). And the bursts originated from node r_0 to node r_3 can be switched to either ℓ_a or ℓ_b, so λ_{ab} is equal to $\bar{\lambda}$. Also by symmetry, we have $\lambda_a = \lambda_b$ and $p_a = p_b = \frac{1}{2}$.

We begin the successive substitution procedure with an arbitrary initial blocking probability of B. We calculate λ_a and λ_b using (4.15) and supply them to (4.12) or (4.13). Notice that by symmetry, $B = P_{\ell_a} = P_{\ell_b}$. We repeatedly apply this process until B converges to a unique fixed point. After B is known, the end-to-end blocking probability of an arbitrary burst is derived by

$$P = \frac{2}{5}\cdot B + \frac{2}{5}\cdot\left[1-(1-B)^2\right] + \frac{1}{5}\cdot\left[1-(1-B)^3\right]. \tag{4.16}$$

The three elements in (4.16) indicate the corresponding blocking probabilities for one-hop, two-hop and three-hop bursts, respectively.

We now look at how to compute the end-to-end burst loss rate in a general Ring network with even number of nodes (the case of odd number of nodes will be addressed shortly). Let N be an even integer representing the number of nodes and $N \geq 4$. For any of the optical nodes with two output links ℓ_a and ℓ_b, it can be easily shown that the respective arrival rates and probabilities are given as

$$\lambda_a = \lambda_b = \frac{\bar{\lambda}}{2} \cdot \left[2 \cdot \varphi + \sum_{i=1}^{\varphi} (2 \cdot (\varphi - i) + 1) (1 - B)^i \right], \tag{4.17}$$

$$\lambda_{ab} = \bar{\lambda}, \tag{4.18}$$

$$p_a = p_b = \frac{1}{2}. \tag{4.19}$$

where $\varphi = N/2 - 1$. Similar to what we have achieved on the six-node Ring, we first calculate B through successive substitution, and the end-to-end blocking probability of an arbitrary burst is thus given by

$$P = \frac{2}{N-1} \cdot \sum_{i=1}^{\varphi} \left[1 - (1 - B)^i \right] + \frac{1}{N-1} \cdot \left[1 - (1 - B)^{\varphi+1} \right]. \tag{4.20}$$

When N is odd and $N \geq 3$, for simplicity's sake, we disregard any out-of-symmetry that may be caused by the extended routes R_1^* and R_2^* as displayed in Figure 4.6 ($L(R_1^*) = L(R_1) + 1$, $L(R_2^*) = L(R_2) + 1$). We project that the possible impact should be very small and this conjecture is verified by the subsequent simulation results. Therefore, we set $\lambda_a = \lambda_b$ and $p_a = p_b = \frac{1}{2}$ as for the even-

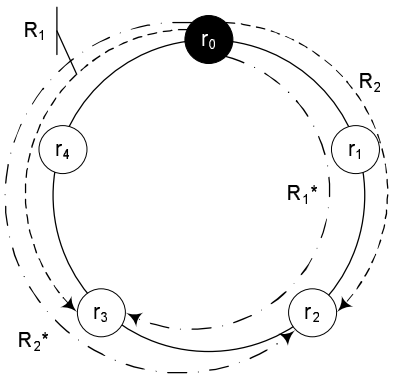

Figure 4.6: A five-node Ring with first-hop adaptive routing (extended).

numbered Rings. Note that here $\lambda_{ab} = 2 \cdot \bar{\lambda}$. Similarly, Equations (4.21) and (4.22) can be deduced by letting $\varphi = \lfloor N/2 \rfloor - 1$.

$$\lambda_a = \frac{\bar{\lambda}}{2} \cdot \left[2 \cdot \varphi + \sum_{i=0}^{\varphi-1} 2 \cdot (\varphi - i) (1-B)^{i+1} + (1-B)^{\varphi+1} \right], \tag{4.21}$$

$$\begin{aligned} P &= \frac{2}{N-1} \cdot \left[\sum_{i=1}^{\varphi} \left(1 - (1-B)^i \right) \right. \\ &\quad + \frac{1}{2} \cdot \left(1 - (1-B)^{\varphi+1} \right) \\ &\quad \left. + \frac{1}{2} \cdot \left(1 - (1-B)^{\varphi+2} \right) \right]. \end{aligned} \tag{4.22}$$

It is desirable to extend our model to analyze the network performance of general mesh topologies. Two tasks would need to be fulfilled to achieve this goal: 1) Since the alternate paths between each node pair in arbitrary networks may share common link(s), it is necessary to take into account

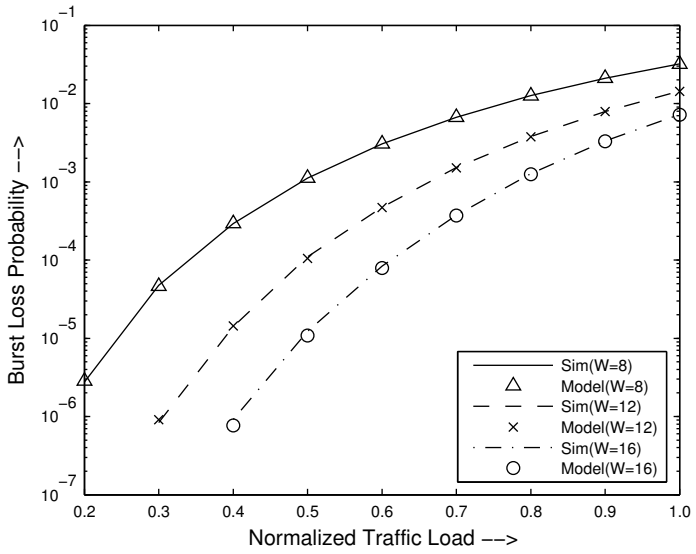

Figure 4.7: Scenario one: $\lambda_a = 0.5\lambda$, $\lambda_b = 0.3\lambda$, $p_a = 0.4$.

the interdependencies between the blocking on alternate routes. This is different from most works in the past [RM02, ZVR07], which usually assume that alternate routes block independently. Instead, the enhanced model may follow the techniques proposed in [GS97]. 2) If a fabric has more than two output links, the proposed two-dimensional Markov chain model may need to be upgraded to multi-dimensional. Unfortunately, this would force the computation complexity to grow exponentially. We leave the modeling of general topologies to be an open problem.

4.5 Numerical Results

In this section, we conduct simulation to evaluate the performance of the proposed schemes and to verify the analytical model. We first compare the simulation and analytical results obtained for a

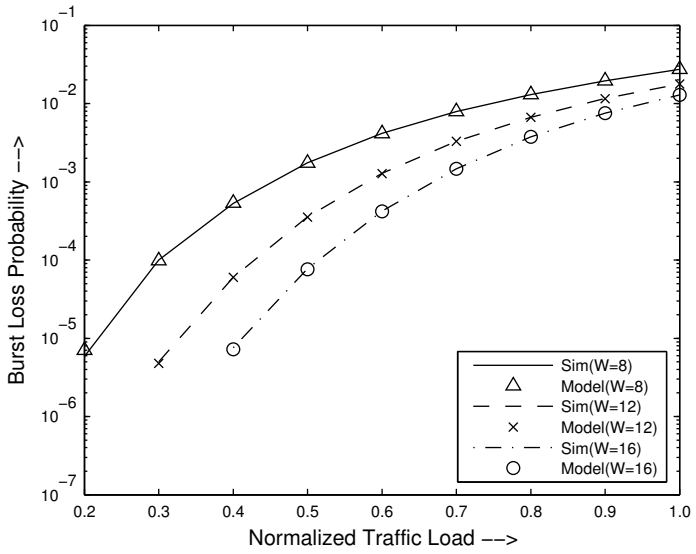

Figure 4.8: Scenario two: $\lambda_a = 0.1\lambda$, $\lambda_b = 0.2\lambda$, $p_a = 0.2$.

single optical switch with two output links and then proceed to present the comparison results for Ring networks. Arrivals follow a Poisson process with total normalized traffic load $\rho = \lambda/(W\mu)$ per optical Ring node. Thereafter we demonstrate performance evaluation in the JET-based OBS networks by simulation. In network simulations, bursts are generated by Poisson model with a network-wide traffic load $\rho = \lambda/\mu$ in Erlangs. Each data point shown in all the simulation graphs is obtained by running 10^7 burst transmission requests.

4.5.1 Validation of Analytical Model

Firstly, we show the total burst loss results at a single optical node in Figures 4.7 and 4.8 for two different scenarios, respectively. In scenario one, $\lambda_a = 0.5\lambda$, $\lambda_b = 0.3\lambda$, $\lambda_{ab} = 0.2\lambda$, $p_a = 0.4$, p_b

= 0.6 and W = 8, 12, 16. On the other hand, in scenario two, $\lambda_a = 0.1\lambda$, $\lambda_b = 0.2\lambda$, $\lambda_{ab} = 0.7\lambda$, $p_a = 0.2$, $p_b = 0.8$ and W keeps the same. In general, the results from the analytical model fit the corresponding simulation curves quite well.

Comparing Figure 4.7 with Figure 4.8, We observe that the optical switch achieves better burst loss performance in scenario one than in scenario two for both simulation and analysis. The reason is explained as follows. In scenario one, most bursts (80% of total arrivals) can flow through only one output link, i.e., $\lambda_a + \lambda_b = 0.8\lambda$, and more importantly the load for the two links is balanced. The rest 20% of total arrivals would be directed to two links (ℓ_a and ℓ_b) proportionally too (i.e., p_a = 0.4 vs. $p_b = 0.6$). On the contrary, in scenario two, the load for ℓ_a and ℓ_b is seriously unbalanced. Although 70% of total arrivals (i.e., $\lambda_{ab} = 0.7\lambda$) shall select one out of them, ℓ_b is given obvious precedence over ℓ_a since p_b is equal to 0.8. In conjunction with the fact that a very small amount of bursts are destined for ℓ_a only (i.e., $\lambda_a = 0.1\lambda$), ℓ_b would consequently be overloaded whereas ℓ_a is kind of underutilized. This results in worse loss performance in the optical switch which proves indirectly that dynamic balanced routing plays a vital role in improving burst loss performance.

Figure 4.9 illustrates the results for the seven-node Ring at both W = 10 and W = 20 (we got similar results for the six-node Ring), while Figure 4.10 shows the comparisons for a variety of Ring networks across different network loads. As a whole, the simulation results are in good agreement with the results obtained from the analytical model. We also observe that the model and simulation are almost identical at low loads, and the model is reasonably accurate at high loads. This is expected because the actual minor blocking interdependencies among different links

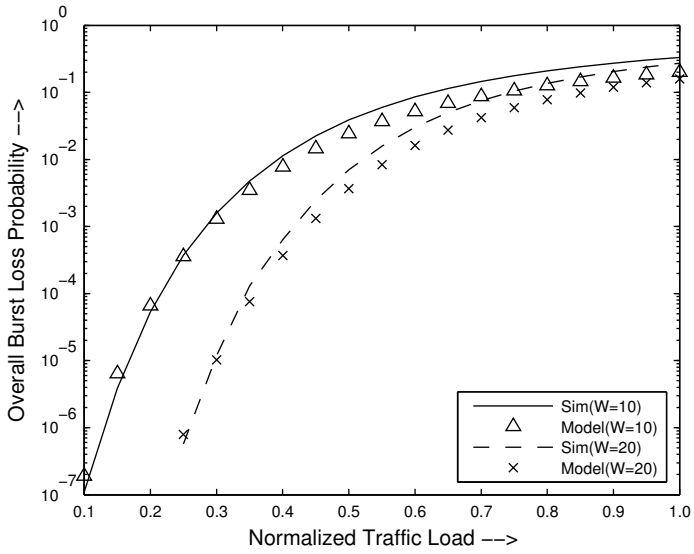

Figure 4.9: Overall burst loss versus load (Seven-node Ring).

are negligible at low loads, but they lead to burst loss underestimation in analysis at high loads. It is also interesting to observe that when N grows the simulation results still match with the corresponding analysis results very well.

4.5.2 Network Performance on Mesh-torus 5 x 5

We investigate the burst lost performance and the fairness of the proposed hop-by-hop dynamic routing schemes in a 5 x 5 mesh-torus network. We also consider another three cases for performance comparison: general JET, BJET-F and BJET-R (with $g = 0.5$ for both BJETs) which all use a static lightpath between any SD pair computed by the shortest-path-first method. Since general

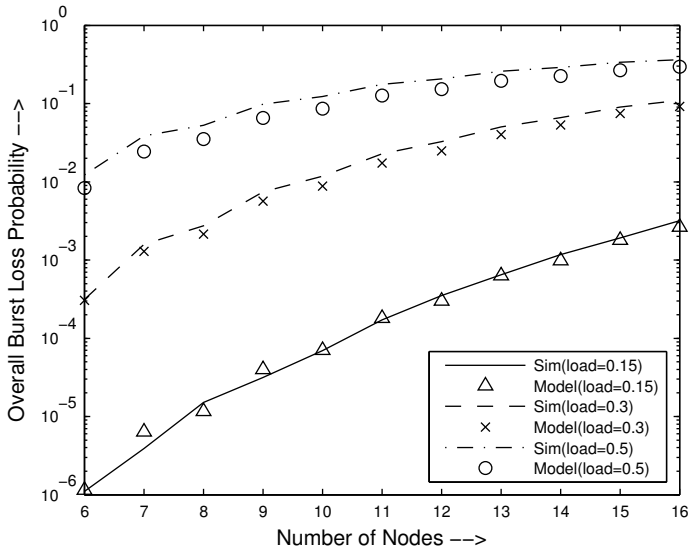

Figure 4.10: Overall burst loss versus load across different Rings at $W = 10$.

JET does not employ any special treatment to deal with fairness, we consider it as the *Base* case for performance comparison.

In the 5 x 5 mesh-torus network, each bidirectional fiber link consists of W data channels, excluding the one dedicated to the control channel. No buffering is assumed in optical nodes. For each burst arrival, the SD pair is uniformly selected; hence all the SD pairs have the same traffic load. The average burst length is 2 ms, and the transmission rate on a wavelength is 2.5 Gb/s.

4.5.2.1 Overall Burst Loss Performance Comparisons

Figure 4.11 plots the overall burst loss probability against load for all the six methods at $W = 4$. The three *FCR*-based dynamic routing schemes are much superior at light and moderate loads.

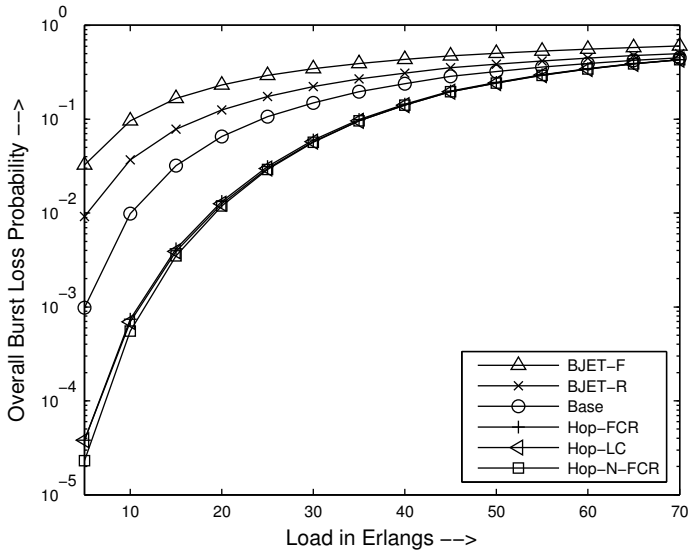

Figure 4.11: Overall burst loss versus load at $W = 4$ (Mesh 5 x 5).

The rationale behind this observation is mainly because dynamic routing can maximize the link utilization as much as possible. Since Hop-LC tries to distribute data bursts to the candidate nodes having a higher forward connectivity index, it has better chances to let bursts go through successfully and thus performs slightly better than Hop-FCR (the discrepancy is too small to discriminate though). As expected, Hop-N-FCR performs best because it utilizes more link state information than others ($\xi = 0.8$ is used for all tests as we found Hop-N-FCR performs best with this value). On the other hand, the *Base* method (general JET) outperforming both balanced JET techniques proves the general concept that fairness can be improved ordinarily at the expense of burst loss performance reduction. BJET-F and BJET-R intentionally block part of short-route bursts which may cause unnecessary burst drops. And besides, although long-route bursts are more likely getting accepted when they are approaching to the destination node, they have the same difficulty (very

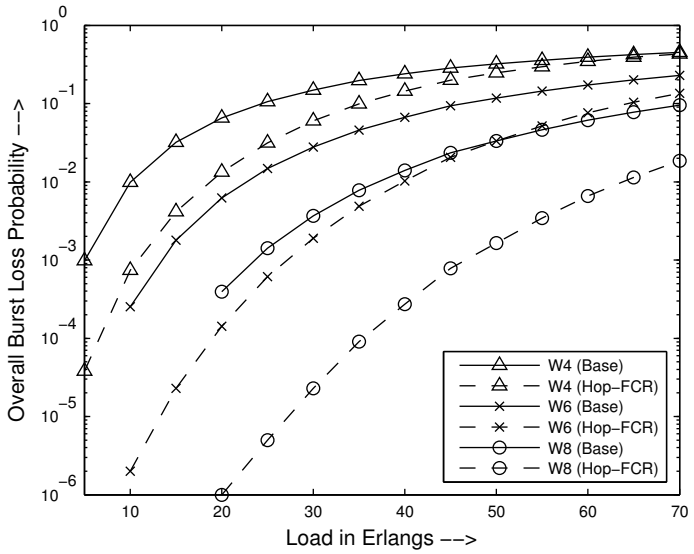

Figure 4.12: Overall burst loss versus load at various *Ws* (Mesh 5 x 5).

limited number of wavelengths to choose) going through the first or even the second hop according to (4.1) as the bursts with shorter total hops. Since BJET-F always searches the limited space $[1, n_i]$ for a free wavelength for incoming bursts at their ith hops, it would cause a larger number of wavelength collisions at the first or second hop, which may result in excessive drops of bursts. BJET-R avoids this drawback by checking the entire wavelength space $[1, W]$ randomly for a free channel as long as the total number of examined channels is also restricted to n_i. This explains why BJET-R is superior to BJET-F.

Figure 4.12 compares the overall burst loss probability against load for general JET and Hop-FCR with different number of wavelengths. It shows at low loads Hop-FCR can improve the performance by one order of magnitude at $W = 4$, and even two orders of magnitude at $W = 6$ and $W = 8$. This growing performance gain over *Base* is because Hop-FCR can dynamically distribute

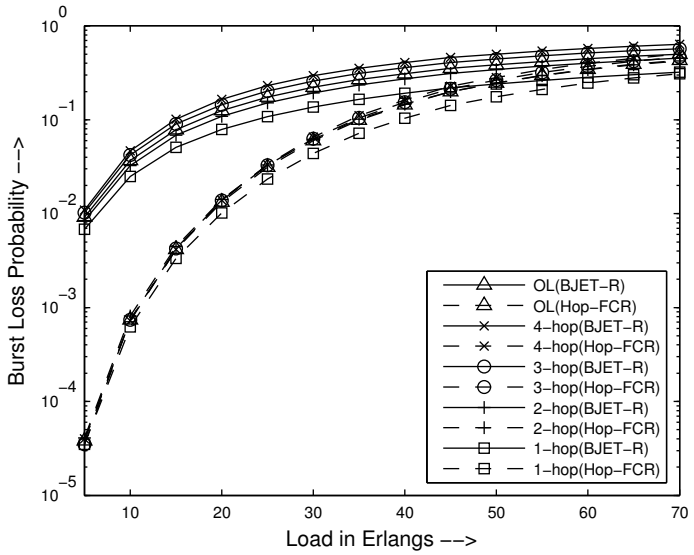

Figure 4.13: Burst loss versus load for different hops at $W = 4$. OL stands for overall burst loss in this and following figures (Mesh 5 x 5).

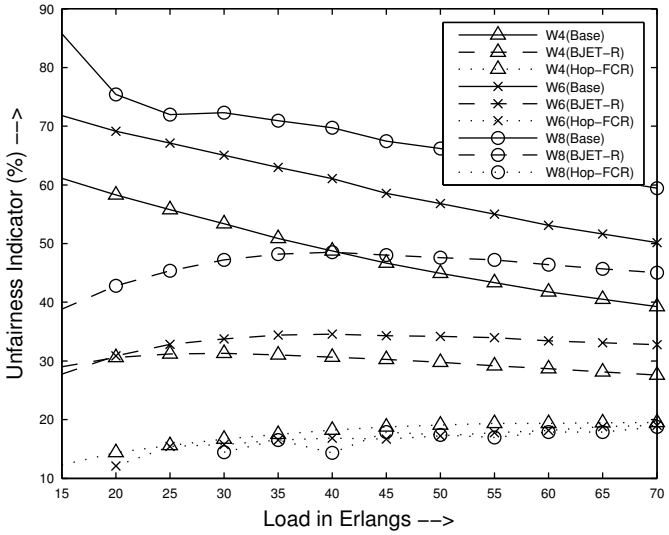

Figure 4.14: Unfairness measure versus load at various *Ws* (Mesh 5 x 5).

the burst arrivals more evenly to the next hops based on the *FCRs* when W gets larger, leading to a higher effective link utilization. When load becomes higher, the performance discrepancies between the two methods vanish gradually as expected and they eventually saturate at a similar level, but at a higher load for a larger W.

4.5.2.2 Fairness Comparisons

Figure 4.13 demonstrates the burst loss performance based on the number of hops for BJET-R and Hop-FCR at $W = 4$. We do not consider BJET-F here because it is not meaningful that someone would appreciate the improved fairness by tolerating a large performance drop. It is clear to see in Figure 4.13 that there are distinguishable disparities between bursts of different hops for almost all loads in BJET-R. On the contrary, very small discrepancies exist in Hop-FCR except for one-hop bursts at medium/high loads. We shall explain why the two schemes behave differently by combining Figure 4.14.

Figure 4.14 shows the modified coefficient of variance against load, which gives the unfairness measurement for the entire network in a quantitative way. Abstractly speaking, it is desirable to achieve two general fairness properties with any scheme: 1) CoV' (the metric of unfairness) starts at smaller values. Since there is a light contention at low loads usually, the system employed with even a simple fairness-improving technique can manage to transmit most bursts end-to-end

regardless of total hops. It thus achieves better fairness than when short-route bursts get more precedences inherently at tight contention; 2) Fairness improves at same loads if W increases or at least keeps a similar level. Nowadays fiber technology continues improving and a fiber link is expected to carry more wavelengths. Apparently, it would be destructive if the fairness problem gets worse when W increases. As displayed in Figure 4.14, *Base* behaves adversely due to lacking of capability to deal with fairness. On the other hand, BJET-R is in compliance with property one but violates property two, whereas Hop-FCR is in good agreement with both properties. It can be explained as follows: BJET-R achieves fairness by limiting the number of wavelengths for searching at smaller hops, but it performs wavelength assignment statically and cannot adapt to the real traffic loads. When W increases, the performance gains obtained by bursts with smaller hop counts grow faster than ones with larger hop counts, which results in poorer fairness as a consequence. Hop-FCR, however, provides a larger proportion of underutilized data channels to long-route bursts dynamically, as demonstrated in the sample Figure 4.2 and Subsection 4.3.5. Therefore, it can improve fairness and overall burst loss performance both to a large extent.

In order to investigate the fairness improvements by the proposed three adaptive schemes in greater detail, we plot the ratio of burst loss probabilities of i-hop bursts to that of all incoming bursts individually in Figures 4.15 and 4.16. Figure 4.17 compares the unfairness measurements based on CoV'. Basically, the three methods perform very closely and all converge at a level of less than 20% CoV', but Hop-LC slightly outperforms the other two when load is greater than 30 Erlangs. It is worth pointing out that since overall burst loss probabilities are almost identical

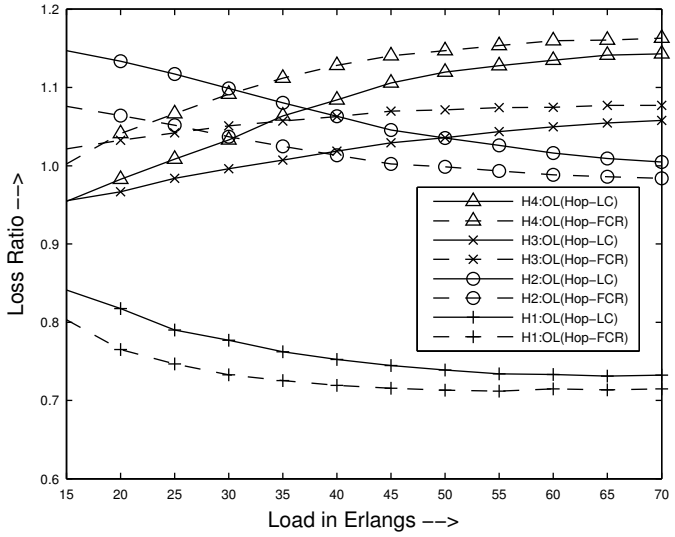

Figure 4.15: Loss ratio for i-hop bursts versus load at $W = 4$ (Mesh 5 x 5).

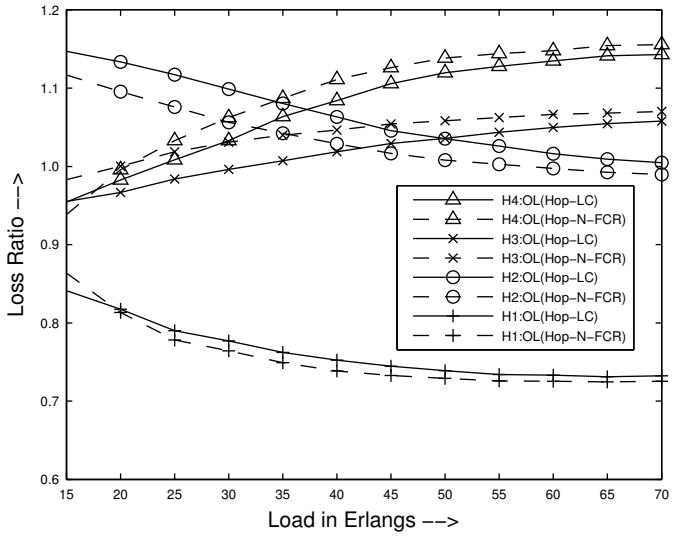

Figure 4.16: Loss ratio for i-hop bursts versus load at $W = 4$ (Mesh 5 x 5).

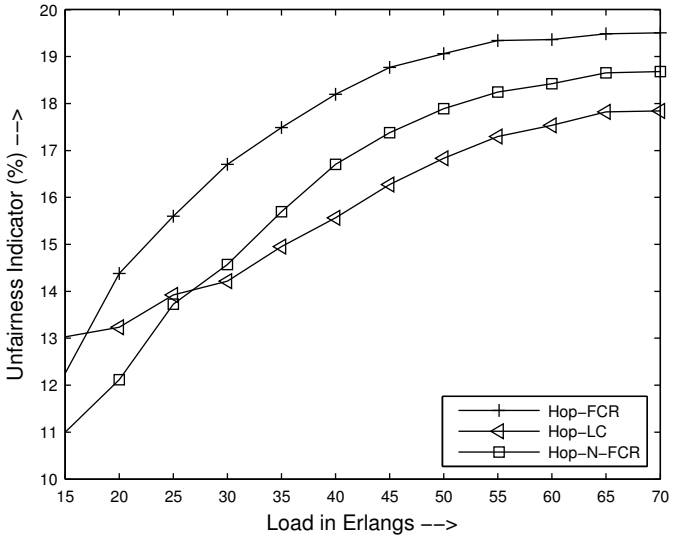

Figure 4.17: Unfairness measure versus load at $W = 4$ (Mesh 5 x 5).

for the three schemes as displayed in Figure 4.11, Figures 4.15 and 4.16 can be used to compare approximately the absolute burst loss probabilities of counterparts in two methods, i.e., one-hop bursts have a higher loss probability in Hop-LC than in Hop-FCR. The two figures show Hop-LC gains better fairness at moderate and high loads by letting more long-route bursts (three-hop and four-hop bursts) go through. We have discussed previously that because Hop-N-FCR considers the *FCRs* both on the immediate candidate links and the next candidate links, it may understand the network congestion state better than Hop-LC. At low loads, this advantage leads to even higher bandwidth utilization in Hop-N-FCR. Hence, the drop performances for all arriving bursts regardless of total hops have been improved, which can be observed in Figure 4.16. Nevertheless, when load grows the second part on the right side in (4.9) may contain too many outdated or conflicting data channel reservations as discussed in Subsection 4.3.4. This negative effect aggravates

when bursts have to pass through more hops which gradually degrades the performance as well as fairness-capability of Hop-N-FCR and makes it less superior to Hop-LC.

4.5.3 Network Performance Summary

We have also conducted tests on the European Optical Network of 19 nodes and 38 links at various *Ws*, and the results are in compliance with those of the Mesh 5 x 5 network (the simulation results are omitted here due to space limitations). Overall, we can summarize our main findings as follows.

- The proposed routing schemes can achieve lower burst loss probability than both BJET methods and the general JET scheme, especially under low loads. This performance gain generally grows when W increases.

- Unlike conventional methodologies which often secure fairness at the expense of burst loss probability, the proposed schemes are meant to improve both performances. By distributing the underutilized link resources dynamically in favor of longer-hop bursts, the proposed schemes can even keep the improved fairness at a similar level when W increases.

- The performance improvement depends on various parameters, including the link state information utilized by the routing mechanism, the network topology and the traffic load. In many cases, the performance improvement over shortest path routing can be considerable. The extended adaptive routing along with a reasonably-set parameter η is suggested for

sparse topologies and may perform better than the regular adaptive routing in general mesh networks.

- Hop-N-FCR routing can further reduce the burst drop probability at low loads. However, considering the increased computation complexity and the support required for information collection and dissemination, it is best to use Hop-LC which is simpler to implement and has better fairness-capability.

4.6 Summary

In this chapter, we proposed three adaptive routing schemes namely Hop-FCR, Hop-LC and Hop-N-FCR to decrease burst losses and solve the fairness problem in OBS networks. They adopt forward channel reservation to dynamically route the burst arrivals hop-by-hop. We evaluated the proposed methods with simulation, and numerical results showed that our methods are highly effective in OBS mesh networks. They can generally achieve dramatic improvement in both burst loss performance and fairness. We also observed that Hop-N-FCR obtains the best fairness at low loads while Hop-LC dominates at moderate and high loads. In short, Hop-LC is suggested in terms of burst loss performance, fairness and implementation complexity. We developed an analytical model to help predict the end-to-end burst loss probability in general Ring networks operated under the simplified first-hop adaptive routing. The analytical model was verified via simulation.

CHAPTER 5

CONVERSION CASCADING IN OBS NETWORKS

In contrast to optical circuit switching, it will incur too much overheads in OBS if we try to develop a wavelength scheduling scheme and/or routing algorithm on the basis of global link state information. This is because bursts are relatively short and link states change too frequently. Therefore, investigations of burst loss performance in OBS often assume that contention resolution is achieved in the wavelength domain through full wavelength conversion [QY99, XVC00, YQD00, WMA00]. Chapters 2 and 3 have shown that the conversion cascading constraint may increase blocking probability in OCS networks substantially, especially in the environment of full wavelength conversion. We expect similar negative side effects to exist in OBS networks. Due to the inherent differences of signaling protocols between the two switching mechanisms, we need to further investigate this negative impact in OBS in order to design effective methods to resolve or alleviate this problem. Based on the fairness-improving adaptive routing presented in Chapter 4, we develop a proactive routing scheme to counteract the negative impact and also extend the proposed mechanism to embrace a variant of regulated deflection routing which can further improve network performance.

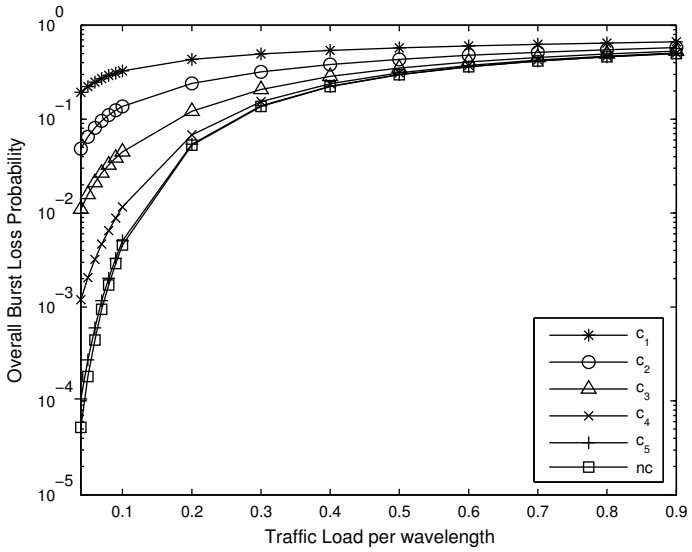

Figure 5.1: Increasing losses under the conversion cascading constraint.

Table 5.1: Negative impact of the conversion cascading constraint on fairness (U.S. Long-Haul, load = 0.06)

constraint	one-hop	two-hop	three-hop	four-hop	five-hop	six-hop	seven-hop
nc	6.19E-4	0.001631	0.003054	0.004532	0.006056	0.007606	0.00704
c_3	6.14E-4	0.001614	0.003036	0.004501	*0.029045*	*0.072899*	*0.107434*
c_2	5.69E-4	0.001491	0.00281	*0.052729*	*0.126291*	*0.200644*	*0.237704*
c_1	3.42E-4	8.62E-4	*0.133151*	*0.268722*	*0.393779*	*0.496653*	*0.537703*

5.1 Preliminary Experimental Examples

As aforementioned, it is expected that the enforcement of the conversion cascading constraint would inevitably degrade the burst loss performance and probably worsen the fairness problem too. In this section, we will demonstrate some preliminary experimental examples about the negative impact of this constraint.

Figure 5.1 illustrates the overall burst loss probability versus traffic load per wavelength in the U.S. Long-Haul network. The number of wavelengths per fiber link (W) is equal to six, and JET is used as the signaling protocol in this simulation. Under c_1 to c_4, burst loss rates are significantly higher than that under *nc* at light and medium traffic loads. The performance degradation at light loads ranges from one order to three orders of magnitude. When the conversion cascading threshold is higher (c_5 or even higher), the performance difference between c_i and *nc* becomes very small or completely disappears. On the other hand, we deduce that when W gets larger more wavelength conversions would appear and possibly there would be more data bursts getting dropped because of the cascading constraint. This conjecture is proved later in the detailed performance evaluation.

Table 5.1 shows the relationship between loss rate and hop count with various thresholds of the conversion cascading constraint. The performance results for *nc* act as the baseline during comparison. It is clear from Table 5.1 that even under no existence of the conversion cascading constraint the unfairness among bursts of different hop counts is still significant. For example seven-hop bursts have ten times the loss rate of one-hop bursts (0.00704 vs. 6.19E-4). We thus can reason that the fairness problem would worsen if we take the conversion cascading constraint into account. Since i-hop bursts require a maximum of $i-1$ wavelength conversions for successful transmission, the loss rate of bursts with four or less hops is not expected to increase because of the presence of constraint c_3. Similarly bursts with three hops or less are not affected by the constraint c_2 and so on. Actually, we observe in Table 5.1 that under c_3 the loss performance of one-hop to four-hop bursts has improved to different extents compared with the case of *nc*, but the losses of

longer-hop bursts have increased adversely which makes the fairness problem much more serious. Similar phenomenon happens for c_2 and c_1. This behavior is understandable because when longer-hop bursts are excessively blocked due to the cascading constraint, more wavelengths are left free for shorter-hop bursts.

5.2 Proposed Work

Most of the previously proposed scheduling and/or routing mechanisms in OBS have assumed full wavelength conversion. Nobody has considered the negative impact of the conversion cascading constraint, nor did anyone attempt to minimize the number of conversions required. we now proceed to describe our proposed proactive routing scheme and an extension in this section, which take the scheduling and routing jointly when bursts are on their way from source to destination. We demonstrate burst loss reduction and fairness improvement simultaneously, among other advantages under the environment of the conversion cascading constraint.

5.2.1 Hop-based Proactive Routing

The fairness-improving adaptive routing scheme called Hop-LC is suggested in Chapter 4 in terms of burst loss performance, fairness and implementation complexity. Therefore, we adapt

Algorithm 1 Hop-LC-CC

Input: New burst $\Gamma_{new} = \langle \lambda_{prev}, \Delta_c \rangle$, c_{max}, current *node i* and current schedule

Output: Grant reservation request of Γ_{new} or not, if yes return chosen next *node* n_x;

$n_x \leftarrow -1, \Lambda \leftarrow \phi, \Omega \leftarrow \phi$;
$\Psi \leftarrow$ neighbor node id's calculated by means of designated routing;
while $\Psi \neq \phi$ **do**
  $j \leftarrow$ next neighbor node;
  if (Γ_{new} can be scheduled via λ_{prev} on link e_{ij} using LAUC-VF) **then**
    $\Lambda \leftarrow \Lambda \cup \{j\}$; /* w/o conversion to reach *node j* */
  else
    $\Omega \leftarrow \Omega \cup \{j\}$; /* w/ conversion to reach *node j* */
  end if
  Remove *node j* from Ψ;
end while
if ($\Omega == \phi$) **then**
  $n_x \leftarrow j$ such that $Pref(j) = \min_{\forall k \in \Lambda} Pref(k)$;
else if ($\Lambda == \phi$ and $\Delta_c < c_{max}$) **then**
  ($\Delta_c \leftarrow \Delta_c + 1$, $n_x \leftarrow j$) such that $Pref(j) = \min_{\forall k \in \Omega} Pref(k)$ and Γ_{new} can be scheduled on link e_{ij} using LAUC-VF;
else if ($\Omega \neq \phi$ and $\Lambda \neq \phi$) **then**
  $n_{nc} \leftarrow j$ such that $Pref(j) = \min_{\forall k \in \Lambda} Pref(k)$;
  $n_c \leftarrow k$ such that $Pref(k) = \min_{\forall j \in \Omega} Pref(j)$ and $\Delta_c < c_{max}$ and Γ_{new} can be scheduled on link e_{ik} using LAUC-VF;
  if ($(Pref(n_{nc}) - Pref(n_c)) > \sigma \times L$) **then**
    $n_x \leftarrow n_c, \Delta_c \leftarrow \Delta_c + 1$;
  else
    $n_x \leftarrow n_{nc}$;
  end if
end if
if ($n_x \neq -1$) **then**
  Reserve resources for Γ_{new}, update λ_{prev} and return n_x;
else
  Drop new burst Γ_{new};
end if

Hop-LC to accommodate the constraint of cascaded wavelength conversions. The new algorithm is named hop-by-hop proactive routing using FCR and neighborhood link connectivity under conversion cascading (Hop-LC-CC). In Algorithm Hop-LC-CC, the wavelength utilized by the previous hop is favorable when it is free at the current hop and thus unnecessary conversions are avoided during the scheduling and routing process. Nevertheless, when converters are required (i.e., a conversion is inevitable when the control packet tries to schedule the burst on any candidate link e_{ij}), we will have to consider the preference value and the conversion cascading constraint together. In the algorithm, λ_{prev} denotes the wavelength used at the previous hop(s), Λ denotes the set of candidate nodes that the burst can be scheduled via λ_{prev} on the corresponding links from the current node i to them, and Ω denotes the set of candidate nodes that can be reached only through wavelength conversion. When Ω is empty ($\Omega = \phi$), it corresponds to the condition that no converters are involved and a neighbor node from Λ with the minimum preference value will be picked. When Λ is empty, it indicates one wavelength conversion will have to be conducted in order to transmit the new burst at the current hop. When both Ω and Λ are not empty, we first need to find both candidate nodes with the minimum preference values from their respective sets. If and only if the preference value along with a conversion (from Ω) is less than the one without any conversion (from Λ) to a certain extent ($\sigma \times L$, L is the average burst duration time and σ is a tunable parameter), the candidate node requiring a conversion is picked. Moreover, if the total number of accumulated conversions (Δ_c) has reached the threshold (c_{max}), no more conversions will be accepted due to the conversion cascading constraint. This scheme tries to balance the trade-

off between wavelength conversion and link utilization, which is proved to be effective in the next performance study section.

The routing method proposed also bears fairness-solving in mind, which distinguishes itself from the other adaptive routing mechanisms [TVJ03, YR06, OA05]. By being offered more routing opportunities, those longer-hop bursts will have a relatively greater possibility of passing through intermediate optical nodes. As a consequence, better fairness can be achieved as desired.

5.2.2 Deflection-enabled Hop-LC-CC (Hop-LC-CC2)

Despite of the buffering issue and the possible oscillation effect at high loads, it has been proved that deflection routing brings great improvement on burst loss performance [WMA00, HLH02, CWX03, LSK03, ZVZ04]. As illustrated in [HLH02], unlimitedly performing deflection does not always bring performance gain. The reason is that more deflection occurrences will cause longer end-to-end delay, which is equivalent to occupying more resources. Consequently, we enable a variant of deflection in the proposed Hop-LC-CC which is subject to the following two conditions:

- Condition I: there is a limit on the additional deflection hops to avoid side effects. This condition is different from the deflection frequency limit applied in [HLH02] which implies the maximum allowed deflection occurrence (f_{max}) cannot exceed a specified number. As we know, whenever a deflection occurs, the original routing path will be lengthened. Let

$d(b)$ denote the additional deflection hops of a burst b. The limit on $d(b)$ indicates the total allowed hops increased because of deflection cannot exceed a network-wide threshold D_{max}, i.e., $d(b) \leq D_{max}$ for any burst b.

- Condition II: another restriction specifies that bursts may not trigger deflection even if they have not reached the pre-set maximum deflection hops. The decision is based on the original hop count $h(b)$ (before any deflection) of bursts in transmission. As described, Hop-LC-CC inherently possesses the capability to solve or alleviate the fairness problem. However, this fairness-relevant capability depends on network topology. For instance, it is expected to acquire better fairness in a densely connected network than in a sparsely connected one where longer-hop bursts may have as few routing options as shorter-hop bursts. This condition ($h(b) \leq H_{start}$, where H_{start} is the bound) specifies particular short-hop bursts cannot carry out deflection routing and leave more free wavelength channels to the rest.

We shall refer to this extension of Hop-LC-CC as Algorithm Hop-LC-CC2. In Hop-LC-CC2, we extend Algorithm Hop-LC-CC to embrace deflection routing when the latter cannot accommodate the new burst Γ_{new}.

Algorithm 2 Hop-LC-CC2

begin Execute Hop-LC-CC to schedule the incoming burst;
  if Hop-LC-CC returns with a failure **then**
    $\Theta \leftarrow$ all unvisited neighbor nodes of the current *node i*;
    $d(b) \leftarrow$ the minimum number of total hops added to the original routing path if deflected to nodes in Θ;
    if $((d(b) > D_{max})$ or $(h(b) > H_{start}))$ **then**
      Drop new burst Γ_{new};
    else
      if Γ_{new} can be deflected to every node in Θ via λ_{prev} using LAUC-VF **then**
        Pick the neighbor node minimizing the number of increased hops and schedule Γ_{new};
      else
        Pick the neighbor node minimizing the number of increased hops such that $\Delta_c < c_{max}$ and schedule Γ_{new} using LAUC-VF;
      end if
    end if
  end if

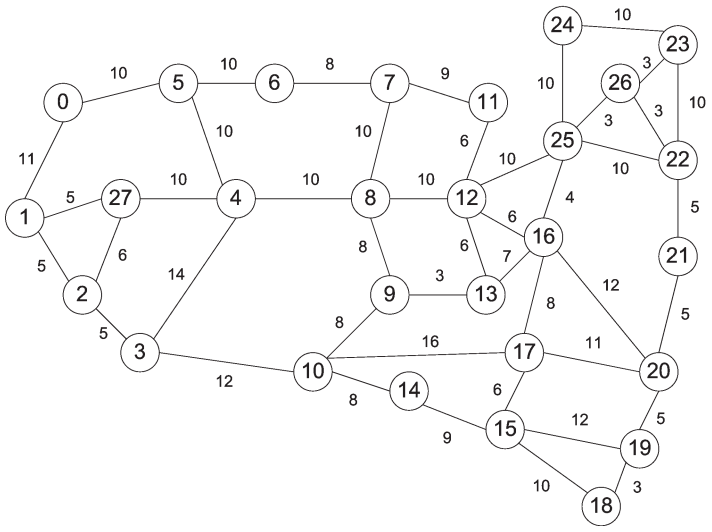

Figure 5.2: U.S. Long-Haul network topology.

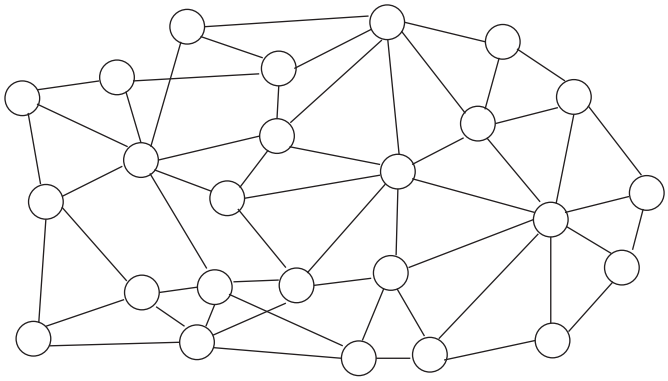

Figure 5.3: Toronto Metropolitan network topology.

5.3 Experimental Results

In this section, we investigate the burst lost performance and the fairness of the two proposed dynamic routing mechanisms. We also consider another three cases for performance comparisons: FSR (fixed shortest-path routing), FSR-CasCt (FSR under the Conversion Cascading Constraint) and FSR-CA (FSR with Conversion Avoidance). They all adopt a static lightpath between any two nodes computed by the shortest-path-first method and the LAUC-VF channel scheduling algorithm. FSR is a general JET method which does not consider the conversion cascading constraint. On the other hand, FSR-CasCt, based on FSR, additionally blocks a burst request if it has already conducted the maximum number of wavelength conversions but still requires another one for its next scheduling. FSR-CA, however, is more intelligent than FSR-CasCt in that it tries to first schedule the bursts on the same wavelengths utilized in the previous hop(s) and thus avoids unnecessary wavelength conversions whenever possible. We consider FSR as the *baseline* case for performance comparisons.

The evaluation network models are the U.S. Long-Haul (Figure 5.2) and the Toronto Metropolitan (Figure 5.3) topologies. The Toronto Metropolitan topology [THT05] which has 25 nodes and 55 links is a high link density sample. The U.S. Long-Haul topology which has 28 nodes and 45 links is a low link density sample. The longest-shortest path between source and destination has six and four intermediate OXCs, for U.S. Long-Haul and Toronto Metropolitan, respectively. Therefore no burst needs more than six or four wavelength conversions to reach its destination. Meanwhile, most source-destination pairs in both networks have lightpaths with a much fewer number of intermediate OXCs. We assume that all nodes have the capability of full-range wavelength conversion. Every link is a bidirectional fiber and consists of W data channels. The burst arrival pattern follows a Poisson process, and the burst duration time is negative exponentially distributed with mean L. For each burst arrival, the source and destination nodes are uniformly selected. The time required for control packet processing in a single node is denoted as δ time units. In U.S. Long-Haul, the propagation delay of a link in milliseconds is 0.5 multiplied by the length label of that link. Thus, the delay for a link with length 6 is 3 ms. Unless specified, in both Hop-LC-CC and Hop-LC-CC2, σ is set to 2.0 or 6.0 for $W = 4$ and $W = 8$ respectively for U.S. Long-Haul. In Toronto Metropolitan every link has the same propagation delay of 0.1 ms, and σ is set to 8.0 for both Hop-LC-CC and Hop-LC-CC2 when $W = 8$ as it is denser than U.S. Long-Haul. Each data point shown in the performance graphs is obtained by running 10 million burst transmission requests.

5.3.1 Overall Burst Loss Performance Results

Figure 5.4 plots the overall burst loss probability against traffic load in U.S. Long-Haul for all the three static routing methods and the Hop-LC-CC algorithm at different *Ws*. The curves labeled with "nc" represent FSR without the conversion cascading constraint. It is easy to observe in Figures 5.4b, 5.4d and 5.4f that when $W = 8$, the conversion cascading constraint causes significant performance degradation to FSR-CasCt at light and moderate loads, in despite of the values of c_{max}. The worst could be over three orders of magnitude for a moderate constraint of c_3 at load 0.04 compared with the no-constraint environment. And it imposes similar negative impacts on FSR-CA and even Hop-LC-CC for $c_{max} \leq 3$. From this point of view, the negative impact of the conversion cascading constraint is *not* negligible at all. On the other hand, the influences illustrated in Figures 5.4a, 5.4c and 5.4e when $W = 4$ are not as distinct as those when $W = 8$. Combining these results with Figure 5.1, we can project that if W gets larger there will be more channels as well as voids available and consequently more conversions would occur. Generally speaking, the larger number of conversions, the more severe the negative impact of the cascading constraint would be. Actually, pure LAUC-VF is a kind of channel scheduling algorithm that is biased to converter utilization. It performs exhaustive searching trying to find the matching void throughout the available ones on all channels. This selection process regardless of wavelength converting is so predominant that it even counteracts the benefit of a larger W. Figures 5.4a and 5.4b show that the absolute overall burst loss probabilities are higher with $W = 8$ under c_1 - c_4 than their counterparts

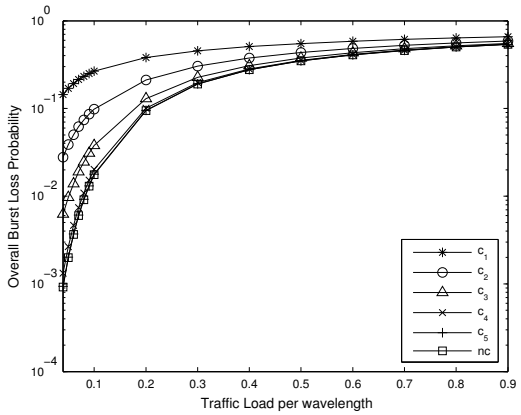

(a) FSR-CasCt, $W = 4$

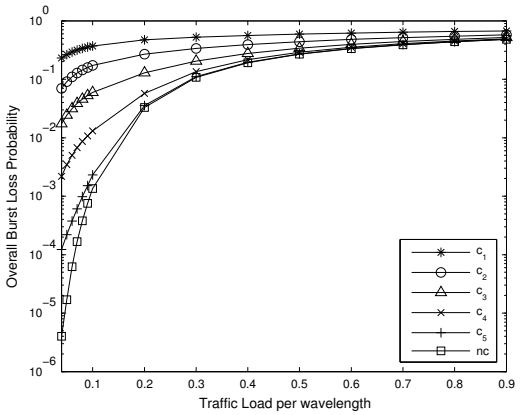

(b) FSR-CasCt, $W = 8$

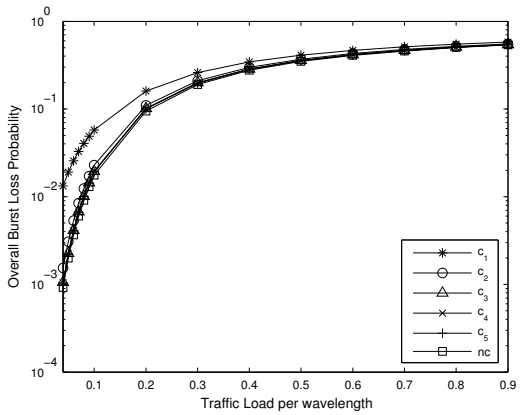

(c) FSR-CA, $W = 4$

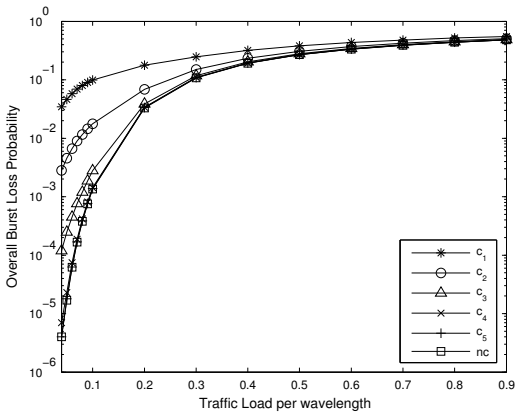

(d) FSR-CA, $W = 8$

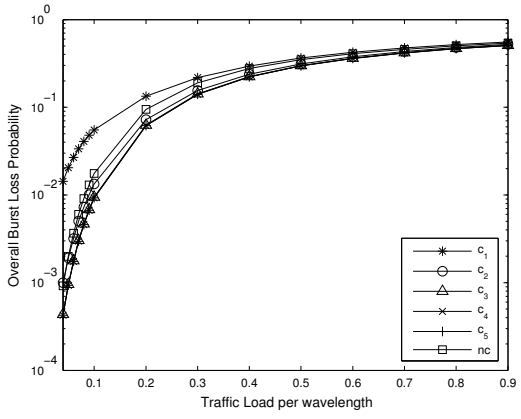

(e) Hop-LC-CC, $W = 4$

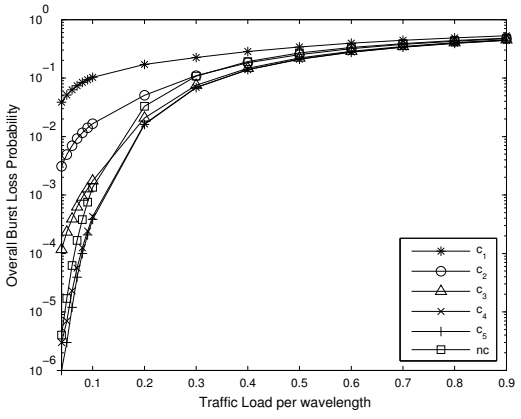

(f) Hop-LC-CC, $W = 8$

Figure 5.4: Overall burst loss probability versus traffic load per wavelength in U.S. Long-Haul ($\delta = 0.01L$).

with $W = 4$, especially at light loads when there are more voids available. Similar phenomenon happens in FSR-CA and Hop-LC-CC too but is much more slim since these two schemes possess certain intelligence to deal with the cascading constraint.

As illustrated in Figure 5.4d, owing to the conversion avoidance technique the burst loss performance of FSR-CA under $c_{max} = 4$ or 5 is almost the same as FSR without the cascading constraint. This indicates that conversion avoidance may be an economic and effective way to diminish or eliminate the impact caused by the cascading constraint in some not very stringent circumstances. Compared with FSR-CA, Hop-LC-CC is much superior especially when $c_{max} \geq 3$ as depicted in Figure 5.4f. It is worth pointing out that FSR-CA performs worse than FSR in all circumstances (i.e., no matter what the value of c_{max} is) due to the conversion cascading constraint, as expected. Nevertheless, Hop-LC-CC has better performance than FSR at all loads when $c_{max} \geq 4$ and at moderate/high loads when $c_{max} = 3$ (Figure 5.4f). The rationale behind this observation is mainly because Hop-LC-CC takes both the cascading constraint and link utilization into account during its dynamic routing and wavelength scheduling process. By distributing data bursts to the candidate nodes having a higher connectivity index as demonstrated in Equation (4.8), Hop-LC-CC obtains better chances to let bursts go through successfully and thus improve the link utilization as much as possible. Furthermore, in traditional deflection routing methods the loss performance is usually worse than that of fixed shortest-path routing at very high loads. As showed in Figures 5.4e and 5.4f, Hop-LC-CC does not preserve this prevalent undesirable property since the proactive routing limits the candidate nodes to only the nodes that are closer to the destination nodes.

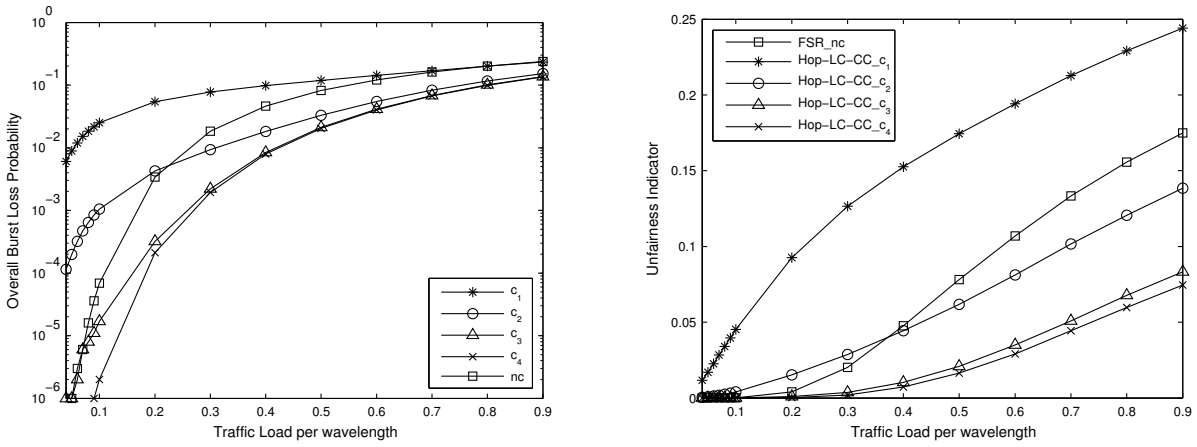

(a) (b)

Figure 5.5: Performance of Hop-LC-CC in Toronto Metropolitan ($\delta = 0.01L$, $W = 8$).

The different routing schemes have shown similar performance results on Toronto Metropolitan network under the environment of cascaded wavelength conversions. Due to the similarity, we only illustrate the loss performance of Hop-LC-CC when $\delta = 0.01L$ and $W = 8$ in Figure 5.5a. Since the diameter of Toronto Metropolitan is smaller but the network is denser, Hop-LC-CC is able to achieve performance gain even at a smaller c_{max}, e.g., when load > 0.2 Hop-LC-CC performs better than FSR_nc at c_2, compared with Figure 5.4f.

5.3.2 Fairness Results

We use a similar way as [HY08] to exploit the fairness achievement in this chapter. The unfairness indicator is defined as the standard deviation of mean burst loss probabilities calculated according

to statistics of bursts with identical total hop count. The lower the unfairness indicator is, the fairer a routing and/or scheduling algorithm is. As shown in Figures 5.6, 5.7 and 5.8 on the U.S. Long-Haul network, FSR acts as a baseline since it does not employ any special method to deal with fairness (the curves labeled with FSR_nc represent the same outcome under no constraint in all the three groups of figures if the two factors W and δ are the same). Basically, for all the three FSR-CasCt, FSR-CA and Hop-LC-CC schemes, we find that unfairness becomes more serious with smaller c_{max}. The reason is obvious: bursts with a high total hop count should suffer from higher loss probability because more of them will be blocked when the conversion cascading constraint is more stringent. We have explained in Subsection 5.3.1 that the above three schemes have worse loss performances with $W = 8$ in stringent cases (small c_{max}) mainly because LAUC-VF "encourages" converter usage. It has similar effect on unfairness which becomes worse when W is equal to 8 since longer-route bursts are more easily affected (Figure 5.6a vs Figure 5.6b under c_1, and so on). Overall, under the same c_{max} and provided the other factors are identical, FSR-CA outperforms FSR-CasCt whereas Hop-LC-CC performs the best and even a lot better than FSR in many cases. This superiority partly lies on more routing choices designated for bursts with a high total hop count in Hop-LC-CC. On the other hand, FSR-CA performs rather well which further proves conversion avoidance can preserve not only the loss performance but also the fairness in certain relaxed conditions.

Figures 5.6c, 5.7c and 5.8c plot the unfairness measurements with a larger packet processing time ($\delta = 0.1L$) for $W = 8$. We omit the corresponding figures for $W = 4$ because the comparison

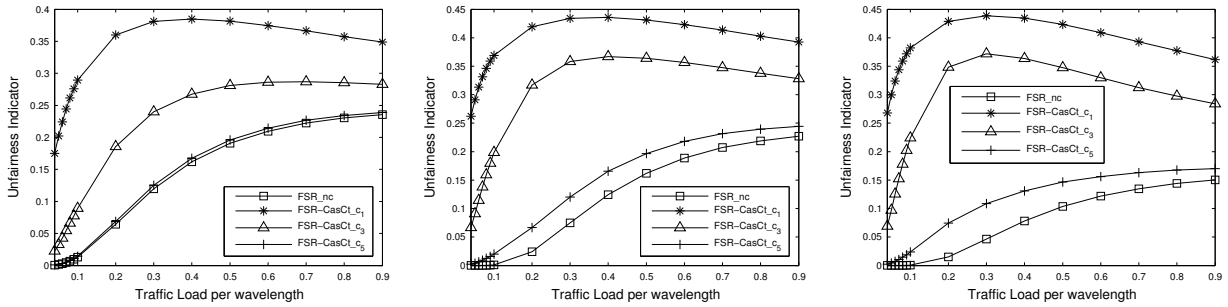

(a) $W = 4$, $\delta = 0.01L$ (b) $W = 8$, $\delta = 0.01L$ (c) $W = 8$, $\delta = 0.1L$

Figure 5.6: Unfairness measure versus traffic load per wavelength in U.S. Long-Haul (FSR-CasCt).

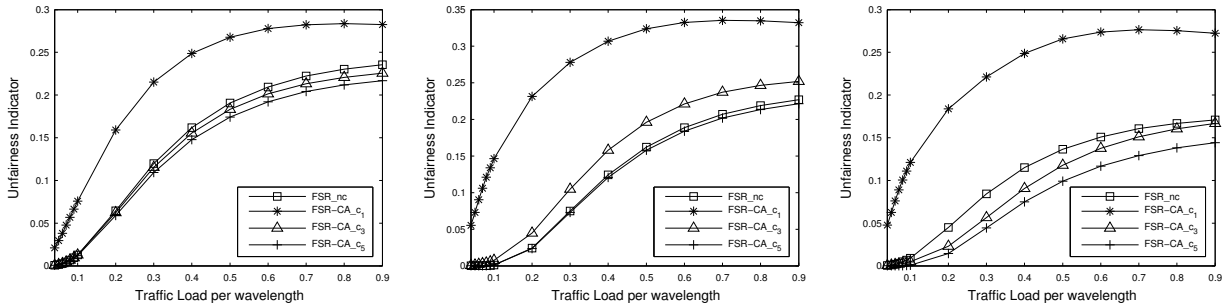

(a) $W = 4$, $\delta = 0.01L$ (b) $W = 8$, $\delta = 0.01L$ (c) $W = 8$, $\delta = 0.1L$

Figure 5.7: Unfairness measure versus traffic load per wavelength in U.S. Long-Haul (FSR-CA).

results are very similar. As the current offset time is determined by the remaining hop count, a larger δ can boost the advantage in the reservation process of longer-route bursts. Compared with the results showed in Figures 5.6b, 5.7b and 5.8b where $\delta = 0.01L$, Figures 5.6c, 5.7c and 5.8c show better performance which is in good agreement with the findings in [HY08]. Hop-LC-CC can achieve similar fairness on Toronto Metropolitan as shown in Figure 5.5b.

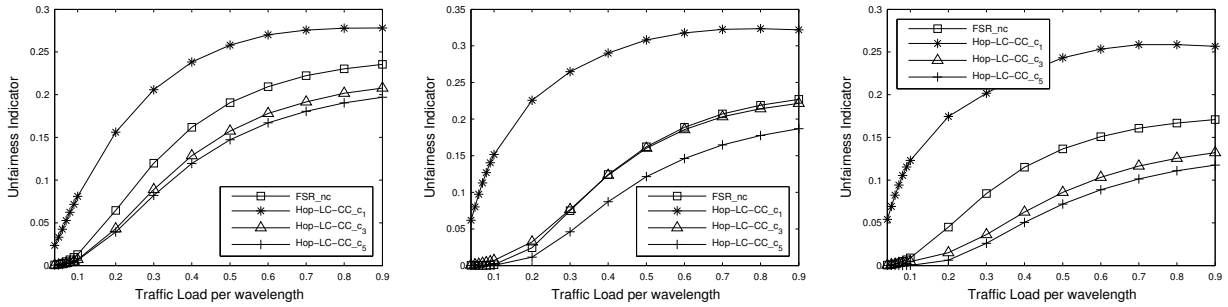

(a) $W = 4$, $\delta = 0.01L$ (b) $W = 8$, $\delta = 0.01L$ (c) $W = 8$, $\delta = 0.1L$

Figure 5.8: Unfairness measure versus traffic load per wavelength in U.S. Long-Haul (Hop-L-C-CC).

Table 5.2: Effect of σ on burst loss in Hop-LC-CC under $c_{max} = 3$ ($W = 8$, $\delta = 0.01L$)

traffic load	σ = 3.0	σ = 4.0	σ = 5.0	σ = 6.0	**σ = 7.0**	σ = 8.0	σ = 9.0
0.1	0.001778	0.001758	0.001754	0.001751	**0.00175**	0.00175	0.00175
0.2	0.020891	0.020841	0.0208	0.020791	**0.02078**	0.020785	0.020789
0.2	0.075895	0.075742	0.075648	0.075623	**0.075574**	0.075624	0.075648
0.4	0.147813	0.147578	0.147451	0.147505	**0.147479**	0.147491	0.147458
0.5	0.22004	0.219746	0.219755	0.219638	**0.219602**	0.21962	0.219806
					↑		

5.3.3 Effect of Sigma on Burst Loss in Hop-LC-CC

In Algorithm Hop-LC-CC, the scheduler will try to balance the tradeoff between wavelength conversion and link utilization in the case that a wavelength conversion is needed to reach some candidate nodes while no conversion is required to reach the rest of candidates. This property is controlled by the tunable parameter σ. It is expected that σ should depend on network topology, c_{max}, W as well as traffic load. When the other conditions are identical, the larger σ is, the more

Table 5.3: Effect of σ on burst loss in Hop-LC-CC under $c_{max} = 5$ ($W = 8$, $\delta = 0.01L$)

traffic load	σ = 1.0	σ = 2.0	**σ = 3.0**	σ = 4.0	σ = 5.0	σ = 6.0	σ = 7.0	σ = 8.0
0.1	3.81E-4	3.79E-4	**3.8E-4**	3.82E-4	3.82E-4	3.82E-4	3.83E-4	3.83E-4
0.2	0.01604	0.016005	**0.015992**	0.01603	0.016053	0.016075	0.016087	0.016096
0.3	0.068377	0.068225	**0.068173**	0.068236	0.068256	0.06833	0.068316	0.068348
0.4	0.138851	0.13854	**0.138386**	0.138465	0.138649	0.138576	0.138717	0.13872
0.5	0.210442	0.210099	**0.20999**	0.20992	0.210114	0.210035	0.21007	0.210033
			↑					

preference to wavelength continuity (bursts are to be scheduled to maintain wavelength continuity) would gain over wavelength conversion. Less wavelength conversions means that less bursts would be blocked due to the cascading constraint. However, extremely large σ would prevent the scheduler from scheduling bursts to a lightly loaded link even though the bursts have conducted no or only very few wavelength conversions so far. Tables 5.2 and 5.3 demonstrate the effect of σ on overall burst loss probability in the U.S. Long-Haul network under $c_{max} = 3$ (a moderate value) and $c_{max} = 5$, respectively. As analyzed above, to achieve the best performance σ cannot be extremely small or large. Approximately, $\sigma = 7.0$ and 3.0 show the lowest losses across various loads, respectively. When c_{max} gets larger, the impact caused by the cascading constraint becomes smaller. Consequently, more wavelength conversions can be fulfilled to improve the link utilization which accounts for why the network under $c_{max} = 5$ reaches the equilibrium state at a smaller σ according to Algorithm Hop-LC-CC.

In reality, the estimation of σ is also pertinent to link load. Thus, in order to obtain the best performance, it is desirable to first estimate the average link load through traffic engineering and then determine which σ should be used via simulation and analysis.

5.3.4 Performance Comparison with Deflection Routing

In order to discover further the effectiveness of Algorithm Hop-LC-CC, we also conduct a study on deflection routing and compare their performances. The deflection routing we implement is based on [HLH02]. We adapt it to the environment of cascaded wavelength conversions by incorporating the conversion avoidance technique used in FSR-CA. As a result, it is named DR-CA. During simulation, f_{max} (maximum allowed deflection occurrence) is set to up to two.

Figures 5.9a and 5.9c plot burst losses at $c_{max} = 3$ for U.S. Long-Haul and Toronto Metropolitan respectively. Figure 5.9a exhibits a typical scenario presented by deflection routing, where DR-CA brings performance gain under light load and the gain is gradually reduced under heavier traffic. On the other side, the two routing schemes perform adversely in Figure 5.9c. It can be interpreted as follows: since the Toronto Metropolitan topology is denser, both Hop-LC-CC and DR-CA have more choices during routing. When load is light, Hop-LC-CC has fewer burst losses owing to its managed routing (bursts are not directed to long lightpaths randomly as in DR-CA). Under heavier traffic the constrained paths in Hop-LC-CC may be congested, although there are still some other

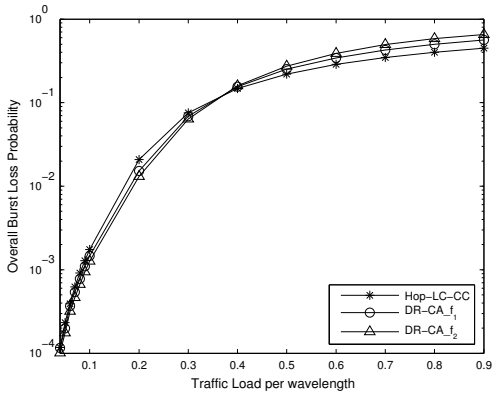

(a) U.S. Long-Haul, $c_{max} = 3$

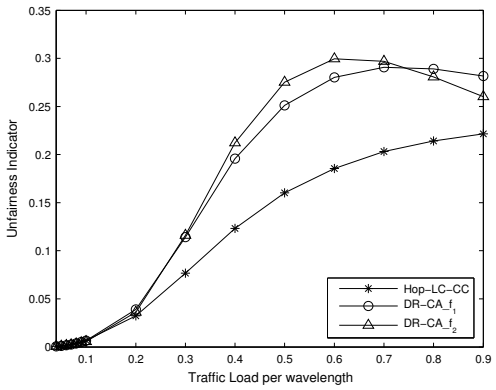

(b) U.S. Long-Haul, $c_{max} = 3$

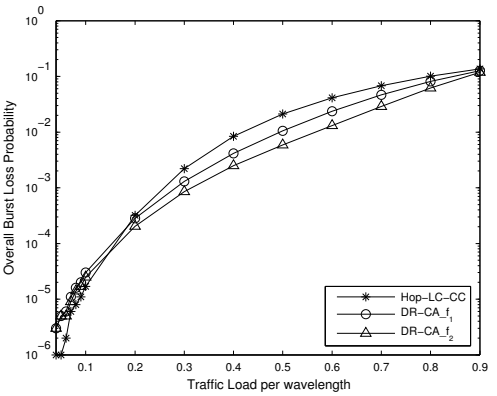

(c) Toronto Metropolitan, $c_{max} = 3$

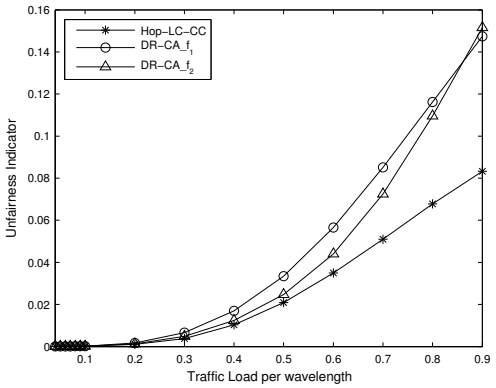

(d) Toronto Metropolitan, $c_{max} = 3$

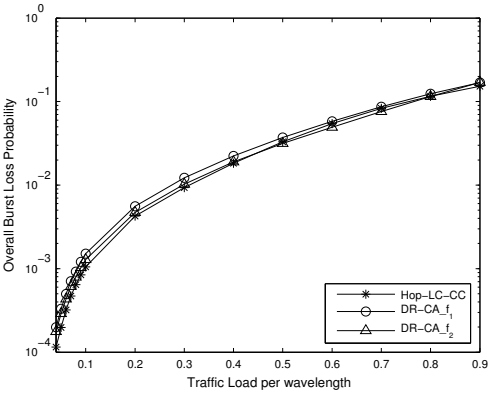

(e) Toronto Metropolitan, $c_{max} = 2$

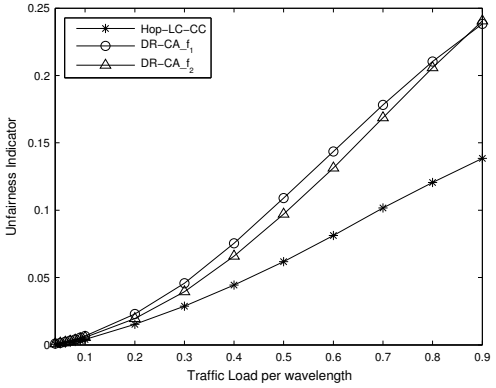

(f) Toronto Metropolitan, $c_{max} = 2$

Figure 5.9: Performance comparisons with DR-CA ($\delta = 0.01L$, $W = 8$).

underutilized links in a dense network as Toronto Metropolitan. DR-CA takes advantage of those underutilized links and consequently decreases its burst losses. However, this property of DR-CA is suppressed when c_{max} gets smaller because deflected bursts, that are expected to experience more wavelength conversions, get dropped more often. Figure 5.9e is in compliance with this inference. Because DR-CA concentrates on reducing burst losses, it has consistently shown poorer fairness than Hop-LC-CC in Figures 5.9b, 5.9d and 5.9f.

5.3.5 Performance of the Extension Algorithm Hop-LC-CC2

Figure 5.10 illustrates the performance comparisons regarding various configurations of D_{max} and H_{start} in Hop-LC-CC2. Since H_{start} is set to be greater than one, all bursts with only one hop will not perform any deflection routing. The curves labeled with Hop-LC-CC exhibit the corresponding performance outcomes of Algorithm Hop-LC-CC under the same circumstances. We have the following observations:

- First of all, Hop-LC-CC2 is superior to Hop-LC-CC for almost all configurations in regard to both loss and fairness. Apparently, the combination with deflection routing brings great improvement on loss performance, especially when traffic load is light as there is more room for improvement by deflection routing.

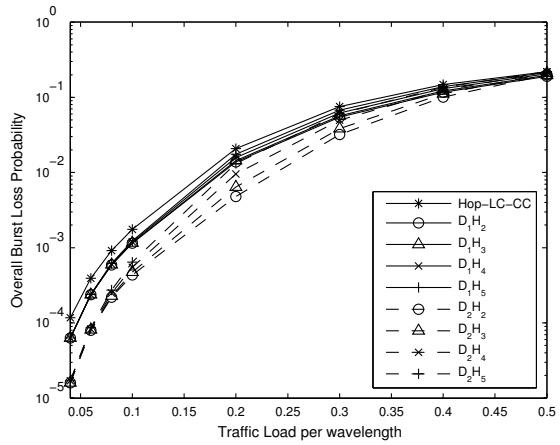

(a) U.S. Long-Haul, $c_{max} = 3$

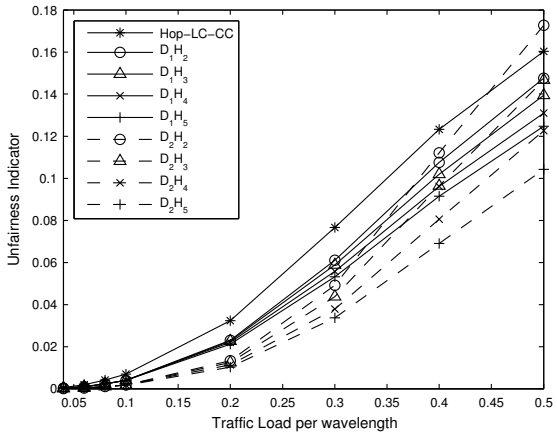

(b) U.S. Long-Haul, $c_{max} = 3$

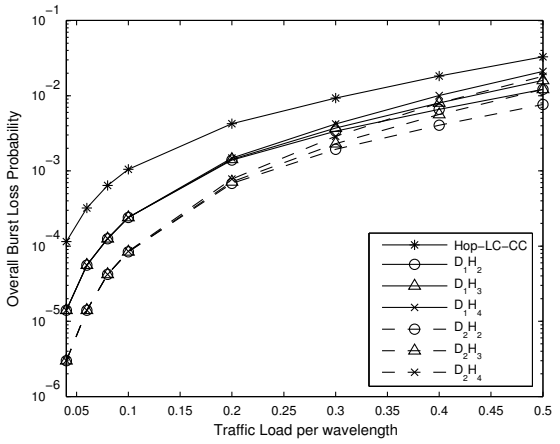

(c) Toronto Metropolitan, $c_{max} = 2$

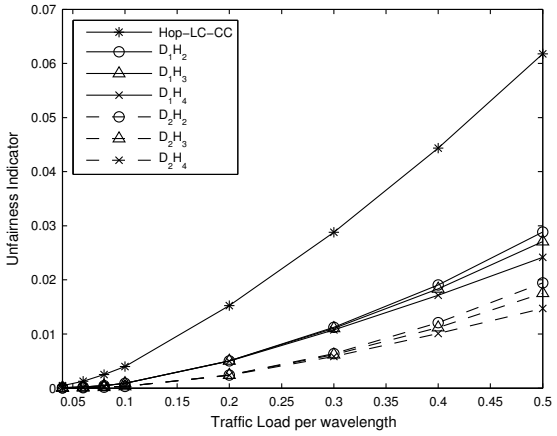

(d) Toronto Metropolitan, $c_{max} = 2$

Figure 5.10: Performance comparisons with Hop-LC-CC2 under various configurations of D_{max} and H_{start} ($\delta = 0.01L$, $W = 8$).

- In general, when the configuration is more aggressive (i.e., higher D_{max} and/or lower H_{start}), Hop-LC-CC2 can achieve even better performance. Although Hop-LC-CC2 has restrained deflection to a minimum level, the more aggressive configurations still bring many excessive deflections under high load. That causes negative impact and the improvement diminishes gradually. Considering fairness specifically, it is expected that Hop-LC-CC2 performs better

with $D_{max} = 2$ than with $D_{max} = 1$ in most cases, especially under light and moderate loads (Figures 5.10b, and 5.10d). However, with the same D_{max} if we want to achieve even better fairness, we should leave more deflection routing to longer-route bursts by setting a higher threshold of H_{start}.

5.4 Summary

In this chapter, we have examined the negative impact of the conversion cascading constraint in the JET-based OBS networks. We have shown that the impact on burst loss performance is quite noticeable or even significant when conditions are stringent. Furthermore, the fairness problem is worsened by this negative impact since bursts with a high hop count usually suffer much more than those with a short lightpath. Motivated by these observations, we proposed a novel proactive scheduling and routing scheme as well as an extension that adopts forward channel reservation to dynamically route burst requests under the cascading constraint. Extensive numerical results have demonstrated that our methods effectively improve burst loss performance and yields better fairness as well.

CHAPTER 6

PREEMPTIVE CHANNEL SCHEDULING

In this chapter we introduce a new preemptive scheduling technique for next generation OBS networks considering the impact of cascaded wavelength conversions. Subject to this practical impediment under full wavelength conversion, we improve a recently proposed fair channel scheduling algorithm to deal with the fairness problem and aim at burst loss reduction simultaneously in OBS environments. In our scheme, the dynamic priority associated with each burst is based on a constraint threshold and the number of already conducted wavelength conversions among other factors for this burst. When contention occurs, a new arriving superior burst may preempt another scheduled one according to their priorities. Extensive simulation results have shown that the proposed scheme further improves fairness and achieves burst loss reduction as well.

6.1 Related Work

In this section, we first discuss the fundamental wavelength scheduling algorithms, the contention problem, and then we shall investigate the fairness problem and several relevant approaches addressed in previous literature.

In JET-based OBS, data bursts are assigned variable offset lengths at edge nodes according to their path distance, and as the bursts are traveling through the network, these offsets will shrink. The presence of this variability and the dynamic random arrival of bursts create a large number of idle periods (voids) on wavelength channels. The scheduler in each optical node faces herein the challenge that it must accommodate efficiently bursts in the absence of global link state information. To overcome this difficulty, Xiong et al. [XVC00] proposed two scheduling algorithms called LAUC (latest available unscheduled channel) and LAUC-VF (LAUC with void filling), respectively. LAUC, which is the same as the Horizon algorithm [Tur99], maintains a single variable recording the latest reservation time of each channel and assigns the channel with the latest starting time that is still earlier than the arrival time of the incoming burst. LAUC is simple but cannot utilize all existing voids. LAUC-VF keeps track of all void intervals within the channel space and assigns the intervals that would give the minimum of gaps or voids. This has the effect of filling channel space more effectively, ensuring that any newly created voids would occur closer to the present time and hence be more capable of being filled by newly arriving bursts. The minimum starting void (Min-SV) algorithm [XQL03, XQL04] uses a geometric approach and organizes the

voids into a balanced binary tree. Min-SV algorithm finds a void that minimizes the distance between the starting time of the void and the starting time of the burst. It can produce efficient burst schedules as LAUC-VF but more quickly. A more efficient scheduling approach proposed in [CTM07] which requires a special hardware-based constant time burst resequencing (CTBR) scheduler can achieve only O(1) runtime complexity. CTBR is similar to the free channel queue (FCQ) burst scheduling algorithm introduced in [BS05, BS06], which fits in with the new dual-header optical burst switching (DOBS) architecture.

One of the primary objectives in the design of an OBS network is to minimize burst loss. Burst loss occurs primarily due to the contention of bursts in the bufferless core nodes. During scheduling, an arriving burst may contend with one or more scheduled bursts on the outgoing data channels. This contention results in the burst being dropped, leading to burst loss. Approaches for resolving contention include wavelength conversion [Gau04, AKD06], optical buffering [XVC00, WL04, CTM07], and deflection routing [WMA00, HLH02, CWX03, LSK03, ZVZ04]. Apart from these three contention resolution approaches, burst segmentation [VJS02, RVZ03] and preemption techniques [CCE03, TUK04, MMI05] were also proposed.

As we have discussed in OBS networks, the fairness problem causes the loss probabilities of optical bursts traveling through lightpaths with larger hop counts to be higher than those whose paths have a smaller number of hops. It is an important topic that we need to face and solve. The works [LTT04, ZBL04, ZBL07, HY08] were dedicated to improving fairness in OBS networks. The monitoring group drop probability (MGDP) approach [LTT04] intentionally drops a burst with a

small total hop count so that more resources can be left for bursts with longer paths. However, this feature may cause unnecessary burst drops and consequently blocking performance is sacrificed to satisfy fairness. Another disadvantage of MGDP is that it focuses on achieving fairness on a single switching node but may worsen the fairness of bursts transmission in the whole network as a result. The balanced just-in-time scheme (BJIT) proposed in [ZBL04] deals with the fairness problem by adjusting the size of the search space for a free wavelength based on the number of hops traveled by the burst. The size for searching is designed to grow gradually as the burst approaches to its destination. Similar to MGDP, BJIT may suffer from higher burst losses because some bursts with a short lightpath have difficulty in finding free wavelengths at their first or even second hop and get dropped excessively.

In addition to providing contention solution and achieving service differentiation as shown in [CCE03, TUK04, MMI05], preemption has also been used to offer fair scheduling in JET-based OBS networks as well. Provided carefully designed, when dropping is inevitable, preemption can pick the one maintaining fairness while causing the least significance to the network performance at the same time. The authors in [ZBL07] proposed to use constrained preemption to improve fairness without degrading network throughput. They set a couple of additional constraints to reduce resource waste and improve efficiency of preemption. On the other hand, the authors in [HY08] first provided an in-depth analysis of the fairness problem in JET-based OBS networks. They then derived a priority function evaluated on a bunch of parameters inferred from their analysis: successful hops, remaining hops, initial offset time, and average burst duration time. Preemption

(taking account of both fairness and loss performance) is triggered based on the priority function in case of any burst contention. The resulting fair prioritized preemption algorithm (FPP) is remarkable and the simulation results showed that it yields better fairness and lower losses than the other two fairness solutions - MGDP and BJIT. Therefore, our proposed preemptive scheduling scheme is based on FPP. To accommodate the conversion cascading constraint that the current converter technology is facing, we reduce the converter usage whenever possible and combine a constraint threshold into a new priority function. The details of the algorithm are presented in the following section. The techniques introduced in [ZBL07] could be incorporated into our preemption solution for further improvement, and we may consider them in real implementation.

6.2 Conversion Reduction and Fair Prioritized Preemption

In this section, we shall describe the proposed wavelength scheduling scheme - conversion reduction and fair prioritized preemption algorithm (CR-FPP) in detail.

We use the following same notations as in FPP [HY08] to present CR-FPP:

- X_i: any arriving burst i
- H_i: total hop counts of burst X_i
- σ_i: successful hop counts of burst X_i

- τ_i: remaining hop counts of burst X_i, i.e., $H_i = \sigma_i + \tau_i$
- L: average burst duration time
- δ: processing time of a control packet at core nodes
- $\triangle_i$: initial offset time of burst X_i, i.e., $\triangle_i = H_i \times \delta$
- θ: the evaluation function for preemption

As pointed out in FPP [HY08], the total number of hops pertains to fairness, the remaining hops can promote the priority of bursts close to its destination, and the number of successful hops is relevant to link utilization. FPP integrates these considerations into the evaluation function θ to achieve fairness improvement and efficient link utilization together. The evaluation function θ biased to longer H_i at some point is given as (6.1):

$$\theta(X_i) = \sigma_i - (\triangle_i / L) \times \tau_i \tag{6.1}$$

In (6.1), the negative term is used to prune the biased preference for bursts with longer initial offset time and the significance is determined by the ratio $\triangle_i / L$. If this pruning is not executed, the above preemptive scheme may apparently over-correct the fairness problem.

To address the negative performance impact caused by the conversion cascading constraint, our proposed scheme CR-FPP shall first try to schedule the incoming burst on its current channel λ_{prev} that it used at the previous hop(s). Only if the channel occupied by the incoming burst is

not available on the outgoing link, LAUC-VF scheduling is applied. If LAUC-VF still can not accommodate the new burst, CR-FPP shall look for the candidate bursts to preempt according to the new evaluation function $\bar{\theta}$:

$$\bar{\theta}(X_i) = \left(1 - \frac{\pi_i}{c_{max}} \cdot \frac{1}{\sqrt{H_i}}\right) \times \sigma_i - \beta \times (\triangle_i / L) \times \tau_i \tag{6.2}$$

where π_i denotes the accumulated number of wavelength conversions conducted for bust X_i so far, c_{max} is the threshold and $\pi_i \leq c_{max}$. Due to the cascading constraint, we determine the eligibility of a candidate burst not only by how many successful hops (σ_i) it has traversed, but also by how many wavelength conversions (π_i) it has experienced. The term $\frac{\pi_i}{c_{max}} \cdot \frac{1}{\sqrt{H_i}}$ represents the latter impactor and should be negative. It is in inverse proportion to H_i, which gives more bias on longer-path bursts to achieve fairness, because as aforementioned those bursts may be affected by the constraint more often in general. In (6.2) a new parameter β is also added to the second term relevant to τ_i. This parameter β provides us with more flexibility determining the significance of τ_i. We can fine-tune β to further reduce the two opposite side-effects brought by the preemption scheme: overcorrection because of the over-preference for bursts with longer initial offset time and over-suppression of longer-hop bursts due to possible increasing packet process time δ. We shall discuss the effects in more detail in Section 6.3. When a burst is preempted, messages are sent to both uplink(s) and downlink(s) to release the resources reserved for this burst.

Algorithm 3 CR-FPP

Input: Burst $X_{new} = \langle H_{new}, \sigma_{new}, \tau_{new}, \triangle_{new}, \pi_{new}, \lambda_{prev} \rangle$, c_{max}, and the current schedule
Output: Grant reservation request of X_{new} or not

```
if X_new can be scheduled into the current schedule on λ_prev then
    Reserve X_new on λ_prev; return;
else if X_new can be scheduled on λ_m (≠ λ_prev) via LAUC-VF then
    Reserve X_new on λ_m; return;
else
    Ψ ← φ;
    for i = 1 to W do
        X_con = ⟨H_con, σ_con, τ_con, △_con, π_con⟩ /* the contending burst on λ_i */
        if θ̄(X_new) > θ̄(X_con) then
            Ψ ← Ψ ∪ {X_con};
        end if
    end for
    if Ψ ≠ φ then
        Pick X_j such that σ_j/H_j = min_{∀X_i} σ_i/H_i;
        Reserve X_new on the channel that X_j was scheduled;
        Send message to release reservations for X_j on both uplink(s) and downlink(s);
    else
        Drop X_new;
    end if
    return;
end if
```

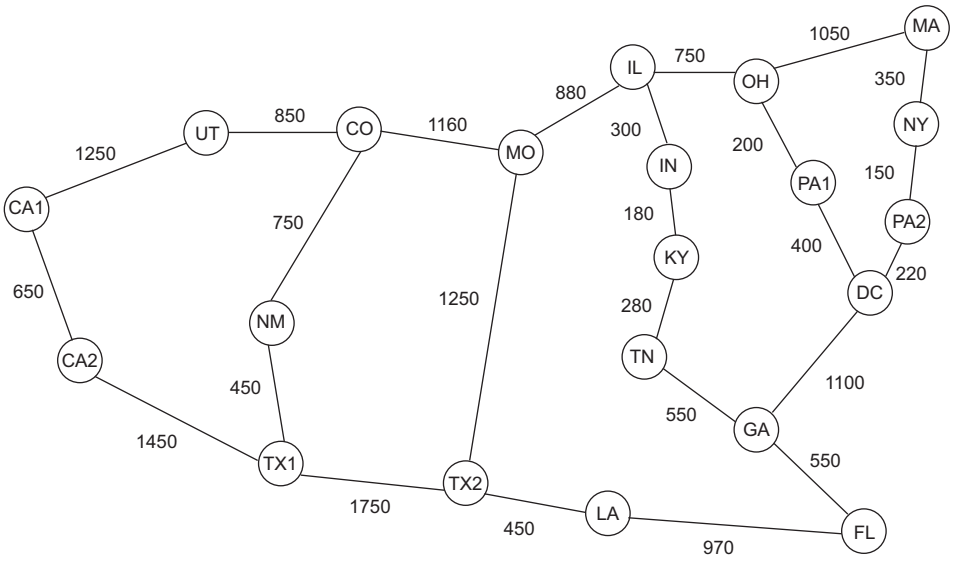

Figure 6.1: 21-node Abilene (Internet2) network with link distance in km.

The resulting algorithm is described in Algorithm CR-FPP. Similar to FPP, in Algorithm CR-FPP if more than one scheduled bursts lose in a contention, the algorithm picks the one with the shortest relative successful path as the victim to be preempted in this contention, i.e., burst X_j such that $\frac{\sigma_j}{H_j} = \min_{\forall X_i} \frac{\sigma_i}{H_i}$. If two or more bursts on a channel are involved in a contention, in other words over one scheduled burst shall be preempted to accommodate the single new burst, we discard the new burst directly to save the possible bandwidth waste.

6.3 Numerical Results

In this section, we investigate the burst loss performance and the fairness of the proposed preemptive scheduling scheme. Since it has been shown in [HY08] that FPP outperforms both BJIT and

MGDP, we shall focus on comparing CR-FPP with FPP only. The evaluation network model is the topology comprising the optical routing nodes extracted from the Abilene (Internet2) network. In the simplified Abilene topology (Figure 6.1), the longest-shortest path between source and destination has seven intermediate OXCs. Therefore no burst needs more than seven wavelength conversions to reach its destination. We assume that all nodes have the capability of full-range wavelength conversion. Every link is a bidirectional fiber and consists of W data channels. The burst arrival pattern follows a Poisson process, and the burst duration time is negatively exponentially distributed with mean L. Traffic load is normalized with $\rho = (\lambda L)/W$ per optical node. For each burst arrival, the source and destination nodes are uniformly selected. Unless specified, $W = 8$, the ratio $\delta/L = 0.01$ and β in CR-FPP is set to 1.0. The unfairness measure is defined as the standard deviation of mean dropping probabilities calculated according to statistics of bursts with identical total hop count. The lower the unfairness measure is, the fairer a scheduling algorithm is. Each data point shown in the performance graphs is obtained by running 10^7 burst transmission requests.

We first briefly illustrate the advantages of FPP over the pure LAUC-VF scheduling algorithm under no effect of the conversion cascading constraint. Figures 6.2 and 6.3 plot the burst loss rate and unfairness measure against traffic load, respectively. When $c_{max} = 7$, FPP shall not be affected by the cascading constraint at all. Because of its intelligent discarding, FPP shows large performance improvement for both burst loss and fairness. In short, FPP would not drop any burst deliberately, and it determines bursts priorities dynamically for preemption.

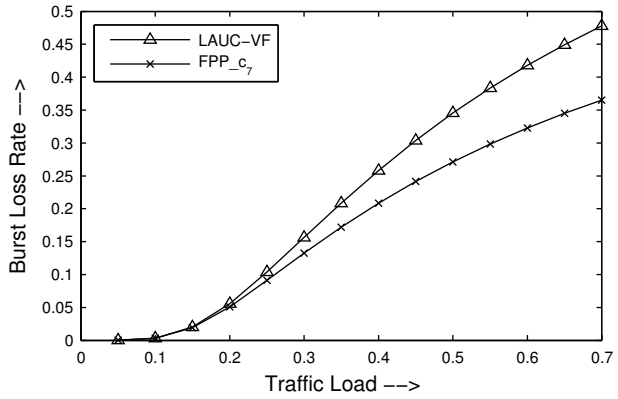

Figure 6.2: Burst loss: pure LAUC-VF versus FPP (c_{max} = 7).

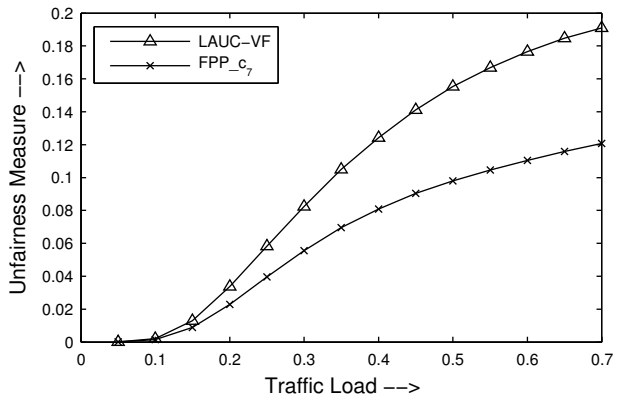

Figure 6.3: Unfairness measure: pure LAUC-VF versus FPP (c_{max} = 7).

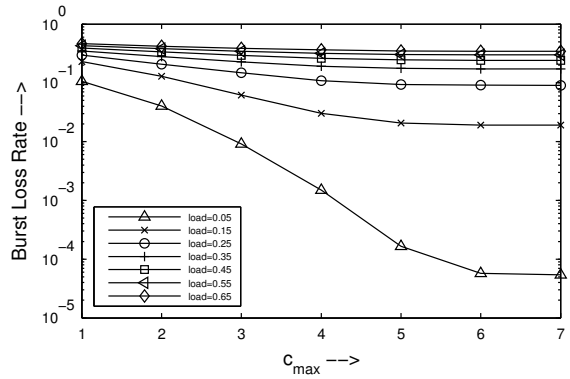

Figure 6.4: FPP: burst loss versus c_{max}.

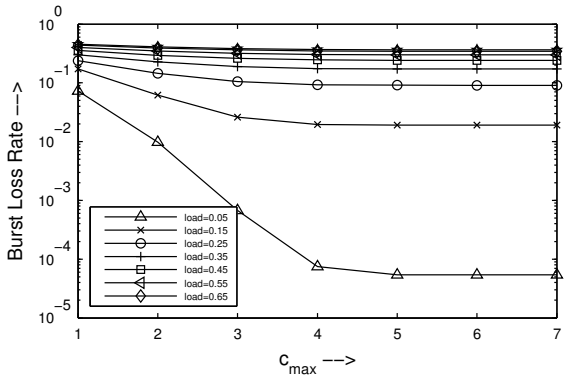

Figure 6.5: CR-FPP: burst loss versus c_{max}.

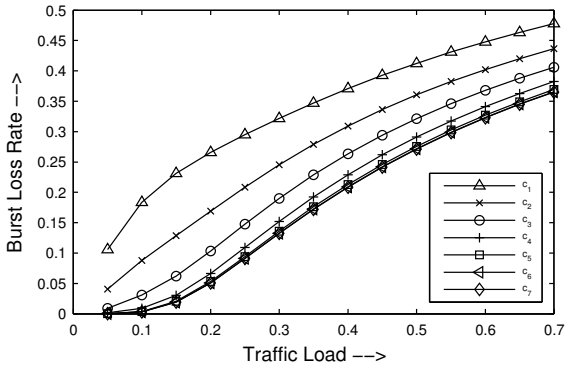

Figure 6.6: FPP: burst loss versus traffic load.

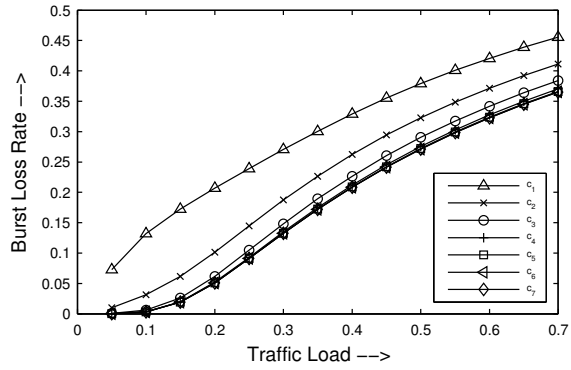

Figure 6.7: CR-FPP: burst loss versus traffic load.

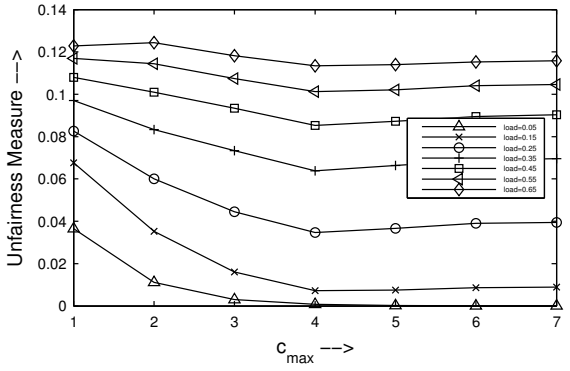

Figure 6.8: FPP: unfairness measure versus c_{max}.

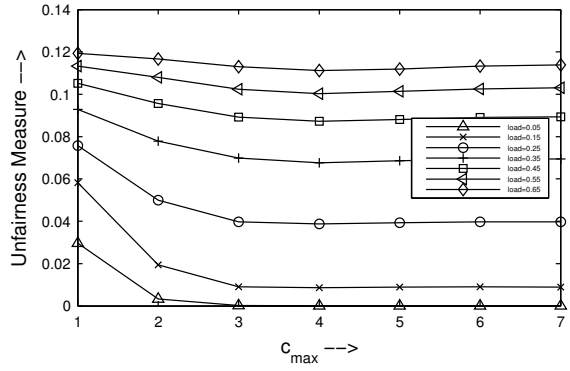

Figure 6.9: CR-FPP: unfairness measure versus c_{max}.

Figures 6.4-6.9 compares the performance achievements between CR-FPP and FPP side by side. We have the following observations:

- CR-FPP achieves lower burst loss rates across almost all kinds of loads, and regardless of the value of c_{max}. Moreover, as depicted in Figures 6.4 and 6.5, for the same load CR-FPP is able to suppress the negative impact of the conversion cascading constraint much faster than FPP when this constraint becomes less stringent (with higher c_{max}), especially under lower loads. For instance, under load 0.05 CR-FPP has reached the stable loss rate at c_4, but FPP still suffers from high burst losses at same c_4 which is over one order of magnitude in disparity. The merit of CR-FPP lies on two aspects: at first it effectively reduces unnecessary wavelength conversions by scheduling the bursts on the channel that they have used at their previous hop(s); secondly, it incorporates the consideration of the cascading constraint into the priority evaluation function for preemption. In this way, some bursts that have experienced relatively too many wavelength conversions, which are very possible to get dropped at their next hop(s) due to the cascading constraint, may be sacrificed at the current hop to accommodate other bursts with less conversions. Consequently, resource wastes have been saved ahead of time.

- Figures 6.6 and 6.7 further prove the above findings. It is clear that starting at c_4 CR-FPP almost gains the same loss performance as the cascading constraint is not in effect (i.e.,

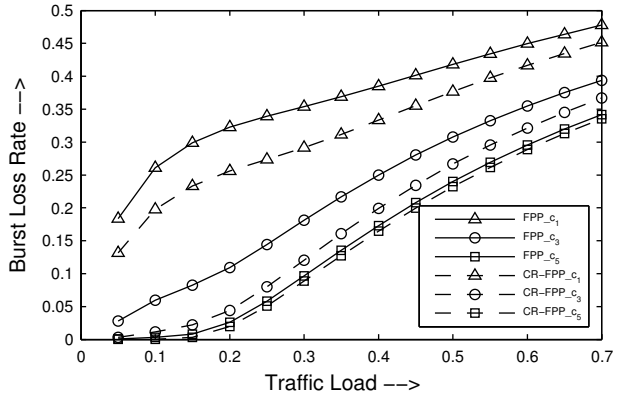

Figure 6.10: Burst loss versus traffic load at $W = 16$.

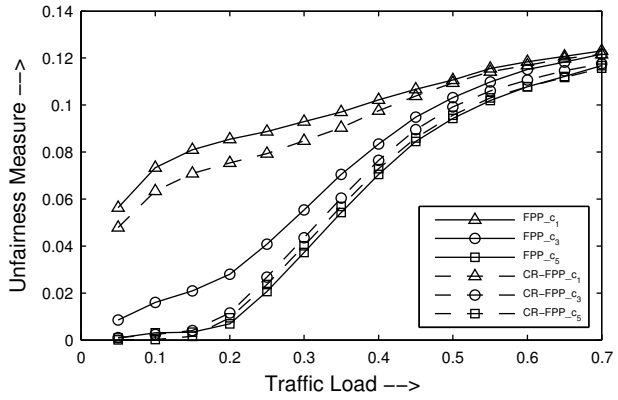

Figure 6.11: Unfairness measure versus traffic load at $W = 16$.

$c_{max} \geq 7$). And the loss rates obtained under $c_{max} \leq 3$ are closer to the counterparts under c_7 in CR-FPP than in FPP.

- Owing to the similar reasons explained above, Figures 6.8 and 6.9 show that CR-FPP achieves better fairness too for the same load.

Figures 6.10 and 6.11 depict the performance comparisons between CR-FPP and FPP for c_1, c_3 and c_5 at $W = 16$. CR-FPP is superior as expected. On the other hand, it is noticeable that

Table 6.1: Impact of β on burst loss under c_1

load / β	-0.5	-0.25	0.0	0.25	0.5	1.0	2.0	3.0	4.0	5.0
0.05	0.072718	0.072696	0.072671	0.072684	0.072681	0.072513	0.072023	0.071857	0.071645	0.07155
0.35	0.307824	0.307779	0.306885	0.302778	0.302713	0.300531	0.295888	0.293615	0.290728	0.289678
0.70	0.483667	0.483264	0.478419	0.458995	0.458594	0.455494	0.448272	0.442965	0.437204	0.43502

Table 6.2: Impact of β on burst loss under c_5

load / β	-0.5	-0.25	0.0	0.25	0.5	1.0	2.0	3.0	4.0	5.0
0.05	0.000054	0.000054	0.000054	0.000054	0.000054	0.000054	0.000054	0.000054	0.000054	0.000054
0.35	0.181062	0.180544	0.179496	0.173313	0.172721	0.172348	0.172114	0.171344	0.170118	0.169275
0.70	0.399438	0.398218	0.393653	0.368539	0.366999	0.366195	0.365374	0.362781	0.359315	0.357135

for either algorithm the performance disparity between c_1 and c_3, or between c_3 and c_5 (e.g., CR-FPP_c_1 vs. CR-FPP_c_3) is bigger than that when $W = 8$, especially at lower loads. It can be interpreted as follows. Both algorithms are expected to use LAUC-VF for scheduling most of the time. Actually, pure LAUC-VF is a kind of channel scheduling algorithm that is biased to converter utilization. It performs exhaustive searching trying to find the matching void throughout the available ones on all channels. When W gets larger, there will be more channels as well as more voids available and consequently more conversions would occur. Generally speaking, the larger number of conversions, the more severe the negative impact of the cascading constraint would be. Whereas, since CR-FPP possesses the intelligence to deal with the cascading constraint, it is still able to maintain a very small performance discrepancy between CR-FPP_c_3 and CR-FPP_c_5.

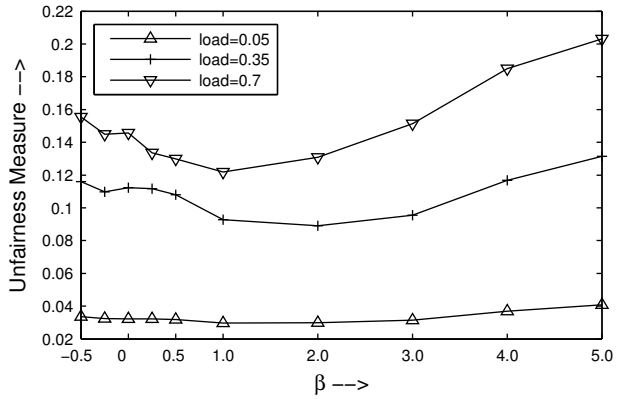

Figure 6.12: Unfairness measure versus β under c_1.

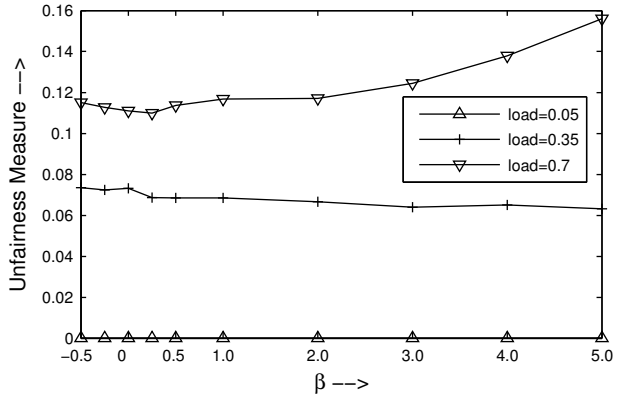

Figure 6.13: Unfairness measure versus β under c_5.

We also exploit the impact on the network performance when the parameter β varies. In the original FPP algorithm, the term $(\triangle_i/L) \times \tau_i$ was designed to suppress the over-preference for bursts with longer initial offset time. However, we expect this significance would also be related to a variety of other conditions such as network topology, traffic load and the cascading constraint threshold in our studying case. Tables 6.1 and 6.2 display burst loss variations when β grows under c_1 and c_5, respectively, while Figures 6.12-6.13 show fairness fluctuations. To ensure completeness, we consider some negative β values too. We can observe that burst loss rates have been decreasing at most cases when β increases for the values of β we select. On the contrary, fairness has shown a different curve roughly decreasing at first, reaching the bottom in the middle and increasing afterwards. Furthermore, the variations on both burst loss and fairness intend to grow larger at higher loads and under more stringent cascading thresholds (i.e., smaller c_{max}). We shall explain these two related phenomena as follows. When β including negative ones is smaller, bursts with longer hop counts (therefore longer initial offset times) would generally gain more preference during preemption. If β is small enough, the overcorrection would occur resulting in fairness deterioration. If β is big enough, bursts with longer hop counts would be suppressed too much, which results in fairness deterioration too. Consequently fairness reaches the equilibrium state only with a reasonable moderate β. On the other side, more longer-hop bursts getting dropped would benefit the other shorter-hop bursts. For example the resources released because of the discarding of one eight-hop burst would probably rescue two or more one-hop bursts. That explains why overall burst loss rates continue to decrease when β grows. Certainly, this trend would stop or go inverse

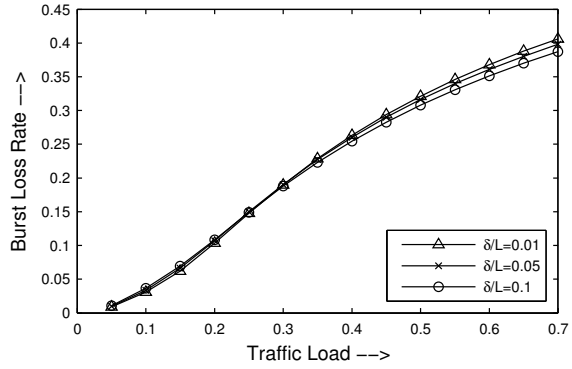

Figure 6.14: FPP: burst loss versus traffic load.

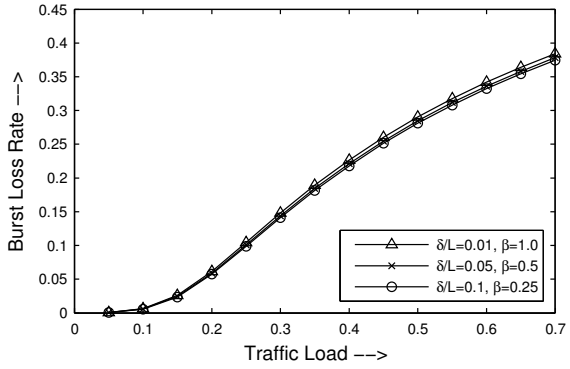

Figure 6.15: CR-FPP: burst loss versus traffic load.

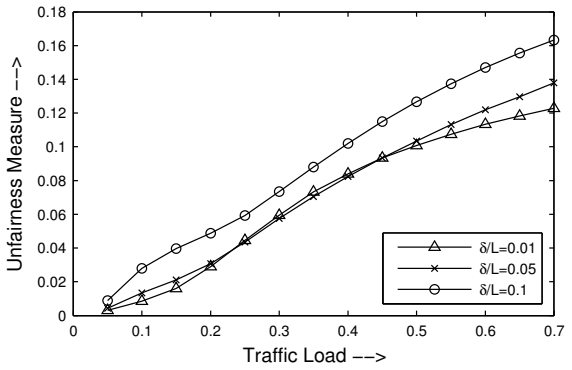

Figure 6.16: FPP: unfairness measure versus traffic load.

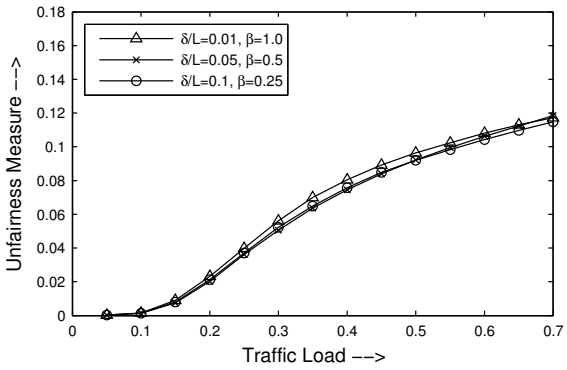

Figure 6.17: CR-FPP: unfairness measure versus traffic load.

if β is rather big. Finally, at higher loads and under smaller c_{max}, more preemptions are expected to being performed. So the variations brought by different β values have occurred faster or appeared larger.

Being able to alleviate the side effect caused by a larger packet processing time δ is another plausible feature through β adaptation. In (6.2) if δ becomes bigger but β keeps unchanged, bursts with longer hop counts will probably be over-suppressed by the preemption process. It may result

in fairness deterioration. Therefore, decreasing β shall solve this dilemma. Figures 6.14-6.17 demonstrate the performance comparisons side by side for CR-FPP and FPP under the effect of different δ values. The c_{max} is set to a moderate value of three. It is obvious that while FPP suffers from a noticeable performance fluctuation (mostly degradation, especially on the fairness problem) when δ increase, CR-FPP maintains a very small performance discrepancy by adjusting β appropriately.

6.4 Summary

In this chapter, we re-examine the fairness problem under the effect of the conversion cascading constraint in OBS networks. Both fairness and burst loss performance may deteriorate when bursts especially those with longer hop counts are dropped due to the cascading constraint. Subject to this conversion impediment, we improve an existing preemptive fair channel scheduling algorithm named FPP by integrating the impact of the constraint into the priority evaluation function. The resulting new preemptive scheme CR-FPP also tries to reduce unnecessary wavelength conversions whenever possible. Simulation results show that CR-FPP yields better fairness and achieves lower burst loss rates simultaneously over FPP. The former also has the flexibility to work with a diversity of network topologies and to mitigate the side effect resulting from a large packet processing time.

CHAPTER 7

CONCLUSION

We have designed and analyzed effective routing and channel scheduling schemes to improve system performance for WDM optical networks. Our main findings and contributions are summarized in this chapter. Possible future research ideas are also discussed.

The new wavelength conversion cascading constraint has been identified. The cascadability of wavelength converters is limited for the resulted reduced signal quality measured by various factors including signal-to-noise ratio, chirp, amplitude distortion, and extinction ratio. It is thus desirable to put a constraint on the maximum number of wavelength conversions we can perform on each data transmitting. This constraint would inevitably cause negative side effects on network performance such as higher blocking probability and worse fairness among transmitted data of different hop counts.

To address the cascading constraint in optical circuit-switched networks, two constraint-aware dynamic routing algorithms were proposed and presented. They perform source routing using link connectivity and the global state information of each wavelength. The simulation results demonstrated that these two constraint-aware algorithms could improve the blocking performance

significantly compared to conventional dynamic RWA algorithms in the environment of full or/and sparse wavelength conversion.

In the literature of optical burst switching, full wavelength conversion is commonly assumed to resolve high burst loss rates. Similar to what we have discovered on the connection blocking performance degradation in OCS networks, it is inferred that the cascading constraint causes negative impact on network performance in OBS too. Due to the inherent differences of signal protocols between the two switching mechanisms, we further investigated this negative impact in OBS. We developed a proactive routing mechanism tailored to the environment of constrained cascaded wavelength conversions on the basis of the proposed routing methods presented in Chapter 4.

The routing schemes proposed in Chapter 4 have the advantage that bursts traversing the same node pairs can utilize the same default offset time, while providing adaptive routing. The proposed hop-by-hop routing schemes also aim to address the intrinsic unfairness defect of existing popular signaling protocols by increasing the effective link utilization. The results showed that the proposed schemes generally outperform shortest path routing and depending on the routing strategy involved, the network topology and the traffic load, this improvement can be substantial. We developed analytical loss models to demonstrate the need for such an adaptive routing scheme at each hop and show its effectiveness. We also verified the analytical results by simulation.

We introduced a new preemptive scheduling scheme for next generation optical burst-switched networks considering the impact of cascaded wavelength conversions. Accordingly, subject to

this practical impediment, we showed how to improve a recently proposed fair channel scheduling algorithm [HY08] to deal with the fairness problem and aim at burst loss reduction simultaneously in optical burst switching. In this scheme, the dynamic priority associated with each burst is based on a constraint threshold and the number of already conducted wavelength conversions among other factors for this burst. When contention occurs, a new arriving superior burst may preempt another scheduled one according to their priorities.

Our research can be extended in a variety of ways. It is desirable to extend our analytical model for ring networks proposed in Chapter 4 to a more robust model that can analyze the network performance of more general topologies. In order to achieve this goal, we will need to extend the two-dimensional Markov chain model to multi-dimensional chains and develop computational methods for the efficient solution of these complex multi-dimensional chains.

Another point worthy of investigation is in the area of computing alternate routes. Although performance analyses of arbitrary networks have been largely researched in the past [RM02, ZVR07], they often assume that alternate routes block independently which is not generally true. It is desirable to derive a new model to cover general network topologies by taking into account the interdependencies between the blocking on alternate routes based on the techniques proposed in [GS97].

A third possible area of future research is to improve our OBS algorithms by utilizing the possible knowledge of burst arrivals in the future. Although it is not generally possible to know

the exact pattern of future burst arrivals, a limited knowledge of future traffic behavior can be used to improve the routing and wavelength assignment decisions of our algorithms. Developing predictive versions of the algorithms proposed in this dissertation is a point of research worthy of future investigation.

LIST OF REFERENCES

[AKD06] N. Akar, E. Karasan, and K. Dogan. "Wavelength Converter Sharing in Asynchronous Optical Packet/Burst Switching: An Exact Blocking Analysis for Markovian Arrivals." *IEEE J. Sel. Areas Commun.*, **24**(12):69–80, December 2006.

[Bir96] A. Birman. "Computing approximate blocking probabilities for a class of all-optical networks." *IEEE J. Sel. Areas Commun.*, **14**(5):852–857, June 1996.

[BS05] N. Barakat and E.H. Sargent. "Dual-header optical burst switching: a new architecture for WDM burst-switched networks." In *Proc. IEEE INFOCOM '05*, volume 1, pp. 685–693, Miami, USA, March 2005.

[BS06] N. Barakat and E.H. Sargent. "Separating resource reservations from service requests to improve the performance of optical burst-switching networks." *IEEE J. Sel. Areas Commun.*, **24**(4):95–107, 2006.

[CCE03] H. C. Cankaya, S. Charcranoon, and T. S. El-Bawab. "A preemptive scheduling technique for OBS networks with service differentiation." In *Proc. IEEE GLOBECOM '03*, volume 5, pp. 2704–2708, San Francisco, USA, December 2003.

[CLZ03] Xiaowen Chu, Bo Li, and Zhensheng Zhang. "A dynamic RWA algorithm in a wavelength-routed all-optical network with wavelength converters." In *IEEE INFOCOM 2003*, volume 3, pp. 1795–1804, March 2003.

[CP99] S. Chatterjee and S. Pawlowski. "All-optical networks." *Communications of the ACM*, **42**(6):74–83, June 1999.

[CTM07] Yuhua Chen, Jonathan S. Turner, and Pu-Fan Mo. "Optimal Burst Scheduling in Optical Burst Switched Networks." *J. Lightwave Technol.*, **25**(8):1883–1894, 2007.

[CTZ07] Yuhua Chen, Jonathan S. Turner, and Zhi Zhai. "Contour-Based Priority Scheduling in Optical Burst Switched Networks." *J. Lightwave Technol.*, **25**(8):1949–1960, 2007.

[CWX03] Yang Chen, Hongyi Wu, Dahai Xu, and Chunming Qiao. "Performance analysis of optical burst switched node with deflection routing." In *Proc. IEEE ICC '03*, volume 2, pp. 1355–1359, Alaska, USA, May 2003.

[CY94] Kit-Man Chan and T.P. Yum. "Analysis of least congested path routing in WDM lightwave networks." In *IEEE INFOCOM '94*, volume 2, pp. 962–969, June 1994.

[EB03] M. El Houmaidi and M.A. Bassiouni. "k-weighted minimum dominating sets for sparse wavelength converters placement under nonuniform traffic." In *11th IEEE/ACM International Symposium on Modeling, Analysis and Simulation of Computer Telecommunications Systems. MASCOTS 2003.*, pp. 56–61, October 2003.

[EB06] M. El Houmaidi and M.A. Bassiouni. "Dependency-Based Analytical Model for Computing Connection-Blocking Rates and Its Applications in the Sparse Placement of Optical Converters." *IEEE Transactions on Communications*, **54**(1):159–168, January 2006.

[Gau04] CM Gauger. "Optimized combination of converter pools and FDL buffers for contention resolution in optical burst switching." *Photonic Network Communications*, **8**(2):139–148, September 2004.

[GB08a] Xingbo Gao and Mostafa A. Bassiouni. "Fairness-Improving Adaptive Routing in Optical Burst Switching Mesh Networks." In *Proc. IEEE International Conference on Communications (ICC)*, pp. 5209–5213, Beijing, China, May 2008.

[GB08b] Xingbo Gao and Mostafa A. Bassiouni. "Modeling and Performance Evaluation of Optical Burst Switched Ring Networks with Efficient Adaptive Routing." In *Proc. The 27th IEEE International Performance Computing and Communications Conference (IPCCC)*, pp. 327–334, Austin, Texas, December 2008.

[GB09] Xingbo Gao and Mostafa A. Bassiouni. "Improving Fairness with Novel Adaptive Routing in Optical Burst-Switched Networks." *IEEE/OSA Journal of Lightwave Technology*, **27**(20):4480–4492, October 2009.

[GBL06] Xingbo Gao, Mostafa A. Bassiouni, and Guifang Li. "Evaluating the impact of wavelength conversion cascading on the performance of optical routing algorithms." In *Proc. The Fourth International Conference on Communications, Internet, and Information Technology (CIIT)*, pp. 112–117, December 2006.

[GBL07] Xingbo Gao, Mostafa A. Bassiouni, and Guifang Li. "Conversion cascading constraint-aware adaptive routing for WDM optical networks." *Journal of Optical Networking*, **6**(3):278–294, March 2007.

[GBL08a] Xingbo Gao, Mostafa A. Bassiouni, and Guifang Li. "On the Routing Improvement in OBS Networks Considering Cascaded Wavelength Conversion." In *Proc. The 20th IASTED International Conference on Parallel and Distributed Computing and Systems (PDCS)*, pp. 135–140, Orlando, Florida, November 2008.

[GBL08b] Xingbo Gao, Mostafa A. Bassiouni, and Guifang Li. "Proactive Routing under Conversion Cascading Constraint in Optical Burst Switching Networks." In *Proc. IEEE International Conference on High Performance Switching and Routing (HPSR)*, pp. 45–50, Beijing, China, May 2008.

[GBL09a] Xingbo Gao, Mostafa A. Bassiouni, and Guifang Li. "Addressing conversion cascading constraint in OBS networks through proactive routing." *Photonic Network Communications*, **18**(1):90–104, August 2009.

[GBL09b] Xingbo Gao, Mostafa A. Bassiouni, and Guifang Li. "New Preemptive Scheduling for OBS Networks Considering Cascaded Wavelength Conversion." In *Proc. The SPIE Enabling Photonics Technologies for Defense, Security, and Aerospace Applications V Conference*, volume 7339, pp. 73390M–73390M–10, Orlando, Florida, April 2009.

[GS97] Albert G. Greenberg and R. Srikant. "Computational techniques for accurate performance evaluation of multirate, multihop communication networks." *IEEE/ACM Trans. Netw.*, **5**(2):266–277, April 1997.

[HBL03] Mounire El Houmaidi, Mostafa A. Bassiouni, and Guifang Li. "Dominating set algorithms for sparse placement of full and limited wavelength converters in WDM optical networks." *J. Opt. Netw.*, **2**(6):162–177, 2003.

[HLH02] Ching-Fang Hsu, Te-Lung Liu, and Nen-Fu Huang. "Performance analysis of deflection routing in optical burst-switched networks." In *Proc. IEEE INFOCOM '02*, volume 1, pp. 66–73, New York, USA, June 2002.

[HY08] Ching-Fang Hsu and Li-Cheng Yang. "On the fairness improvement of channel scheduling in optical burst-switched networks." *Photonic Network Communications*, **15**(1):51–66, February 2008.

[IM99] Jason Iness and Biswanath Mukherjee. "Sparse Wavelength Conversion in Wavelength-Routed WDM Optical Networks." *Photonic Network Communications*, **1**(3):183–205, November 1999.

[JX01] J.P. Jue and Gaoxi Xiao. "Analysis of blocking probability for connection management schemes in optical networks." In *IEEE GLOBECOM '01*, volume 3, pp. 1546–1550, 2001.

[KA98] E. Karasan and E. Ayanoglu. "Effects of wavelength routing and selection algorithms on wavelength conversion gain in WDM optical networks." *IEEE/ACM Transactions on Networking*, **6**(2):186–196, April 1998.

[LGV97] RB Lee, DF Geraghty, M Verdiell, M Ziari, A Mathur, and KJ Vahala. "Cascaded wavelength conversion by four-wave mixing in a strained semiconductor optical amplifier at 10 Gb/s." *IEEE Photon. Technol. Lett.*, **9**(6):752–754, June 1997.

[LL93a] K.-C. Lee and V.O.K. Li. "Routing and switching in a wavelength convertible optical network." In *IEEE INFOCOM '93*, volume 2, pp. 578–585, 1993.

[LL93b] K.-C. Lee and V.O.K. Li. "A wavelength-convertible optical network." *Journal of Lightwave Technology*, **11**(5):962–970, May-June 1993.

[LS99] L. Li and A. Somani. "Dynamic Wavelength Routing Using Congestion and Neighborhood Information." *IEEE/ACM Transactions on Networking*, **7**(5):779–786, October 1999.

[LSK03] SuKyoung Lee, K. Sriram, HyunSook Kim, and JooSeok Song. "Contention-based limited deflection routing in OBS networks." In *Proc. IEEE GLOBECOM '03*, volume 5, pp. 2633–2637, San Francisco, USA, December 2003.

[LTT04] Hailong Li, M. Tan Wei Liak, and I. Thng Li-Jin. "A distributed monitoring-based fairness algorithm in optical burst switching networks." In *Proc. IEEE ICC '04*, volume 3, pp. 1564–1568, Paris, France, June 2004.

[MMI05] E. Magana, D. Morato, M. Izal, and J. Aracil. "Evaluation of preemption probabilities in OBS networks with burst segmentation." In *Proc. IEEE ICC '05*, volume 3, pp. 1646–1650, Seoul, Korea, May 2005.

[OA05] N Ogino and N Arahata. "A decentralized optical bursts routing based on adaptive load splitting into pre-calculated multiple paths." *IEICE Transactions on Communications*, **E88B**(12):4507–4516, December 2005.

[OAM01] I. Ogushi, S. Arakawa, M. Murata, and K. Kitayama. "Parallel reservation protocols for achieving fairness in optical burst switching." In *IEEE Workshop on High Performance Switching and Routing*, pp. 213–217, Dallas, USA, May 2001.

[QY99] Chunming Qiao and Myungsik Yoo. "Optical burst switching (OBS) - a new paradigm for an Optical Internet." *Journal of High Speed Networks*, **8**(1):69–84, January 1999.

[QY02] Xiangdong Qin and Yuanyuan Yang. "Nonblocking WDM switching networks with full and limited wavelength conversion." *IEEE Transactions on Communications*, **50**(12):2032–2041, December 2002.

[RM98] B. Ramamurthy and B. Mukherjee. "Wavelength conversion in WDM networking." *IEEE J. Sel. Areas Commun.*, **16**(7):1061–1073, September 1998.

[RM02] Ramu Ramamurthy and Biswanath Mukherjee. "Fixed-alternative routing and wavelength conversion in wavelength-routed optical networks." *IEEE/ACM Trans. Netw.*, **10**(3):351–367, June 2002.

[RS97] R. Ramaswami and A. Segall. "Distributed network control for optical networks." *IEEE/ACM Transactions on Networking*, **5**(6):936–943, December 1997.

[RVZ03] Z. Rosberg, Hai Le Vu, M. Zukerman, and J. White. "Performance analyses of optical burst-switching networks." *IEEE J. Sel. Areas Commun.*, **21**(7):1187–1197, September 2003.

[SAS96] S. Subramaniam, M. Azizoglu, and A.K. Somani. "All-optical networks with sparse wavelength conversion." *IEEE/ACM Transactions on Networking*, **4**(4):544–557, August 1996.

[SS02] M. Sivakumar and S. Subramaniam. "On the performance impact of wavelength assignment and wavelength conversion architecture and placement algorithms." *SPIE/Kluwer Optical Networks Magazine*, **3**:44–53, Mar/April 2002.

[THT05] Yu Tanaka, Yusuke Hirota, Hideki Tode, and Koso Murakami. "Wavelength assignment algorithm considering the state of neighborhood links for OBS networks." In *Proc. SPIE Optical Transmission Systems and Equipment for WDM Networking IV*, volume 6012, pp. 56–65, Boston, USA, October 2005.

[TUK04] T. Tachibana, M. Ueda, and S. Kasahara. "A preemptive scheme with two-way release message transmission in optical burst switching networks." In *Proc. IEEE GLOBECOM '04*, volume 3, pp. 1994–1998 Vol.3, Dallas, USA, November 2004.

[Tur99] JS Turner. "Terabit burst switching." *Journal of High Speed Networks*, **8**(1):3–16, January 1999.

[TVJ03] G.R.V. Thodime, V.M. Vokkarane, and J.P. Jue. "Dynamic congestion-based load balanced routing in optical burst-switched networks." In *Proc. IEEE GLOBECOM '03*, volume 5, pp. 2628–2632, San Francisco, USA, December 2003.

[VJ03] V.M. Vokkarane and J.P. Jue. "Prioritized burst segmentation and composite burst-assembly techniques for QoS support in optical burst-switched networks." *IEEE J. Sel. Areas Commun.*, **21**(7):1198–1209, September 2003.

[VJS02] V. A. Vokkarane, J. P. Jue, and S. Sitaraman. "Burst segmentation: an approach for reducing packet loss in optical burst switched networks." In *Proc. IEEE ICC '02*, volume 5, pp. 2673–2677, New York, USA, April 2002.

[WL04] Bin Wang and N. Lella. "Dynamic contention resolution in optical burst switched networks with partial wavelength conversion and fiber delay lines." In *Proc. IEEE GLOBECOM '04*, volume 3, pp. 1862–1866, Dallas, USA, November 2004.

[WM00] John Y. Wei and Ray I. McFarland. "Just-In-Time Signaling for WDM Optical Burst Switching Networks." *J. Lightwave Technol.*, **18**(12):2019–2037, December 2000.

[WMA00] X. Wang, H. Morikawa, and T. Aoyama. "Deflection Routing Protocol for Burst-Switching WDM Mesh Networks." In *Proc. SPIE/IEEE Terabit Optical Networking: Architecture, Control, and Management Issues*, pp. 242–252, Boston, USA, November 2000.

[XL99] Gaoxi Xiao and Yiu-Wing Leung. "Algorithms for allocating wavelength converters in all-optical networks." *IEEE/ACM Transactions on Networking*, **7**(4):545–557, August 1999.

[XQL03] J. Xu, C. Qiao, J. Li, and G. Xu. "Efficient channel scheduling algorithms in optical burst switched networks." In *Proc. IEEE INFOCOM '03*, volume 3, pp. 2268–2278, San Francisco, March 2003.

[XQL04] Jinhui Xu, Chunming Qiao, J. Li, and Guang Xu. "Efficient burst scheduling algorithms in optical burst-switched networks using geometric techniques." *IEEE J. Sel. Areas Commun.*, **22**(9):1796–1811, November 2004.

[XVC00] Yijun Xiong, Marc Vandenhoute, and Hakki C. Cankaya. "Control architecture in optical burst-switched WDM networks." *IEEE J. Sel. Areas Commun.*, **18**(10):1838–1851, October 2000.

[YAK03] Younghwan Yoo, Sanghyun Ahn, and Chong Sang Kim. "Adaptive routing considering the number of available wavelengths in WDM networks." *IEEE J. Sel. Areas Commun.*, **21**(8):1263–1273, October 2003.

[Yoo96] S.J.B. Yoo. "Wavelength conversion technologies for WDM network applications." *Journal of Lightwave Technology*, **14**(6):955–966, June 1996.

[YQD00] Myungsik Yoo, Chunming Qiao, and Sudhir Dixit. "QoS performance of optical burst switching in IP-over-WDM networks." *IEEE J. Sel. Areas Commun.*, **18**(10):2062–2071, October 2000.

[YR06] Li Yang and G.N. Rouskas. "Adaptive path selection in OBS networks." *J. Lightwave Technol.*, **24**(8):3002–3011, August 2006.

[ZBL04] Bin Zhou, Mostafa A. Bassiouni, and Guifang Li. "Improving Fairness in Optical-Burst-Switching Networks." *Journal of Optical Networking*, **3**(4):214–228, March 2004.

[ZBL05] Bin Zhou, Mostafa A. Bassiouni, and Guifang Li. "Routing and Wavelength Assignment in Optical Networks Using Logical Link Representation and Efficient Bitwise Computation." *Photonic Network Communications*, **10**(3):333–346, September 2005.

[ZBL07] Bin Zhou, Mostafa A. Bassiouni, and Guifang Li. "Using constrained preemption to improve dropping fairness in optical burst switching networks." *Telecommunication Systems*, **34**(3):181–194, April 2007.

[ZJM00] Hui Zang, Jason P. Jue, and Biswanath Mukherjee. "A review of routing and wavelength assignment approaches for wavelength-routed optical WDM networks." *SPIE Optical Networks Magazine*, **1**(1):47–60, 2000.

[ZVJ04] Qiong Zhang, V.M. Vokkarane, J.P. Jue, and Biao Chen. "Absolute QoS differentiation in optical burst-switched networks." *IEEE J. Sel. Areas Commun.*, **22**(9):1781–1795, November 2004.

[ZVR04] A. Zalesky, Hai Le Vu, Z. Rosberg, E.W.M. Wong, and M. Zukerman. "Modelling and performance evaluation of optical burst switched networks with deflection routing and wavelength reservation." In *Proc. IEEE INFOCOM '04*, volume 3, pp. 1864–1871, Hongkong, China, March 2004.

[ZVR07] A. Zalesky, H.L. Vu, Z. Rosberg, E.W.M. Wong, and M. Zukerman. "Stabilizing deflection routing in optical burst switched networks." *IEEE J. Sel. Areas Commun.*, **25**(6):3–19, August 2007.

[ZVZ04] A. Zalesky, Hai Le Vu, M. Zukerman, Z. Rosberg, and E. W. M. Wong. "Evaluation of limited wavelength conversion and deflection routing as methods to reduce blocking probability in optical burst switched networks." In *Proc. IEEE ICC '04*, volume 3, pp. 1543–1547, Paris, France, June 2004.